

Master's thesis

NTNU
Norwegian University of Science and Technology

Nils Storås

Energy related occupant behaviour - In situ thermal sensing

Master's thesis in
January

Abstract

Energy use in buildings has been a major substance of reducing total energy consumption. Concerning both residential and non-residential buildings, 50 % of the energy in Norway is used to achieve thermal comfort by space heating or cooling [1, 2]. New buildings have seen improvement by utilising this energy more effectively by appointing this thermal energy where it is needed but the development must continue. As Norway, along with many other countries, aiming to reduce energy consumption, finding an efficient way to utilise energy for maintaining thermal comfort is the target in the industry.

Human thermal sensation and comfort is a subject of increased interest and relevance for people who spend their time in an indoor environment. Occupant behaviour is a substantial element in thermal perception. It is directly connected to persons clothing and activity level and can be difficult to predict. Ambient parameters, such as temperature and air velocity, are other parameters to consider along with the psychological element. Thermal comfort becomes a complex field of study where many aspects could be considered, and should in addition be done with caution to the energy consumption.

This study aims to cultivate more knowledge about occupant behaviour inside an office cell under certain given thermal conditions. An experiment was carried out, which took place in Trondheim during spring when the climate conditions are considered warm. Brief investigations of relevant subject were conducted and interesting findings from other studies are presented. By obtaining a thermal model, inspired by the 'Fanger's model' and the 'adaptive model', an evaluation form was prepared for the participant. Sensation about indoor thermal conditions was reported among psychological and personal parameters. Utilisation of a depth registration camera (Microsoft Kinect) recorded the participant's behaviour during the experiment. Collection of qualitative data by the subject, produced a cloud of information about the perception of certain thermal environments.

To procure information about the thermal environment, a CFD model was carried out to be a representation of the reality. The model was first drawn in SolidWorks CAD program, and transferred further to the simulation program, ANSYS. There were build two geometries, a pipe model and a chamber model, to represent the experiment. The geometries had to be meshed by applying different mesh methods to ensure the quality. By simulating the conditions in ANSYS Fluent, four different turbulence models were tested and evaluated. The $k-\epsilon$ RNG was, after tuning the model characteristics, found to present the reality to an acceptable level. To narrow the number of ambient parameters to examine, only 'temperature' and 'air velocity' was examined in this study.

Four different air flows were induced in to the chamber. There was also investigated the impact of a radiator, which rendered temperatures up to 30 °C by applying different effects. The data from the simulation was directly appointed to the registered joint locations conducted by the Kinect. Each joint location, for every time step during the experiment, had a certain value of temperature and air velocity attached. Exposure of temperature and velocity, for 25 location points, through a period of a full working day, could now be thoroughly analysed. This quantitative data makes it possible to pinpoint reasons for the subject's evaluations during the experiments.

The participant adapted to what could be considered as unpleasant conditions. Two equal scenarios were run with some days in between and the evaluation was different in those two. The quantitative data are equal for those two scenarios but the qualitative data were different. The subject also reported a physical change. The personal parameter; 'sweat rate', had been reduced. Adaption towards indoor environment was, in this case, present during very warm indoor conditions.

Sammendrag

Energibruk i bygninger har vært et viktig tema for å redusere det totale energiforbruk. For både boliger og industribygg er 50 % av energien i Norge brukt til å oppnå termisk komfort ved romoppvarming eller -kjøling. Nye bygninger har sett forbedringer ved å benytte denne energien mer effektivt ved å anvende den termiske energien kun der den er nødvendig, men utviklingen må fortsette. I Norge, sammen med mange andre land, tar sikte på å redusere energiforbruket, og målet i bransjen er å finne en effektiv måte å utnytte energi på for å opprettholde den termiske komforten.

Menneskelig termisk oppfattelse og komfort er et emne av økt interesse og relevans for folk som tilbringer sin tid i et innemiljø. Brukeroppførsel er et betydelig element i termisk oppfatning. Det er direkte forbundet med personlig bekledning og aktivitetsnivå og kan være vanskelig å bestemme. Omgivende parametere, for eksempel temperatur og lufthastighet, er andre faktorer som kan vurderes sammen med det psykologiske elementet. Termisk komfort blir et komplekst studieområde hvor mange aspekter kan vurderes, og bør i tillegg gjøres med hensyn til energiforbruket.

Denne studien tar sikte på å øke kunnskapen om adferd i en kontorcelle under visse gitt termiske forhold. Et eksperiment ble gjennomført, som fant sted i Trondheim på våren når klimaforholdene regnes som varme. Korte undersøkelser av det relevant emneet ble gjennomført og interessante funn fra andre studier er presentert. Ved utviklingen av en termisk modell, inspirert av "Fanger's modell" og den "adaptive modellen", ble det utarbeidet et evalueringsskjema for forsøkspersonen. Oppfattelse av termiske forhold ble rapportert med hensyn på psykologiske og personlige parametere. Utnyttelse av et dybderegistreringskamera (Microsoft Kinect) registrerte deltakerens oppførsel under forsøket. Innsamling av kvalitative data produserte en sky av informasjon om oppfatningen av enkelte termiske miljøer.

For å skaffe seg informasjon om det termiske miljøet ble en CFD-modell utarbeidet til å være en representasjon av virkeligheten. Modellen ble først tegnet i SolidWorks CAD-program, og overført videre til simuleringsprogrammet, ANSYS. Det ble bygget to geometriske modeller, en ventilasjonsmodell og en modell for kammeret, som representerer eksperimentet. Geometriene måtte «meshes» ved å anvende forskjellige metoder for å sikre kvaliteten. Ved å simulere forholdene i ANSYS Fluent ble fire forskjellige turbulensmodeller testet og evaluert. $K - \epsilon$ RNG ble etter å ha justert modellegenskapene funnet egnet til å representere virkeligheten. For å begrense antall omgivende parametre å undersøke, ble bare 'temperatur' og 'lufthastighet' undersøkt i denne studien.

Fire forskjellige luftstrømmer ble induisert i kammeret. Det ble også undersøkt virkningen av en radiator, som ga temperaturer opp til 30 °C ved å bruke forskjellige effekter. Dataene fra simuleringen ble koblet direkte til de registrerte bevegelsene utført av instrumentet Kinect. Hvert punkt på forsøkspersonens kropp, hadde en viss verdi av temperatur og lufthastighet. Eksponering av temperatur og hastighet, for 25 steder, gjennom en periode på en full arbeidsdag, kunne nå analyseres grundig. Disse kvantitative dataene gjør det mulig å fastslå årsaker til evalueringene under forsøkene.

Deltakeren tilpasset seg det som kunne betraktes som ubehagelige forhold. To like scenarioer ble gjennomført med noen dagers mellomrom, og evalueringen var forskjellig i de to. De kvantitative dataene er like for de to scenarioene, men de kvalitative dataene var forskjellige. Forsøkspersonen rapporterte også en fysisk endring. Den personlige parameteren; "svette", hadde blitt redusert. Tilpasning til innemiljø var i dette tilfellet tilstede under svært varme innendørsforhold.

Preface

This master's thesis marks the end of a five-year long education at Norwegian University of Science and Technology (NTNU) in Trondheim, at the Department of Energy and Process Engineering as my final destination. The thesis is a continuation of the project work carried out in the fall semester of 2018.

I would like to thank NTNU and supervisor Vojislav Novakovic for handing me this interesting task to accomplish and the guidance along the way. Thanks to my co-supervisor Jakub W. Dziejczak for thorough help in every step to complete this study, good moments and teaching along the way. Thanks to all other employees at NTNU for guidance, support and access to necessary equipment in the last five years. Especially Håvard Karoliussen, I hope you do well in the future.

Thanks to everybody I have met during my education in the past five years.

Special thanks to all friends and family, you are my heroes!

Nils Storås

Trondheim, 16.06.2019

Contents

Abstract	i
Sammendrag	ii
Preface	iii
List of figures	vii
List of tables	viii
Nomenclature	ix
1 Introduction	1
1.1 Background and objective	2
1.2 Method of work and structure	3
1.3 Limitations	3
2 Framework	4
2.1 Heat transfer	4
2.2 Thermal sensation	6
2.2.1 Thermal alliesthesia	9
2.3 Parameters	11
2.3.1 Clothing level	11
2.3.2 Metabolic rate	12
2.3.3 Temperature	14
2.3.4 Air movement	15
2.3.5 Relative humidity	16
2.4 Thermal comfort models	17
2.4.1 Fanger’s model	18
2.4.2 The adaptive model	20
2.5 Behaviour energy impacts	21
2.5.1 Predicted versus real energy use	22
3 Tools and instruments	24
3.1 Test chamber	24
3.2 SolidWorks	24
3.3 ANSYS	25
3.4 MATLAB	25
3.5 Microsoft Kinect	26
3.6 Supplementary	27
4 Methodology	28
4.1 Construction and set up in SolidWorks	28
4.2 Align geometry in DesignModeler	30
4.3 Meshing in ANSYS	33
4.3.1 Elements in mesh	34
4.3.2 Mesh methods	37

4.4	Simulating in ANSYS	41
4.4.1	Validation of simulation	44
4.4.2	Sensitivity analysis of the Standard and RNG model	47
4.4.3	Appending radiator inside the chamber	50
4.5	Design of experiment	51
4.5.1	Setting up and initiate the experiment	51
4.5.2	Evaluation	52
4.6	Data processing	57
5	Results	60
5.1	Meshing	60
5.1.1	Quality of pipe mesh	60
5.1.2	Quality of chamber mesh	62
5.2	Simulation	64
5.2.1	Pipe model	64
5.2.2	Chamber model	66
5.3	Validation	67
5.4	Modifying the Standard and RNG model	69
5.5	Radiator	72
5.6	Evaluation	73
6	Discussion	77
7	Conclusion	87
8	Further Work	88
	Appendix	94

List of figures

1	Layers inside human body to maintain core temperature.	8
2	Pleasantness of thermal stimuli applied towards hands which either suffers from hypothermia, hyperthermia or which is neutral.	10
3	Values of clo for a different kind of clothing.	12
4	Metabolic rate for different activities.	13
5	Predicted percentage dissatisfied (PPD) as a function of the predicted mean vote (PMV).	19
6	Adaptive model chart showing acceptable indoor operative temperature as a function of mean monthly outdoor air temperature	20
7	Influential factors that are directly connected to occupant behaviour. In addition, there are also external influential factors like political, economic and cultural factors.	22
8	Tracked skeleton using Kinect for 25 different joint locations.	26
9	TSI VelociCalc 8388-M-GB	27
10	TSI Transducer 8475-300	27
11	DPM TT 470 S	27
12	Three-dimensional drawing of the chamber measured in millimetres. The holes located at floor level are occurring on all four walls.	29
13	Transparent view of the chamber with pipe, chair, table and PC.	30
14	Display of how the chamber was cut into 48 zones with a the use of a Cartesian coordinate system. Each zone is defined by different colours and separated by lines.	31
15	Section overview of zones and containing furniture articles. The chair is coloured in orange, the table is red, PC is blue, and the pipe is drawn green.	32
16	Transparent zone in the chamber with the table and PC cut out from the air	32
17	Pipe model divided into two zones. The grey part is the separation ahead of the nozzle, and the green part is the main part.	33
18	Two different types of element order. Quadratic element order on the left side with more nodes. The linear element order on the right side with reduced nodes.	34
19	Geometrical 3D element shapes which appear in ANSYS meshing. From left: tetrahedron, pyramid, a prism with quadrilateral base, a prism with triangular base (wedge) and arbitrary polyhedron.	35
20	Generation of elements applying the hex dominant method. The part on the left is a cross-section at one outlet. The part on the right is a cross section along with the ceiling. Adjacent elements are removed.	38
21	Generation of elements applying the automatic method. The part on the left is a cross-section along the pipe. The part on the right is a cross section where the pipe is cut out. Adjacent elements are removed.	39
22	Generation of elements applying the body fitted Cartesian method. The part on the left is a cross section of the pipe. The part on the right is the surface of the pipe nozzle. Adjacent elements are removed.	39
23	Steps from the SolidWorks geometry to the generation of mesh. Left pink column represents the chamber model and the right blue column the pipe model. First steps are done in DesignModeler while the last two steps were performed in ANSYS mesh feature.	40
24	Simulation residuals for the pipe at 0.0167 kg/s with the Realizable model. The simulation was set to 1000 iterations but stopped at roughly 600 because of convergence.	43

25	Flowchart of the working process in ANSYS Fluent. Four turbulence models were examined along with a combination of four levels of mass flow.	44
26	Measuring locations in the chamber as viewed from Z- and X-direction, respectively from left. This was the probing points used in Fluent.	45
27	Polyline displaying the recordings of the participant inside the chamber carried out by the Kinect. Right illustration is an adjustment of the polyline.	58
28	Linear plot of temperature of 25 joint location points compared to accumulative plot.	59
29	Element quality of pipe mesh. Displaying volume (y-axis), the shape of the element and the quality of elements (x-axis).	61
30	Aspect ratio of pipe mesh. Displaying volume (y-axis), the shape of the element and the quality of elements (x-axis).	61
31	Skewness of pipe mesh. Displaying volume (y-axis), the shape of element and quality of elements (x-axis).	62
32	Element quality of chamber mesh. Displaying volume (y-axis), shape of the element and the quality of elements (x-axis).	63
33	Aspect ratio of chamber mesh. Displaying volume (y-axis), the shape of the element and the quality of elements (x-axis).	63
35	Cross-sectional view of the pipe showing streamlines from the inlet to the outlet. Range of colours represents the variety of air velocities through the pipe.	65
36	Cross-sectional view of the outlet of the pipe for the four turbulence models. The face was then transferred to the chamber inlet which is in a different geometry model. . .	66
37	Cross-sectional view illustrating the movement of air in the chamber. The vertical, pink line represent the adjacent cross-section. Contours ranging from 0 to 10 m/s for all four turbulence models.	67
38	Measures of air velocities for five locations points inside the chamber. Grey, transparent boxes represents the actual measurements. The coloured columns represent each of the turbulence models.	68
39	Comparison of air velocity between the Standard and the RNG model for the five locations in chamber. Including a sensitivity analysis of features and model characteristics for both turbulence models.	70
40	Comparison of air velocity when experimenting with RNG model characteristics at five locations in the chamber.	71
41	Cross-sectional view illustrating the temperature of the air in the chamber. The vertical, pink line represent the adjacent cross-section. Contours are ranging from 293 to 313 Kelvin for all simulations.	73
42	Accumulative exposure of temperature and air velocity at segregated locations on the participant's body. Results from 23.05 with the heater on (II/III) and an air flow of 0.0667 kg/s.	74
43	Accumulative exposure of temperature and air velocity at segregated locations on the participant's body. Results from 28.05 with the heater on (II/III) and an air flow of 0.0667 kg/s.	75

List of tables

1	Advised limits for the parameters given in NS-EN ISO 7730:2005.	19
2	Categories of a thermal environment based on PMV and PPD.	19
3	The value of C for each type of geometry that an element can have.	35
4	Mesh settings	40
5	Fluent settings	44
6	The five locations in the chamber and in the model that was compared against each other. Type of instrument is described in the right column.	45
7	The six scenarios which were conducted in the chamber. Two different air flows were tested together with different radiator settings.	51
8	The original RNG model and experiments with model characteristics, values and activated feature.	71
9	Fluent settings	72

Nomenclature

Abbreviations

<i>ANSYS</i>	Analysis Systems
<i>API</i>	Application Program Interface
<i>ASHRAE</i>	American Society of Heating, Refrigerating and Air-Conditioning Engineers
<i>BIM</i>	Building Information Models
<i>CAD</i>	Computer-Aided Design
<i>CAE</i>	Computer-Aided Engineering
<i>clo</i>	Clothing level
<i>CPU</i>	Central Processing Unit
<i>EN</i>	European Standard
<i>EPT</i>	Energy and Process Engineering
<i>HVAC</i>	Heating, Ventilation and Air Conditioning
<i>ISO</i>	International Organization of Standardization
<i>MATLAB</i>	Matrix Laboratory
<i>met</i>	Metabolic rate
<i>MPC</i>	Model Predictive Control
<i>NTNU</i>	Norwegian University of Science and Technology
<i>PMV</i>	Predicted Mean Vote
<i>PPD</i>	Predicted Percentage of Dissatisfied
<i>RNG</i>	Renormalization Group
<i>situ</i>	<i>here:</i> Field
<i>SST</i>	Shear-Stress Transport
<i>tog</i>	Rate of the area covered with clothes
<i>ZEB</i>	Zero Emission Buildings

Symbols

α	Inverse effective Prandtl number
β	Pressure gradient
\dot{m}	Mass flow
ϵ	Equation for turbulent dissipation rate
η	Strain rate
\hat{U}	Angular velocity of the system rotation

μ	Turbulent viscosity
ω	Equation for specific dissipation rate
ϕ	Ratio between measured and maximum containment of water vapour pressure
ρ	Air density
σ	Turbulent Prandtl number for epsilon
AH	Absolute humidity
A	Mean strain and rotation rates
A	Surface area
B_m	Basal metabolic rate
C, β	Constants
C_a	Vapour concentration in the air
C_{sk}	Vapour concentration for skin
C	Convective heat transfer
C	Value of element quality
d	Distance
E	Evaporation
G_b	Generation of turbulence kinetic energy due to buoyancy
g_i	Gravitational vector
G_k	Generation of turbulence kinetic energy due to the mean velocity gradients
h_c	Convective heat transfer coefficient
h_D	Diffusion transfer coefficient
h_r	Radiative heat transfer coefficient
K	Thermal conductivity
k	Equation for turbulent kinetic energy
k	Valve position
L	Thermal load
M_M	Metabolic rate due to whole-body movement
M_P	Metabolic rate due to body posture
M_W	Metabolic rate due to type of work
M	Metabolic rate
m	Rate of mass transfer
p_1	Pressure difference

P_a	Water vapour pressure of air
P_{sa}	Water vapour pressure of saturated air
Pr_t	Prandtl number
Q	Rate of energy flow
q	Volume flow
Re_ϵ	Reynolds number
R	Radiative heat transfer
S	Heat storage
S	User-defined source terms
T_a	Air temperature
T_r	Radiative temperature
T_{op}	Operative temperature
T	Temperature
t	Time
u	Velocity
W	Mechanical work
x_{ij}	Vector of direction
Y_M	Fluctuating dilatation in compressible turbulence to the dissipation rate

1 Introduction

In the last years, there has been an increasingly interest in indoor climate where thermal comfort is a key indoor environmental quality concern, both at home and at the office. Studies show that satisfying indoor climate has a significant impact on productivity and performance as well as humans daily well-being [3, 4]. Several comfort models have been presented over the decades to measure peoples satisfaction with the indoor climate. This in terms of environmental factors, physiology, psychology and peoples freedom to interact with the building. [5, 6]

The sensation of the thermal climate is decided upon a large number of factors, e.g. clothing, the activity level, which climate that person were before arriving the typical room etc. With extensive factors to consider, it becomes difficult to predict a person's thermal expectations. Therefore, setting the optimum temperature without any knowledge about the people in the room is not an easy task. Every individual sense the temperature different based on the respective factors mentioned along with many more. Then the question arises if this is best suited to be controlled manually or automatically.

Together with keeping the environmental conditions at a pleasant level, there is also deference of energy use and energy efficiency. Especially energy use in buildings has been a major substance of reducing total energy consumption. As Norway, along with many other countries, has made a commitment to reduce their total energy use, looking at how to spend less energy is an important measure because it is relatively simple and it is not as expensive compared to other measures. This has created building standards with strict requirements to use equipment and materials which reduces the energy consumption of the building.

In residential buildings in Norway, between 65-80 % of the electricity is used for space heating [1, 7]. For non-residential buildings, approximately half of the electricity consumption is either used for heating or cooling, depending on the utilisation of the building [2]. Then, it becomes intelligible how important it is to avoid wasting more heat than necessary. Newer buildings also have the capability to reduce the amount of energy used by regulating the temperature or provide fresh air automatically depending on, e.g. activity level or time of day. This avoids wasting energy by keeping the room in satisfying conditions without anyone occupying it.

By recording occupant's behaviour inside a building it is possible to set guidelines for how the building should allocate its energy use. Testing participants in experimental studies to map out their sensation in given conditions will bring numerical information to the table. The number of uncertainties are, however, extensively large in such surveys and detailed studies are necessary. Covering aspect by aspect through sensitive analyses under controlled environments would render valid and reliable results which will be useful for further research.

1.1 Background and objective

Occupant's and their energy-related behaviour has a significant impact on the total energy use in buildings. Building occupant's behaviour is a key parameter for building design optimization, energy diagnosis, and performance evaluation as well as for building energy performance simulation. To increase the general understanding of building occupants, it is necessary to develop a reliable tool for evaluation of occupant's energy needs. Currently, there is a method under development (depth registration) that can be used for such purposes, but its performances have to be carefully tested. If the selected method delivers information, proofing its accuracy and usability, it should be used for the development of the occupant behaviour numerical model.

The objective of this master thesis is to give support to the development of knowledge regarding occupant's energy-related behaviour. It will lead to the development of more accurate occupant behaviour models. Monitoring and identification of occupant's thermal comfort preferences is key in occupant behaviour studies. The assignment comprises processing of monitored data regarding human body exposition to the various thermal conditions and comparing it with a subjective sensation of the thermal indoor environment state. The assignment is connected to the current PhD research entitled "Modelling and Simulation of Occupant Behavior in Buildings".

The following tasks are to be considered:

1. Prepare a design of experiment protocol, supported by a knowledge obtained during the semester project.
2. Developed a detailed three-dimensional representation of the test chamber, followed up with a simulation mesh for further numerical investigations.
3. Perform a series of parametrical simulations studies, with limitations given by the technical capabilities of the test chamber.
4. Conduct field measurements of the indoor environment and develop a comprehensive report regarding the subjective sensation of thermal comfort inside the thermal chamber.
5. Analyze and compare gathered information from field studies and numerical simulations

According to "Utfyllende regler til studieforskriften for teknologistudiet/sivilingeniørstudiet ved NTNU" § 20, the Department of Energy and Process Engineering reserves all rights to use the results and data for lectures, research and future publications.

1.2 Method of work and structure

The method of work will be divided into three sections and follows a rational succession. First, a literature study will be conducted to gain knowledge and prepare for forthcoming work. Then, thoroughly set up the experiment to create conditions that minimize the erroneous of the field work. At last, the models set up will be simulated in the ANSYS software and analysed together with the evaluation of thermal comfort.

The literature study is part of the project work and contains a review of several papers, journals, books and relevant websites. The study was then updated to correspond better to the topic in question. Information gathered will build up the framework for the thesis and is presented in chapter two. It gives insight into the study substance and provides useful knowledge about the subject.

Setting up the model and the experiment is furthered developed from the project work and will describe the creation of the investigation. Every tool and instrument will be described along with the application of them. The goal of this part is to appoint a CFD model that precisely can represent a real-life scenario. Equipment and the methodology will be rendered in chapter three and four respectively. Details and settings are described to reproduce the field work and for further investigation

To complete the study, several models will be simulated under given boundary conditions and compared against the indoor environment the models are replicated from. Several cases will be evaluated to find coherence between different thermal and ambient conditions and the sensation of the subjective. The results from the simulation and experience inside the chamber are then to be analysed. Results from the study will be presented in chapter five.

A discussion will be following in chapter six, where relevant topics of the given objective will be addressed. Possible sources of error and suggestions for improvement will also be mentioned. To summarize the work conducted, there will be given a conclusion to the work in chapter seven. Proposal for further work will be given in chapter eight.

1.3 Limitations

The study is a commencement of the topic involving occupant behaviour and energy use. It will not include any energy-efficiency solutions for this particular case. The energy use is also not measured to any extent. How to utilise tools to trace movement is used, but the occupant data in interaction with the energy use in the chamber is not furthered examined. Occupant space is limited to a few square meters, and office work is the only activity performed. Behaviour inside is thereby restricted by the space and furnishing.

During the experiment, there will only be one person present. Evaluation towards the indoor environment is thereby not representative as there is no information about the person's history. Neither creates this any basis for the indoor environment as the person's sensation is not compared to any other objects.

The examination itself tests air flow up to 0.0667 kg/s at the ventilation inlet. This renders only minor air velocity gradients across the chamber. The experiment will conduct testing inlet temperature of 20°C and different settings with a radiator. The subject will thereby not be exposed to temperatures that could be considered as 'low'. The investigation is performed in the middle part of Norway, where the climate is cold.

2 Framework

The framework is based on a literature study and gives the basis for fieldwork and research throughout the thesis. The review of literature should also render necessary background information to better understand the topic and show the state of existing research. This theory also emphasises decision making through the experiment and the following evaluation of the experiment.

2.1 Heat transfer

Adjusting towards thermal comfort requires an understanding of what is influencing human's perception of the thermal environment. Thermal comfort can often be related to the correct balance between heat production of the body and the ambient conditions. Which implies that the heat transferred to or from the human body extends towards the body's thermal neutrality. If a person is cold, that person wants to minimize heat loss from the body, and if possible, receive heat from the environment. Likewise, for a person that is hot, increased heat loss from the body is desired. Heat transfer represents those processes that have an impact on a person's thermal equilibrium with the surroundings and is a key concept in this study.

According to the second law of thermodynamics, heat will always flow from hot to cold when no external force is involved [8]. Heat flow that occurs because of such temperature differences is called *sensible heat* and can happen in three different ways; *conduction*, *convection* and *radiation*. Heat transferred without temperature differences, but by the change of state, is called *latent heat*. This can happen through *evaporation* (liquid to gas) or *condensation* (gas to liquid). One or several of these five mechanisms are driving forces when heat is transferred between the human body and the environment. [9]

Conduction

Heat transferred through physical contact is called conduction. It means that a solid or stationary fluid is the heat conducting device, in which the heat transfer is driven by temperature differences. Note that steady-state conditions are here assumed along with one-dimensional bodies and applies for all the three mechanisms. Although such situations rarely exist, a simplification is used just for the introduction and establish the principles behind heat transfer.

The conduction heat transfer is presented mathematically in equation 1, where the rate of heat flow through the physical entity is proportional to the temperature difference between the layer. The thickness of the layer, in which the direction of heat is flowing, is represented by the notation d . The cross-sectional area normal to the heat flow direction is A . The thermal conductivity is represented by k , and is depending on the physical properties of the material. The quantity of heat that is passed through per unit time over the cross-sectional area is then denoted as q . [9]

$$q = \frac{k(T_2 - T_1)A}{d} \quad (1)$$

Conduction is of relevance for many scenarios of heat transportation, which is of interest for the subject's thermal comfort. Heat is transported by conduction from the core of the body and out to the ambient environment through layers of fat, muscle and skin. Heat loss is depending on the thickness of these layers, and the physic of a person is, therefore of the matter when evaluating the

ability to maintain the core body temperature. The thermal conductivity of the clothing, as well as the thickness, plays a role for how well insulated the body is, and the material of clothing can be specifically created to either increase or decrease heat loss from the skin. Conductive heat loss can also take place in contact with, e.g. cold floors or chairs, but also gained through heated seats or similar.

Convection

Convection is a compound mechanism of heat transfer which involves conduction as part of the process and is therefore not a separate mode of heat transfer. Convection is heat transferred as the cause of fluid in motion. Without any fluid in motion, the calculation can be simplified to conduction. The moving fluid absorbs heat amplified dependent on the velocity of the fluid, and the concept of boundary layer becomes relevant. The boundary layer is a region adjacent to the solid object where large velocity gradients exist and become thinner with high fluid velocity. When the boundary layer becomes thin, thermal insulation decreases and more heat is transferred from the surface area. [9, 10]

As with conduction, heat transferred by convection is also a function proportional to the temperature difference. A simplified mathematical expression for the convective heat transfer per time unit is shown in equation 2. The convective heat transfer coefficient h_c is dependent on several factors, including both the properties of the fluid and the solid surface. Water and air have different thermal transferring characteristics, but both viscosity and turbulence of the flow also impacts the heat transfer coefficient. The roughness and shape of the solid surface affect friction, which subsequently have an affect on the boundary layer, and with that also the coefficient h_c . [10, 11]

$$c = h_c(T_2 - T_1) \quad (2)$$

Dependent on how the fluid motion is initiated, convection can be classified into two categories; forced convection and natural or free convection. Natural convection is where the fluid movement is driven by natural causes and is generally confined to air velocity lower than 0,2 m/s. Such as the buoyancy effect where the warm fluid around the body rises, and the body loses heat. Forced convection is where an external source dominates, typically wind or air movement created by a circulating fan. Generally, forced convection is when air velocity exceeds 1,5 m/s. Between the two limits, there is a region named mixed-mode convection. [6, 10, 11]

Radiation

Radiation is the energy emitted or transmitted from a surface as particles or waves. It is the carrying of energy from one object and to the surrounding space. It differs from the other two heat transfer mechanisms as radiation does not require any movement, or interaction with other substances. The importance becomes significantly at high absolute temperature levels, but all objects emit and absorbs radiation. The warmer the object, the more it radiates, because increased heat means shorter wavelengths and frequency intensifies, hence the energy level increases. [9, 12]

Temperature plays a significant role in this kind of heat transfer as the energy released is temperature raised to the fourth exponentiation. This is shown in the mathematical expression for radiation heat transfer energy per time unit in equation 3. The coefficient h_r is given as a mean radiation coefficient and is dependent on the emissivity and area of the body and includes Stefan-Boltzmann constant. [10]

$$r = h_r T^4 \quad (3)$$

Radiation is invisible to the eye but can be caught up a thermal imaging camera which detects radiation emitted by any object and is shown as infrared waves in different colour scales. One example of radiation sources is heat and energy that comes from the sun. Another example is electric equipment like computers, lamps etc., which all contributes to increasing heat in the room through radiation. [10]

Evaporation and condensation

Evaporation and condensation happen as mentioned without any temperature differences but by a change of state. Respectively liquid to gas and gas to liquid. The two mechanisms for latent heat is driven by vapour concentration differences between two spaces. Latent heat can also involve a change of state from solid to liquid, but as this is not relevant for this study, it is left out in this framework. For analysis of human thermal environments, it is common to replace the mass concentration, denoted as (m), with vapour pressure. The mathematical expression for heat energy flow is shown in equation 4. The notation h_D is the diffusion transfer coefficient, while C represents vapour concentration. [13]

$$m = h_D(C_1 - C_2) \quad (4)$$

In this study, the vapour concentration difference is relevant as heat is transferred between the skin and air when it is different. Evaporation occurs when the heat is taken from the skin to evaporate water. For this type of process, the temperature does not change, but energy is used to change the state from liquid to gas. Evaporation typically occurs when stepping out of the shower or when the human body is sweaty. Then heat is removed from the body as the vapour differences remove heat energy. As with condensation, this process has close relations to convective heat transfer. [13]

Condensation is the reverse process of evaporation, where energy is released when the state changes from gas to liquid, also without change of temperature. Moist air gets cooled down by a cold medium and water vapour condenses. While evaporation is a cooling process to the relevant object, condensation is a heating process. Condensation is, however, a very unusual phenomena for the human body in cold climates. [13]

2.2 Thermal sensation

How the human body responds to the thermal indoor environment has an impact on health, comfort and performance. People desire an environment that is fit for the given work task and can subconsciously contribute to maximize effort. Unpleasant conditions make humans physical uncomfortable, leads to distraction and is an unfit environment for performing. This applies to office work, as well as physical activities. An environment that is not suited for the task drags the focus away, and the work effort drops as a cause. [14, 15]

The importance of having a satisfying indoor thermal environment has led to an increased interest studying the field. Several models have been made to map out the demand of humans when it comes to thermal comfort. Parameters that affect humans in different degrees, along with the most important comfort models will be presented later. In the European and the ASHRAE standard, which concerns thermal environmental conditions, thermal comfort is defined as:

That condition of mind which expresses satisfaction with the thermal environment [16].

The thermal sensation is generally about how people feel and is, therefore, a vague concept because it is a subjective opinion. It contains psychological, physical and physiological factors and is a complex composition. Distinguishing between what a person feels and would like to feel in terms of thermal comfort is important, and there are individual conceptions that must be evaluated in an analysis. There should also be a distinction between the environment and what a person feels to avoid confusion. Cold climate does not necessarily mean cold sensation. A person with good clothing and the high metabolic rate could even feel warm despite the cold climate. [17]

To understand this better, there are studies that show the correlation between climate and thermal comfort. A study by Yau and Chew found out that people that come from different climates, preferred different indoor environment and that neutral conditions are sometimes not the favourable option [18]. The study discovered that occupants in warm climates favour slightly cooler environments. While the opposite was found in colder climates where the occupants preferred slightly warmer environments. Kalz and Pfafferoth studied the expectation based on the outdoor temperature and the influence of individual experience [3]. Studies like these are examples of psychological factors that influence the sensation of thermal comfort.

Both these two studies ascertain that neutral conditions can deviate from what is satisfying conditions, which implies that thermal sensation is not just a physical sensation. Rohles was a psychologist who tried to correlate his field of study with thermal comfort and concluded that thermal comfort definitely was a matter of state of mind [19]. In one of his experiment, two groups of people were put in different environments with the same temperature. One group has told that a heater was one, the other group knew there was an existing heater, but did not know if it was on or not. The group that was told the heater was on expressed to feel warmer than the other group.

Thermal comfort is not easy to predict. Each individual human has a different perception of the thermal environment and each, and everyone has different physic. In terms of thermal sensation, the perception of the thermal environment is a matter of psychological factors as seen. Since ambient parameters are physical quantities, such parameters also affect the human body physically.

Inside the human body, there are mechanisms to detect thermal conditions and give a response to the condition. This is the system of human thermoregulation. By moving around, the metabolic rate will increase and hence also the heat production. The body can also contribute to heat loss by starting to produce sweat to cool down the skin. Another way to regulate body temperature is by changing the blood flow distribution to regulate the thermal state of the body. These are the most common examples of physiological responses to keep thermal balance. [6]

Other factors like age, gender and physical characteristics also play a role. A review of several studies by elderly people done by van Hoof and Hensen shows that age has more to do with physicality than psychological effects [20]. With increasing age, elderly people have less control over body temperature and the ability to transfer heat from the core of the body to the skin. The sweat rate is reduced, and vasoconstriction (narrowing of blood vessels) can be restrained.

Karjalainen compared well over thirty studies that highlighted thermal comfort between genders [21]. Some of them concluded that there is no significant difference between genders, while most of them find women more sensitive to temperatures that deviate from human's comfortable indoor temperature (22 - 24 °C). This, in particular for cold temperatures where women tend to become aware of discomfort quicker. This was also supported by the study done by Hashiguchi et al., which also found women more sensitive to unequal distribution of temperature across the body [22].

The goal of reaching thermal comfort is by keeping the body temperature at balance. If a person is in an inner normal physical state, the core temperature of the body normally lays around 37 °C [23]. A rise of this temperature leads to a decrease in mental and physical performances and continues to decrease with rising core temperature. A decreased core temperature can, on the other hand, lead to shivering, vasoconstriction and lack of consciousness. [6]

For extreme conditions, it could in both cases result in severe harm of the body and in worst cases death. This, however, is unlikely in an indoor environment as the building is made for protection against such extreme conditions. The peripheral body parts tolerate a broader range in temperature. For precise modelling, evaluating both the local body parts and the body as a whole is crucial as the differences can be vast. Determining if the environment is cold or warm when the most of the body feel warm and comfortable, while the hands or feet are freezing is inaccurate and can give measures that are not representative for the actual sensation. [6]

The body is build up by layers from the core to maintain the body temperature and keep it stable. These layers can be complicated for some parts of the body, and the thickness of each layer varies across the body. The most essential layers are shown in a simplified illustration in figure 1, based on M. Taleghani et al. work [24]. These layers work as insulation and protection against the external environment, in addition to their primal functions. Muscle and fat vary typically from each person and therefore has different capability to maintain the body core temperature. Thin layers of muscle and fat means that the body reacts faster to cold temperature as the body is poorly insulated. The cold receptors respond to this and send signals to the hypothalamus that the body is cold and act accordingly to prevent damage. [5, 25]

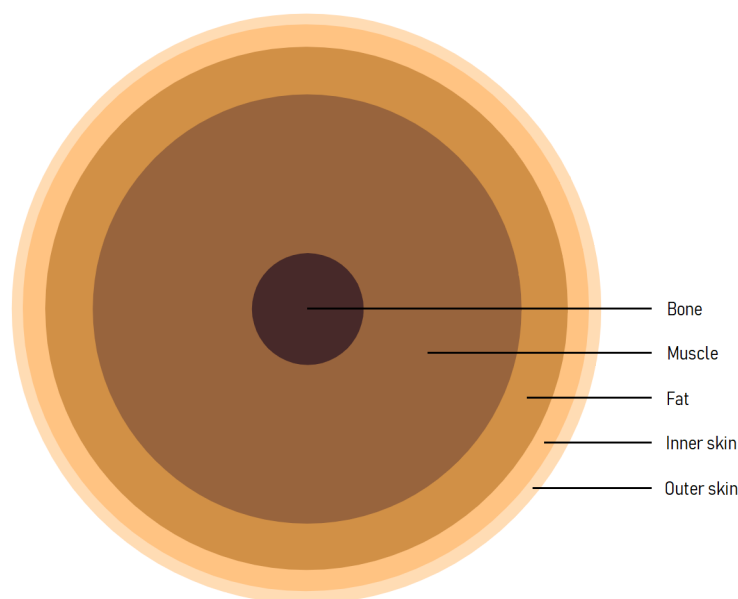


Figure 1: Layers inside human body to maintain core temperature [24].

Discomfort is a function of deviation from the comfort temperature. This applies to every region of the body and every part must be in comfort in order to achieve complete satisfaction with the thermal environment, meaning there is no local thermal discomfort. Causes of local discomfort can be draughts, vertical temperature differences, cold surfaces or radiant temperature asymmetries. Local discomfort appears usually on body parts where the skin is particularly sensitive, e.g. neck and ankles. [26, 27].

To obtain thermal comfort, the heat flowing from and to the body needs to be in balance, so that there is no positive or negative heat accumulation in the body. In addition to this, the skin temperature and sweat rate must be in a certain range depending on the metabolic rate. Equation 5 is the conceptual heat balance but can be acquainted in many forms if furthered derived. [5]

$$M - W = E + R + C + Q + S \quad (5)$$

On the left side of the equation is the metabolic rate (M) subtracted by the energy to do mechanical work (W). This is heat generation, and M-W becomes the released heat from the body's cells. On the right side, there is heat transfer that can go both directions, respectively evaporation (E), radiation (R), convection (C) and conduction (Q). Combining heat production and heat loss, the summation becomes heat storage (S). When balanced, the storage becomes zero. If there is heat gain, S will become positive, and body temperature will rise. If there is heat loss, S will become negative, and body temperature will fall. M-W can only be positive, while the transfer coefficients (E, R, C and Q) can be positive or negative depending on heat gain or loss. [6]

2.2.1 Thermal alliesthesia

Alliesthesia is a concept that describes the physiological basis for thermal pleasure or delight. It was first proposed by the psychologist Cabanac in 1971 and revisited by de Dear in 2011 [25, 28]. This phenomenon is used to separate thermal comfort from what is neutral and acceptable conditions. It is also a way to differentiate thermal comfort in non-steady environments from neutral conditions associated with steady-state environmental exposure, such as the PMV/PPD model [29]. In addition, it describes why some environmental configurations are uncomfortable for some but comfortable for others. De Dear define thermal alliesthesia like this:

Thermal alliesthesia states that the hedonic qualities of the thermal environment are determined as much the general thermal state of the subject as by the environment itself. A peripheral thermal stimulus that offsets or counters a thermoregulatory load-error will be pleasant perceived, and vice versa, a stimulus that exacerbates thermoregulatory load error will fell unpleasant [29].

Thermal alliesthesia emphasises that pleasurable sensations are generated by perceiving an external stimulus and restore thermal stress toward a neutral condition. It temporarily changes the local skin temperature by stimulating the cold or warm receptors on the skin. When occupants are exposed to a certain condition over long periods, the thermoreceptors adapt to the given condition. As a result, the skin temperature slightly changes without caution. By exposing the occupant with a brief change in temperature or air flow, it creates an awareness of the thermal sensation which previous was either slightly too cold or slightly too warm. This can happen in two scenarios, one is called 'temporal alliesthesia', and the other is called 'spatial alliesthesia'. [30]

Temporal alliesthesia is the example of experiencing a very pleasant condition for a short period of time. If exposed to conditions far from neutral over a period, a sudden sensation of a condition that brings the person closer to a neutral thermal state is desirable. Examples are being outside on a hot day and then walk into a cold supermarket or any other cold room. Or being outside on a cold day and then finally getting inside where the room is already heated. In order for this to happen, the body can not be in a neutral state, and the stimulus needs to bring the person towards the direction of thermal neutrality. [4, 29]

Spatial alliesthesia is the phenomena that cause thermal pleasure on a specific part or region of the body without changing the overall body temperature. Meaning that it is not confined to the whole-body experience but restricted to local areas on the body. Examples of spatial alliesthesia are sunrays hitting the face a cold morning. Or a breeze around the head when it is warm outside or touching metal with bare hands outside. Similar to temporal alliesthesia, stronger positive sensation occur when the localised change in a thermal parameter happens in the opposite direction of the original thermal state. Figure 2 is the result of an experiment done by Mower that shows which thermal conditions that were bringing the hands of objects toward thermal pleasure under given physical conditions [31]. From this it becomes clearly that when subjects had cold hands, they find the very high surrounding temperature to be most pleasant and vice versa. [4, 29]

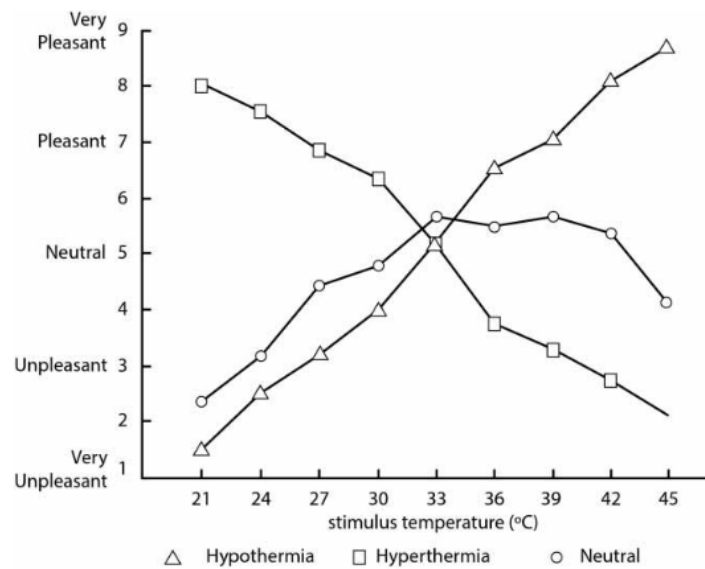


Figure 2: Pleasantness of thermal stimuli applied towards hands which either suffers from hypothermia, hyperthermia or which is neutral.

Spatial alliesthesia is generally more conventionally used than temporal alliesthesia due to the fact that spatial alliesthesia happens to occupants more often in real life scenarios. There is also an interaction between negative and positive alliesthesia. Negative is referred to incidents where the thermal state moves further away from the neutral point, and positive alliesthesia is coming closer to the neutral state. [29]

Thermoreceptors are unevenly distributed over the body and there are different weighting between cold and warm receptors. The cold receptors are more sensitive because they are located more superficial in the skin tissue. Cold receptors also send more impulses to the central nervous system, and humans are therefore more sensitive to the cold environment than warm environments [29, 32, 33].

Becoming aware of the thermal environment with variances in temperature or air flow is examined to have a positive effect. Traylor et al. ask the question if varying the temperature within the building could increase the human comfort [34]. This could also save energy as the temperature does not necessary have to be at a constant level. A possible solution is cold lobby spaces where occupant only moves through and do not stay for long periods. This will not only create awareness of the thermal environment as mentioned but also save energy since less space heating is needed.

Another solution is personalised heating and cooling by exploiting spatial alliesthesia. This solution is discussed by Deng et al. as well as by Brager et al. [4, 35]. This creates a non-uniform thermal

environment and aims to more personal control. Simultaneously, less monitoring of the overall thermal environment is needed and could save up to 10 % of the energy use per degree misalignment from the set-point temperature [35].

2.3 Parameters

Humans sensation of thermal comfort is decided upon several factors. Some are more important than others and these are presented in this chapter. What is interesting is that some of the parameters can have extreme values, but by balancing it up by adjusting or regulating one of the others, thermal comfort can still be achieved. Yet, extreme values that pass beyond what is possible to balance creates discomfort. This happens when one of the parameters passes a limit where the person or environment is no longer capable of balancing it.

There will be presented in a total of five factors. The first two are the clothing level and metabolic rate. These two can be described as personal parameters because the values of them are decided by the person itself. That also implies that these two factors can vary from person to person, even exposed to the same environment. The other three parameters presented are environmental factors. These are the conditions of the thermal environment and the ones discussed will be temperature, air movement and relative humidity.

Even though these are considered as some of the most important factors, there are also others that influence humans sense of the thermal environment. Age, gender and physical characteristics, called organic factors, also play a role but are not investigated further here. In addition to these, there are also cultural and psychological factors. Understanding that these factors cannot be overseen when considering thermal comfort is important to avoid misinterpretation of a field study. With so many variable factors, evaluating thermal comfort can be a complex process and knowing all the input parameters is critical for comparison between studies on the subject.

2.3.1 Clothing level

Clothing is an insulating layer protecting the body from the environment, and its function is to maintain a satisfying condition. Clothes cover most of the human body and leave only small skin parts exposed to the environment. The level of clothing should be based on the activity and the environment to keep a balance between heat loss and heat gain. This leaves a person with great control to balance clothing as the level of clothing can be decided personally and is, therefore, a behavioural adaptation. However, certain occasions require a dress code where this does not apply. Such events or workplaces can make us wear an undesirable amount of clothes that are not adapted to the thermal environment. [18]

Because calculating heat transmission through clothes is rather difficult and inaccurate, there was a necessity to find a more suitable parameter. Clothing is expressed by the unit *clo*. First proposed by Gagge and Winslow in 1941 [14]. For conveniences, *clo* uses its units from heat transmission and can, therefore, be further derived to $\text{m}^2\text{K}/\text{W}$, similar to the R-value for insulation in buildings. 1 *clo* has the average value of $0,155 \text{ m}^2\text{K}/\text{W}$ and is approximately the value to keep a person comfortable at 21°C [6]. To get this in a better perspective, the value of *clo* has been allocated to different clothing's, and a brief overview of this is given in figure 3. Each person in the figure represents a value of *clo*, given beneath each person.

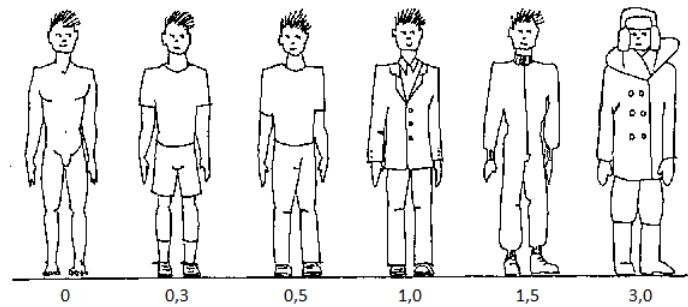


Figure 3: Values of clo for a different kind of clothing [36].

It is important to know that the area (m^2) for clo represents the body surface and not the area of clothes wore. The value of $0,155 m^2K/W$ represents an average value covering all the of the body. The unit *tog* is therefore sometimes used, which is the area of the material. The value of 1 tog is $0,1 m^2K/W$. It is created to avoid confusion since the unit clo is distributed evenly over the whole body. This can lead to a misunderstanding that 1 clo is a suitable amount of clothes wear. While a unbalanced distribution of the clothes across the body can leave some body parts exposed to uncomfortable thermal conditions.

The level of clo is important and can make a person comfortable in extreme conditions of both cold and heat. For some professions, clothing is an essential part, like firefighters or winter travellers. It is made for protection and to keep humans comfortable under such circumstances, but also in daily life. With the opportunity to wear several layers, a person can adapt to the thermal environment as desired. [37]

The heat transmission through the clothes happens through conduction, which was examined earlier in chapter 2.1 about heat transfer. The temperature gradient between all the layers is therefore important. Hence, the metabolic rate is a major participant of the skin surface temperature and plays an essential role in humans perception of comfort. During intensive work, there is a high metabolic rate, and the heat must be transferred away in order to keep thermal balance. With too much insulation in terms of clo, there will be an accumulation of heat on the skin surface and eventually lead to dissatisfaction with the thermal environment.

For colder environments, there is usually a desire to keep the heat produced by metabolic rate. If the clothing can not provide enough insulation, the cold environment will draw more heat away from the body than it can produce and will eventually lead to a sensation of being cold and uncomfortable. Clothing also protects us from other external influences like wind and rain. By wearing a wind protective layer, the convection heat loss will be reduced. The clothing also protects the skin from becoming wet and consequently prevent heat loss. It is also important to keep the clothes dry as wet fabrics have less thermal insulation than dry fabrics [37].

2.3.2 Metabolic rate

Metabolic rate can be described by the activity level of a person. The more physical work a person does, the higher the metabolic rate and hence, the more heat that person produces. As the body wants to keep its temperature close to $37\text{ }^\circ\text{C}$, with too much heat produced, it is desirable to also lose an equal amount of heat. In addition, heat production plays an important role in keeping the internal organs functioning at an optimal state. Metabolic heat production happens across the whole body, and the thermoregulatory system regulates how much is transferred to the skin. One example

of how this works is hypothermia. Where blood flow is reduced to avoid heat loss, and the sensation of cold hands or feet will appear. Shivering is another example where movement in muscles increases the metabolic rate to produce heat. [5, 6, 26]

The heat produced by the body is a product of creating adenosine triphosphate (ATP). A mechanism to provide energy to cells which again releases energy to do its function in the body. During these processes, heat becomes a product from converting the energy from food into necessary energy for the cell. Being full or hungry can, therefore, influence a person's thermal sensation. With increasing activity, there is a need for more energy and so will the heat production also increase. And if the production exceeds the amount of heat loss, heat will get stored in the body, and the person will eventually feel warmer than what is comfortable. [38]

The metabolic rate is measured by the unit *met* and is measured in W/m^2 . Joules, calories or kilocalories per unit time are also measurements that can be used. 1 met is equal to approximately $58 \text{ W}/\text{m}^2$ and is the metabolic rate for a seated person at rest [6, 36]. Note that this value assumes a man at 70 kg and $1,8 \text{ m}^2$ body surface area or a woman at 55 kg and $1,6 \text{ m}^2$ surface area [6]. This implies that a deviation from these physical properties can lead to a different metabolic rate when seated.

To predict a correct metabolic rate, there is a need to consider a person's physical characteristics and not just the activity level. Different size, weight, age, gender and level of fitness all play a role affecting the metabolic rate. It is therefore difficult to correctly estimate the metabolic rate just based on a personal activity level and more detailed derivation is necessary to predict it precisely. In general, the metabolic rate for the "average" person described earlier has the metabolic rates shown in figure 4. [39]

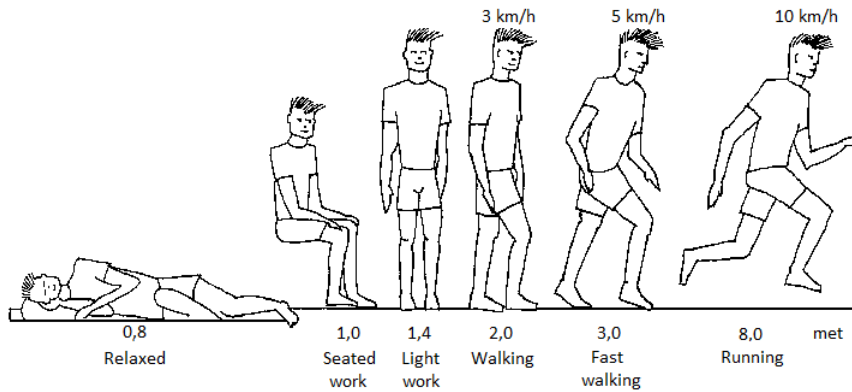


Figure 4: Metabolic rate for different activities [36].

More detailed the metabolic rate can be divided into four parts. The first one is basal metabolic rate, B_m , and can be described as the baseline metabolism to keep an organism alive. This means maintaining the body temperature and keep the cardiac and respiratory function. The second one is due to body posture, M_P (e.g. sitting, standing). The third one is due to the type of work, M_W , and the fourth one is due to whole-body movement, M_M . Adding these together equals metabolic rate as shown in equation 6. [6]

$$M = B_m + M_P + M_W + M_M \quad (6)$$

To put it in a better perspective, a change in metabolic rate from 0,9 to 1,5 met can result in 3,2 °C variance in thermally neutral temperature or around 1,5 unit on the PMV scale [40]. This implies a variation in activity levels between persons, requires different thermal environment to satisfying indoor climate for each person. An example is retirement homes, where the elderly persons in need of nursing have very low basal metabolism and activity level comparing to the nurses who work there. Different clothing is therefore needed to achieve thermal comfort for both groups. [18]

By continually changing body position, the metabolic rate varies greatly. Lou et al. highlight the variation in metabolic rate for different activities at the office [40]. Concluding that metabolic rate is the most problematic parameter to predict accurately and better tools than what exists today are necessary in order to do so. Even at the office, predicting metabolic rate can be difficult to estimate for persons doing the same task. Some persons can be sitting quietly and doing deep work in front of a computer for long periods. Others tend to move around more, go from sitting to standing and generally have more whole-body movement. This results in various metabolic rates and leads to abnormal results during a simulation. More exact tracking of movement will lead to more accurate evaluations.

There is also a question on how the activity level and the thermal environment affect each other. In some cases, if a person is set to do a job, that person will work on that task regardless of the thermal environment. Examples are persons doing tasks which requires being at the same spot and does minimal movement. The possibility of changing the activity level is limited. An unfit thermal environment in regard to the activity will, therefore, leave that person dissatisfied. In other cases, where there are tasks that require hard physical work. The degree of how much a person can do, will be dependent on the thermal environment if that person can adjust the activity level. Under unpleasant warm conditions, the person will slow down the activity level, and hence, also the work productivity will decrease.

2.3.3 Temperature

Temperature is the most important physical parameter there is because heat flow is determined by temperature differences. If heat energy is lost from a body, the body's temperature will fall. If heat energy flows into the body, the body's temperature will rise. According to the second law of thermodynamics, there will be a net energy flow from one object or surface with higher temperature to an object or surface with a lower temperature [8].

In order to keep the core temperature of the body around 37 °C, the surrounding temperature must fit into the equation of heat balance to maintain comfort. The human body is very sensible to this particular temperature, and a deviation from this temperature with a few degrees can be very harmful to the human body. The driving forces for heat flow can be through fluid, solid or gas. As the human body always is in contact with air, the temperature of the air is important for the body's heat transfer. [6]

Temperature can also be divided further into two separate parameters; air temperature and radiant temperature. A combination of these two gives what is called the operative temperature. This parameter is what is normally used in thermal comfort models and can be calculated by taking the average of the air and radiant temperature as shown in equation 7.

$$T_{op} = \frac{T_r + T_a}{2} \quad (7)$$

This equation, however, only applies when air speed is below 0,1 m/s. As the airspeed increases, the operative temperature will emphasise air temperature at a greater extent. In the next chapter, there will be presented more details around air movement and how it affects thermal comfort.

By definition, the air temperature is the temperature of the air surrounding the body. It is the dry-bulb temperature, which means that radiation or moisture in the air does not affect what is read on the thermostat. Measuring the air temperature also has its weaknesses because it will vary across a given room. For a representative value, the measurement must be as close to the experiment's subject as possible. [6]

Radiant temperature can again be divided into two categories; mean radiant temperature and plane radiant temperature. Mean radiant temperature is defined as 'the temperature of a uniform enclosure with which a small black sphere at the test point would have the same radiation exchange as it does with the real environment' [6]. Plane radiant temperature is in ISO 7726 defined as 'the uniform temperature of an enclosure where the radiance on one side of the small plane element is the same as in the non-uniform, actual environment [41].

This means that the surface area which is exposed to the other body matters. Imagine the body was shaped like a cube. Then the body top and bottom would have a smaller area exposed compared to the back and front. If all the six faces of the cube are known, equation 8 in ISO 7726 can be utilised to estimate the mean radiant temperature for a standing person [41].

$$t_r = \frac{0,08(t_{pr1} + t_{pr2}) + 0,23(t_{pr3} + t_{pr4}) + 0,35(t_{pr5} + t_{pr6})}{2(0,08 + 0,23 + 0,35)} \quad (8)$$

In general, the radiant temperature is about how much heat the human body emits or absorb towards other objects or surfaces through radiation. Radiant temperature is, however, not affected by the air temperature. For cold surfaces, e.g. a window, the body emits heat in form of radiation, and likewise, for warm surfaces, e.g. the sun or ovens, the body will absorb the heat from those sources. Many people are not aware of this, but radiation temperature has a by small portion a bigger impact on humans sensation of thermal comfort than the air temperature. Radiant temperature can also vary by a large magnitude.

2.3.4 Air movement

The air movement across the room is the most fluctuating parameter of those to be mentioned here. Movement in the air can come from the ventilation system where the air comes into a room through a fan or a resembling installation. Movement can be caused by wind through an opened window. It can come from an adjacent room because of different air pressure, which leads to transfer of air and experienced as draught. Air movement can also come from an internal source like a fan or similar.

With air coming from one of these sources, the air will not be evenly divided through the room. With a good projected ventilation system, however, there is possible to have good control over the air movement in the occupant zones. For people nearby windows or close to a fan, they will naturally feel more draught than others in the same room. It is therefore essential to both know the mean air velocity and the standard deviation from the average air velocity. In order to achieve physical comfort in the occupant zone, it is beneficial to keep the source as far from the occupant zone as possible and at the same time maintain a minimum air velocity for comfort.

Air velocity is one of the parameters that are easily changeable. By opening a door or window, or change position in the room, a person can sense the effect of different air movement immediately. Either it is heat loss or heat gain, the heat transfer is approximately proportional to the square root of the air velocity [26]. It is important to notice that movement in the air can contribute to thermal comfort without variation in air temperature [42]. Several studies show that when the temperature in the room reaches exceeds approximately 26 °C, the importance of sufficient air movement increases exponentially with increasing temperature to maintain thermal comfort [30, 43, 44].

This is because flow of air increases the convective heat transfer from the body. It also promotes evaporation of sweat on the skin surface. The higher the speed of air close to the skin is, the thinner the boundary layer across the skin is. Hence, this will lower the thermal insulation and heat loss from skin increases. Since this works between two fluids, the direction of the air velocity also plays a role. Air velocity that directly hits the surface area at a 90° angle causes a higher convection heat transfer coefficient, and more heat is lost. [10]

Which value of air velocity that is optimal to achieve satisfying indoor environment has been discussed in several papers and seem to not agree with each other [5, 30, 42]. What is decisive which air velocity that provides thermal comfort, there must be a consideration of the air temperature. It is also important to know if the occupants in the room even want a cooler environment. With the correct and comfortable temperature, air velocity levels down to 0,2 m/s can be sufficient [5].

A study by Wang and Lian looked upon air velocities at 0,6 and 1,35 m/s at different temperatures [43]. As these air velocities are considered as relatively high values, the percentage of dissatisfied decreased with rising temperatures. At 28 °C, the subjects were more satisfied with an air velocity at 1,35 m/s, than 0,6 m/s. For lower temperatures, 0,6 m/s air velocity was the preferred choice. A study by Du et al. backs up these results where different air velocities were tested at temperatures between 28 °C and 34 °C [30]. What is more interesting, at 26 °C, the six subjects showed more discomfort with increasing air velocity. Based on these two studies, it could be fair to say that the tipping point between comfort and discomfort with relatively high air velocity is somewhere between 26-28 °C.

2.3.5 Relative humidity

The relative humidity is in percentages a measurement of the saturation of water vapour in the air. If it reaches 100 %, it means that the air can not hold anymore water. Relative humidity can also be described as the ratio between the measured water vapour pressure and the maximum containment of water vapour pressure held by the air at a known temperature [5]. Equation 9 shows this coherence.

$$\phi = \frac{P_a}{P_{sa}} \quad (9)$$

Relative humidity becomes important when a human body is sweating, and the sweat evaporates. Evaporation was explained more detailed in chapter 2.1 about heat transfer. Then heat goes from the body to the environment and sweating works as a cooling system for the body. How much heat that is transferred is determined by the difference in partial vapour pressure. The partial vapour pressure, P_a , is connected with temperature, T , as shown in equation 10. Absolute humidity, denoted as AH , is the amount of moisture the air can hold given in weight per volume. [6]

$$AH = 2,17 \frac{P_a}{T} \quad (10)$$

The amount of vapour the air can hold is dependent on temperature, as seen in the equation. Fick's first law of diffusion states that when the concentration is high, the mass transfer goes faster [45]. This was tested with molecules where two systems with different concentration of the molecules were interacting with each other. Fick's law was later further derived by Hancock to also apply for heat transfer [46].

The Norwegian Labour Inspection Authority recommends that the indoor relative humidity is somewhere between 20-60 % [47]. In wintertime, it is typically 15-25 % outside while in summer, it can typically reach levels between 50-90 % when considering Nordic climate [48]. Humans sense of the relative humidity is low and would therefore not feel these differences unless the values are in the outer part of the scale. Dry eyes and irritation can occur if relative humidity becomes beneath 20 % [3, 49]. Depending on the temperature, too high relative humidity can lead to the growth of mould inside the building and again lead to very expensive repairing costs. Mould can also lead to sickness among people who spend substantial time in the building. [49]

Too high relative humidity also affects the evaporation rate from the skin. This because of the partial vapour pressure differences as mentioned. The effect of this, however, only seems to occur when high relative humidity is measured along with a significantly high temperature. According to a study done by Zhu et al. which looked upon the correlation between thermal comfort and variate heart rate, thermal comfort decreased when relative humidity passed above 80 % in an environment with high indoor temperature [44].

Air with high relative humidity, together with high temperatures can become problematic for achieving comfort because sweat no longer evaporate. Then the body's cooling system does not work because the difference in partial vapour pressure becomes low and natural heat transfer decreases between body and environment. In warm climates, high humidity is claimed to have the same effect as rising the temperature by 1 °C [26].

2.4 Thermal comfort models

There will always be differences between a model and what it actually represents. If a model gives the altogether picture or not, becomes a question of whether the lack of thoroughgoing is significant in terms of the application of the model. Generally, a model should give a describing sensation and give an indicator of how satisfied an occupant is with the thermal indoor environment.

Achieving thermal comfort is one of the most important objectives of HVAC systems and has wide exposition, including both physiological and psychological aspects. As thermal pleasure is mainly decided by a person's heat balance, there are two main groups of factors that need to be considered. First one is personal parameters like clothing insulation and metabolic heat rate. The other one is ambient parameters, such as air temperature, air velocity and relative humidity [5].

From the first model by Fanger, there has been presented several models trying to determine the thermal sensation mathematically. Both the European and ASHRAE standard is based on Fanger's model, which solves the heat balance equation between a person and the surroundings. In addition to Fanger's model, there is the adaptive comfort model. As some models are restricted to certain

climates, groups of people, etc., there was a need for models that could adapt to this and therefore give more precise results.

2.4.1 Fanger's model

The Predicted Mean Vote (PMV) model was developed by Fanger in the late 1960s. It combines the four physical variables and the two personal variables to measure the perception of occupants in a certain thermal condition inside a building. PMV is an index using a psychophysics 7-point scale, as shown below.

-3	Cold
-2	Cool
-1	Slightly cool
0	Neutral
+1	Slightly warm
+2	Warm
+3	Hot

Fanger related PMV to the difference between the actual heat flow from the body and the heat flow required for comfort specified by the metabolic rate, M , and the thermal load, L . By a test of a vast amount of subjects, it was created an equation to calculate how the subjects would rate their thermal sensation based on metabolic rate and thermal load.

$$PMV = [0,303e^{-0,036M} + 0,028] * L \quad (11)$$

The thermal load is defined by Fanger as 'the difference between the internal heat production and the heat loss to the actual environment for a man hypothetically kept at the comfort values of the mean skin temperature and the sweat secretion at the actual activity level' [50]. A resembling notation is 'S' (heat storage) in equation 5, described more detailed in chapter 2.2. In the comfortable environment, the thermal load would be zero. For any value unlike zero, the thermal sensation is a function of metabolic rate and thermal load.

Derived from PMV, there is possible to calculate the Predicted Percentage Dissatisfied (PPD) and gives information about the number of potential occupants that is dissatisfied with the thermal environment. Based on PMV, PPD can be calculated by equation 12.

$$PPD = 100 - 95e^{-0,03353PMV^4 - 0,2179PMV^2} \quad (12)$$

As PMV diverges further away from zero, PPD increases, as shown in figure 5. Since thermal load expresses the balance in the thermoregulatory system and is related to PMV, the PMV model can be called the heat balance model. According to Fanger, there are also two other conditions besides heat balance that influences the whole-body thermal comfort. The sweat rate and mean skin temperature also needs to be within certain limits and no local discomforts must be present, like draughts or temperature gradients [18, 50].

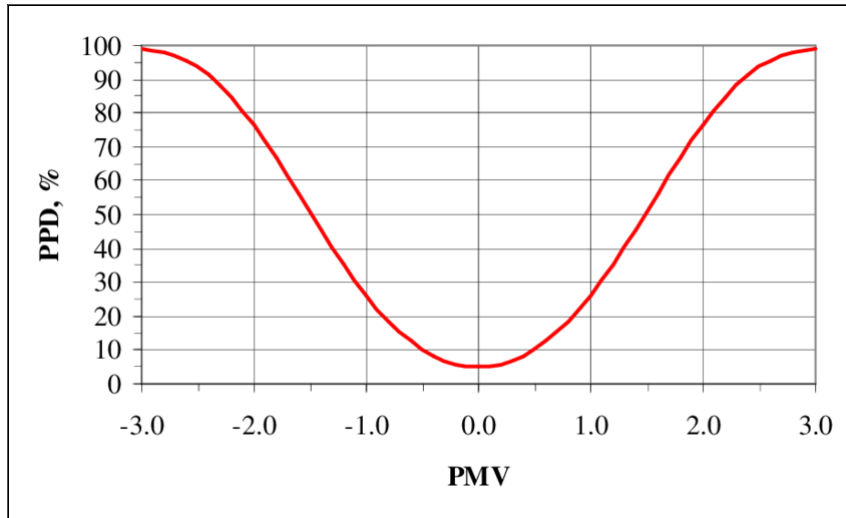


Figure 5: Predicted percentage dissatisfied (PPD) as a function of the predicted mean vote (PMV) [51].

NS-EN ISO 7730:2005 states that the index should be only used when the PMV is between -2 and +2 [16]. The standard also suggests that the six parameters and air pressure are between certain intervals. These are given in table 1.

Table 1: Advised limits for the parameters given in NS-EN ISO 7730:2005 [16].

Parameter	Unit
Metabolic rate	46 - 232 W/m ² (0,8 - 4 met)
Clothing	0 - 0,310 m ² K/W (0 - 2 clo)
Air temperature	10 - 30 °C
Mean radiant temperature	10 - 40 °C
Air velocity	0 - 1 m/s
Air pressure	0 - 2700 Pa

It is nearly impossible to create a thermal environment that satisfies every occupant as they have individual differences. This is also illustrated in figure 5 where the predicted mean vote is 0, or neutral still engenders some dissatisfied occupants at some degree. The indices PMV and PPD can also be divided into categories, as shown in table 2.

Table 2: Categories of a thermal environment based on PMV and PPD [16].

Category	PPD %	PMV
A	< 6	- 0,2 < PMV < 0,2
B	< 10	- 0,5 < PMV < 0,5
C	< 15	- 0,7 < PMV < 0,7

Furthermore, NS-EN ISO 7730:2005 also states that the PMV index is derived for steady-state conditions, but can still be applied if the variables exceed the limits. For different metabolic rates, a time-weighted average over one hour should be used.

2.4.2 The adaptive model

The adaptive approach to thermal comfort has seen increased interest and status in recent years. It derives from several field studies from all around the world and been presented in both the ASHRAE standard and the European standard EN 15251 along with other national standards. It has the purpose to analyse the real acceptability of the thermal environment depending on the context, occupants behaviour and their expectations. The theoretical background of the adaptive model has been around for years, undergoing a long development process and has become more reliable in different climates with increased research. [52]

The model objective is that thermal comfort temperature is a function of the outdoor temperature, using the monthly mean outdoor temperature as a reference, as shown in figure 6. Since the adaptive model is based on field measurements, field votes already account for both general and local discomfort since people are an integrated part. The adaptive model does, to a certain degree, ignore the four ambient and the two personal parameters because they can be related to the outdoor temperature. It turns out that some of the parameters are sufficiently accounted for in the underlying model. [52–54]

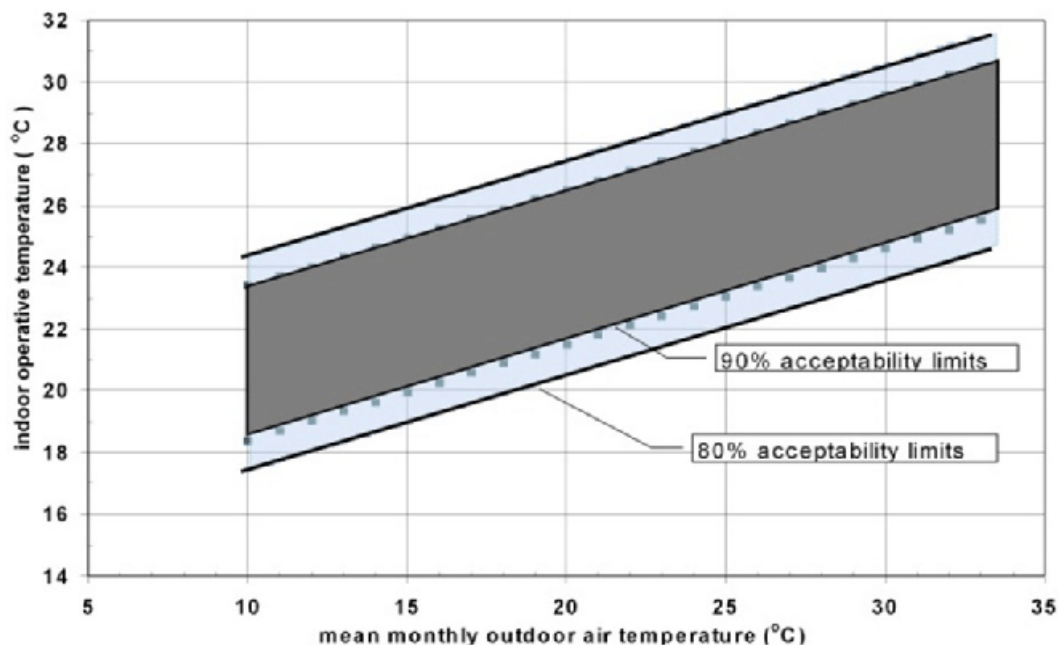


Figure 6: Adaptive model chart showing acceptable indoor operative temperature as a function of mean monthly outdoor air temperature [55].

The adaptive model has three different approaches or categories, which are physiological adaption, psychological adaption and behavioural adjustments. All these are a consequence of each individual subjective sensation of the thermal environment. The adaptations also change as a cause of the climate the occupants stay in, hence the outdoor temperature as the main function of the model. People in warmer climates can tolerate and even prefer higher indoor temperatures than people living in colder climate zones, according to Hensen and van Hoof [53]. Which is opposite to the assumptions in Fanger’s model. [17, 18, 52, 54]

This brings in the behaviour adjustment or adaption, but also strongly related to behaviour expectations. Occupants in naturally ventilated buildings tend to be more active in thermoregulatory adaption through changes in activity level or clothing. While occupants in air-conditioned buildings have higher expectations and adapt to a narrower range of comfort temperature [53]. Yau and Chew

divide behaviour adjustment into three classes: personal adjustment, which involves a change of activity, posture, clothing's etc. Technological adjustments which include modifying the environment or surroundings by opening or closing windows or adjust the air-conditioning. Cultural adjustments which could, for example, involve taking more breaks in the shadow because of the hot weather [18].

The physiological adaptation is basically about genetic adaptation and acclimatisation. The body using different processes like sweating, shivering, vasoconstriction and vasodilatation in order to try to keep the body temperature at a balanced level. This is a change in a person's thermoregulatory system and is a response to acclimatise to the surroundings. When the physiological effort is at the minimum, body temperature is within certain ranges, and skin moisture is low, then there is a sense of thermal comfort. The genetic adaptation involves the heritage of a person and can be evolved over a long period, even before that person's life begun [18, 56].

The psychological adaptation is the principal explanation of how occupants can have different tolerations even within the same indoor environment. Psychological adaptations cannot be measured but describe the feeling of thermal perception based on past experiences. A static thermal heat balance model, like Fanger's, is not able to account for psychological effects as the relation between thermal sensation, and the psychological strain is fixed. This sensitivity will decrease if exposed to a certain climate over longer periods. Due to psychological factors, adaptation to the thermal environment occurs because of the occupant's condition of mind. [18]

2.5 Behaviour energy impacts

Energy consumption is an essential element as every technology development needs to be economically sustainable or at least evaluated against the benefits it provides. Occupant behaviour inside a building has an impact on energy consumption and therefore spreading consequences on the building's operating costs and CO₂-emissions as primary direct impacts. Several other factors, directly or indirectly, is moreover influenced as a cause of human behaviour inside a building. Occupant interactions and behaviour patterns were first to be studied in the early 1950s. [57]

Over the years, such relevant topics were discussed separately by engineers, architects and indoor health specialist. It has now come to the point that comfort and energy requires a compiled approach and must be processed accordingly. Reaching thermal comfort requires a good building design and conditioning of spaces, like heating, cooling and ventilation. This needs to be achieved without the expense of energy use. On the other side, saving energy is pointless if the performance of the building is not sufficient to provide a comfortable indoor environment. [27]

An energy efficient building that does not provide good working conditions will either positively affect well-being or productivity. This could drive the occupants to take action that may compromise the energy economy of the building. However, allowing the temperature floating over a broader range in zones, where this could be accepted, could save large amounts of energy. If the operating temperature is within the range of 22-24 degrees. It is possible to reduce the annual HVAC energy consumption by 10 % per degree expansion in either direction [4]. [3, 58]

There is a need for an optimum between energy efficiency and comfort with respect for the building's sustainability and profitability. Suggestions by Brager et al. is to increase feedback from the system status and energy use [4]. This way, the occupants become aware of the influence they have on the building's energy consumption. Gaining more insight by understanding how the system works and how this affects the energy performance is important to come across this. [3]

2.5.1 Predicted versus real energy use

Occupants behaviour is the most variable factor there is when it comes to the building's energy use. According to Tam et al., occupant behaviour accounts for 64 % of the differences between real and predicted energy use [57]. The remaining is divided between an operation of the HVAC system schedule, which accounts for 24 %. And the last 12 % is divided between equipment inefficiencies, conductive heat loss and discrepancy in minimum outdoor-air rates. Therefore, understanding and accurately modelling behaviour play a crucial role to reduce this gap between predicted and actual energy use and optimising energy efficiency. [59–61]

Behaviour inside a building is a complex thing. Aspects like lifestyle, demography, economy, interaction with building features and equipment affect the occupant's perception of comfort and consequently, the behaviour and energy use [57]. Figure 7 shows a chart of influential factors that affect occupant behaviour. Belafi et al. state that one of the most effective ways to predict and understand human behaviour is through a cross-sectional questionnaire survey tool or a software tool where behaviour is a profound input in *Building Information Models* (BIMs) [59]. This will gain more insight into patterns and drivers for behaviour. It also helps to find connections between human, social and local comfort parameters. Bridging the gap for the future can only be achieved by fully understand how humans react and respond to the condition they are in.

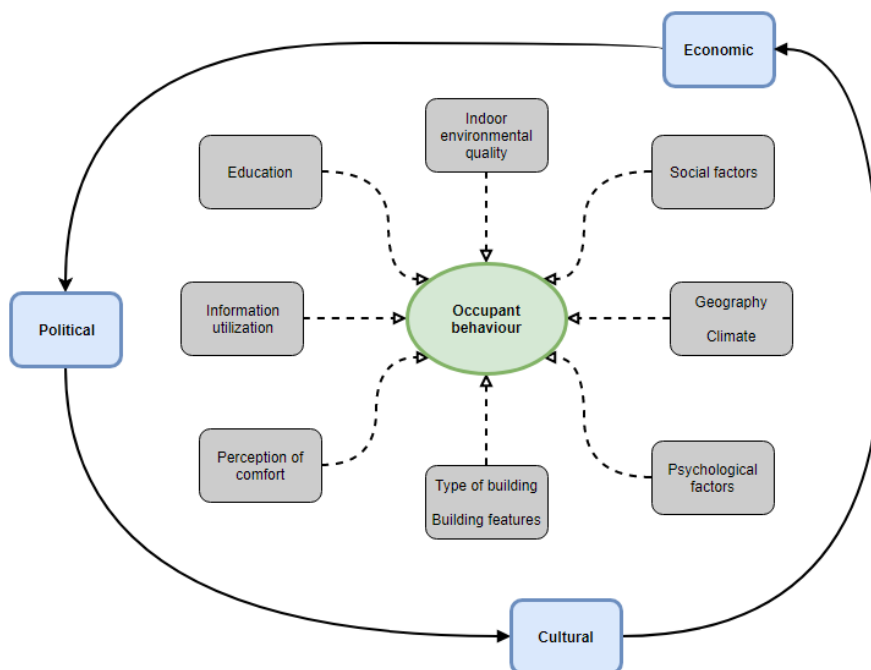


Figure 7: Influential factors (grey) that are directly connected to occupant behaviour. In addition, there are also external influential factors (blue) like political, economic and cultural factors.

Belafi et al. mention three reasons which cause the gap between predicted and actual energy use [59]. The first is oversimplified or disregarded occupant behaviours throughout the building process. The second thing is the lack of common agreement on the validity and applicability of occupant behaviour modelling and simulation approaches. The third one is unclear human-centred interdisciplinary solutions. With the introduction of Smart meter, the step towards surveillance of behaviour becomes easier and could, therefore, be a measure to decrease this gap [59].

With greater complexity of the building, the number of elements to control can be extensive [57]. Researches also agree that with more control, occupant satisfaction increases when able to interact with the building systems. This, however, does not lead to reduced energy use. A study by Nicol shows that highly controlled indoor environments are linked to high energy use [26]. Occupants tend to rather select thermal comfort than energy efficiency and the two outcomes become non-reconcilable. With better instructions on how to use the equipment, this gap could be reduced as the occupants gain knowledge and hence, know the consequences of their actions.

There are owners, design professionals, operation staff and occupants whom all can control different measures to improve the indoor environment. More automation can improve to be more efficient in terms of energy use. This will, however, be at the expense of occupant satisfaction as occupants tend to be more comfortable when they can interact with the system themselves instead of having an automated control system. [57]

Personalised conditions are a possible solution to this, where a non-uniform thermal environment is acceptable and can occur. If occupants tend to be on the same spot over a long period, the occupants have the opportunity to set the temperature, lighting and other parameters by themselves. Since the larger zones then no longer need complete heating or cooling this could also help saving energy. Then the principle of alliesthesia also could be applied in order to increase thermal comfort. [34, 35]

3 Tools and instruments

To conduct a complete study of the thermal environment and occupant behavior, there is necessary to utilise various tools and instruments. How they are applied are described in the methodology, and this chapter will only provide background information about their engagement. It will be described what function each of them has in this study along with other features they can render.

3.1 Test chamber

Examination of this experiment is going to take place in the indoor environmental laboratory at the Norwegian University of Science and Technology (NTNU) Gløshaugen and has the coordinates of 63°25'10"N 10°24'9"Ø. This implies a rather cold outdoor climate compared to the rest of the world. The inside laboratory is on the first floor and has no walls to the exterior, but is surrounded mainly by offices and hallways.

In this laboratory, there is a full-scale climate chamber where the experiment and the measurements will proceed. The laboratory contains several test rigs and provides the opportunity to carry out experimental studies within energy efficiency, energy supply, thermal comfort, and indoor environmental quality. The climate chamber was developed by the Department of Energy and Process Engineering (EPT) by Prof. Hans Martin Mathisen, Associated Prof. Natasa Nord and Prof. Guangyu Cao [62].

The climate chamber is 3,65 m long, 2,75 m wide and 2,70 m high and has been used for different indoor environment related experiments. This includes testing ventilation equipment, like supply air terminal devices, and room heating device with supply air flow up to 2000 m³/h. The climate chamber is also used to run tests of air quality and thermal comfort. The room will contain a simple layout that should portray an office with a desk, a chair and a computer. A ventilation pipe will also be attached to the chamber's ceiling to provide fresh air. There will be one person present during the experiment that is practising conventional office work during a certain time span.

3.2 SolidWorks

SolidWorks is a computer-aided design (CAD) and computer-aided engineering (CAE) software program created by Dassault Systèmes [63]. CAD software is used to create, modify, analyse and optimise any design to improve quality, document a product, or to create a database for manufacturing. While CAE is used to analyse CAD geometry by testing the performance of the components or assemblies. It provides the user with information about the design and can help with decision-making in the engineering sector.

Evident by the name, SolidWorks is a solid modelling application to create a 3D model as a part or in an assembly containing several parts put together. The software utilises a parametric feature-based approach and has users in multiple industries. SolidWorks has an integrated simulation tool to evaluate design or materials before actually creating the physical concept.

SolidWorks lets the user create a 2D sketch with certain parameters to decide relations to make a particular shape or geometry of the model. The sketch consists of lines, curves or marks and dimensions are created to define size. The parts, or sections of parts, can interact with each other if certain parameters are changed. The parts or features can have fixed relations to each other,

or change accordingly to an external adjustment. Such relations can be tangency, parallelism or concentricity. Then the sketch can be extruded to make it a complete 3D model.

3.3 ANSYS

ANSYS is a software used to simulate interactions of all disciplines of physics and structure, fluid dynamics, heat transfer, vibration and electromagnetism. CAD data can be imported into ANSYS, but also enables to build a design on its own. Using the variety of graphical tools lets the user visualise the result of the simulation to see how the model works in real-life conditions. [64, 65]

ANSYS uses the finite element method to numeric generate an analytic solution to the studied subject. Comprehensive and complex problems are divided into smaller, simpler parts which are called finite elements. Space- and time-dependent problems are usually expressed in terms of partial differential equations which numerical model equations approximately can give a solution to. Numerical model equations are in turn an approximation of the real solution to the partial differential equation. The finite element method can, therefore, be said to turn all designed approximations and convert it into an estimate of how a real-life scenario would look like. [66]

The software uses the ANSYS Workbench as a platform which integrates these simulation technologies and the parametric CAD systems. Physical properties can be put into each part of the assembly to determine weak spots or foreseeing any other physical problems in a virtual environment. Temperature distribution or fluid movements can then be analysed graphical or numerical [65].

3.4 MATLAB

MATLAB is a programming platform for technical computing made for people in sectors like engineering, science and economy and is developed by MathWorks. The software integrates several user applications into one environment where problems and solutions are expressed by mathematical notations. These applications mainly include:

- Math and computation
- Algorithm and application development
- Modelling, simulation and prototyping
- Data analysis, exploration, visualisation and graphics

MATLAB uses matrices and vector formulations that can be inputted in a script and allows the user to solve many technical computing problems. This is mainly done with flow statements, functions, data structures and inputs/outputs to quickly reach a solution to the problem that is required to solve. MATLAB also contains toolboxes, allowing the user also to use symbolic computing and give application-specific solutions. These toolboxes give the user an introduction to a specific subject so that the user can learn and apply specific technology. [67, 68]

The MATLAB system can be said to consist of five parts. First one is the MATLAB language. This is the matrix/array language, allowing the user to create small or large and complex computational application programs. The second one is the MATLAB working environment, which is the set of tools and facilities to manage variables and constants in the workspace. Developing, managing, debugging and profiling MATLAB files and to import and export data. The third one is handling graphics in two- or three dimensions, including data visualisation, presentation or animation. Fourth is the MATLAB mathematical function library with numbers of computational algorithms with functions

from the elementary *sum* or *sine* function to the more advanced functions in the software. The fifth one is the MATLAB Application Program Interface (API); this allows the user to interact with other programs. Translating into its language, programs like C, Fortran, Python etc. can be linked up with MATLAB. [68]

3.5 Microsoft Kinect

To register occupant behaviour, the Microsoft Kinect instrument was used to collect information about movement made by the person inside the climate chamber. It is made popular with the growing video game industry but has several areas of applicability in other industries which is beneficial to science. For this study where occupant behaviour is of particular interest, such a device can precisely provide information about every activity detail that otherwise could be overlooked.

Microsoft Kinect tracks segments of the skeleton using the joint location at specific parts which are to be examined. Figure 8 is an example of how these joint location can be placed, based on Dziejczak et al. work with monitoring indoor occupant behaviour [69]. Evenly placed across the body and upon limbs that represents the utmost parts of the body. Kinect uses an infrared projector and a camera to give depth perception by measuring the time emitted infrared light takes to reflect from the object it encounters. Kinect can also figure out the room's layout and adjust if something is rearranged differently. [70]

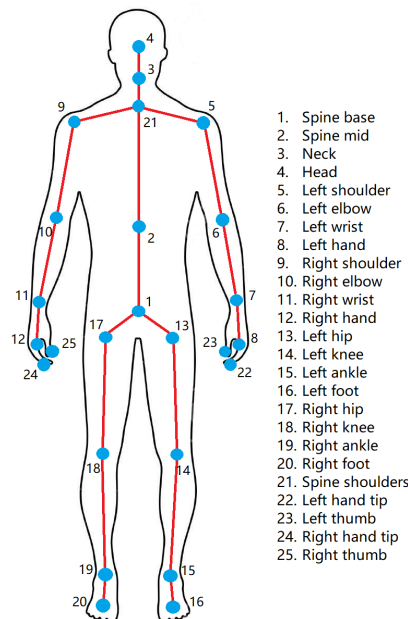


Figure 8: Tracked skeleton using Kinect for 25 different joint locations [71].

The skeleton model, which represents the occupant, is connected through links between each limb made sensible to make movement between links human-like. Information about body position then comes through the position of joint locations. It implies that spine locations are easier for the Kinect to detect compared to the location points at hand, which is tightly situated. The Kinect has a bounded observation radius around 5 m, which will be sufficient to cover the area of the chamber the experiment will take place. The device can record up to six people at once and collect data from all of them in a separate way. [69]

3.6 Supplementary

Devices mentioned in this chapter did not play any significant role, but they still are valuable for carrying out the experiment. Meaning they are not crucial and could be replaced by any other device that could do the same job. A description of their ranges, features etc. are presented in this chapter.

TSI VelociCalc 8388-M-GB is an anemometer that is used to measure the velocity of air in the range between 0,15 - 50 m/s. The significant figures decrease with increasing velocity. It can also measure temperature, relative humidity and static pressure, to name a few. The device read every 1 second but can extend the time constant up to twenty seconds. Then it displays the average last twenty seconds. The device itself is connected to a telescoping probe that can be extended, as shown in figure 9. It is at the tip of this rod the probe read results from. The tip has protection on the sides, which means it can only measure in one direction. The calibration data of this device is shown in appendix A.



Figure 9: TSI VelociCalc 8388-M-GB



Figure 10: TSI Transducer 8475-300

TSI Transducer 8475-300 is a device which exclusively measures air velocity with low values. The device can measure with a precision down to 10^{-3} m/s. It reads continuously the value of air velocity, then which is displayed momentarily. The display and the measuring point is separated from each other, as seen in figure 10. The cable is approximately 2 m long, and the person reading the measures would not interrupt results. The probe tip has a 360° angle for omnidirectional reading.

DPM TT 470 S is a micromanometer is a device that works with the principles of the manometer to continuously measure differential pressure [72]. With micromanometer, the capillary effects and reading errors are kept to a minimum. The device can measure pressure differences down to a precision of 10^{-1} Pascal. On top of the device, there are two inlets that can measure the difference between two locations as seen in figure 11. It is done by connecting each inlet to the topical locations, using tubes as extensions. The pressure difference can then be read on the display.

CKS 355 is a radial, axial fan that provides the chamber with air through a duct. It has a maximum capacity of $3082 \text{ m}^3/\text{h}$, or $0,71 \text{ kg/s}$ if calculating further, assuming an air temperature of 20°C . The fan has an input power of 353 W and can switch between five gears to increase rotation speed in which can reach 1380 rpm . [73]

Siemens 2ND4 103 is a radiator that generates heat into the chamber. It is a small-sized oven that is meant for minor rooms and stands at the floor. It has an integrated adjustable fan for faster distribution and a maximum effect of 2000 W divided by four notches. [74]



Figure 11: DPM TT 470 S

4 Methodology

With a basis in the software and other tools presented, it will now be explained how they are applied. The procedure of how the work is conducted will be given in this chapter, framed as a step-by-step process and covers and describes it from start to finish. Each step is passively discussed, and a thorough review of the method will be endured later in the discussion. As the steps in this process include several features, a brief theory introduction will be presented along with how they were applied. The methodology is primarily divided into three main parts and some intersecting chapters to fulfil these. The three principal sections are the construction of the model, simulating the model and executing a real-life scenario.

Construction of the model is basically drawing, put the experiment up and prepare it for simulation. This is precision work and should put a fundamental base to continue the further process. The software chosen to carry this out was SolidWorks. ANSYS is also a part of the construction, but the application of the two software programs was different. All the settings, features etc. are described in this chapter in order to replicate the work.

After the construction has rendered a complete model, it is ready to be simulated in ANSYS. The simulations should give the basis for analyses of scenarios that are later to be examined. This allows the user to go deeply into the CFD analysis and investigate the details inside. Description of the different and most important settings are also included. Since ANSYS is a very complex and profound program, steps are done carefully and tried validated against real-life scenarios.

When the simulation of the model is completed and results become reasonable, they can be used in correlation with the scenarios executed in the indoor environmental laboratory at NTNU Gløshaugen. The procedure of how this will be executed will be described. With each scenario, there is an evaluation of the thermal environment and other internal and external factors. How this evaluation will be performed along with a detailed description of the parameters will be presented.

4.1 Construction and set up in SolidWorks

Any other CAD program could also be used, but SolidWorks was the preferred option. Mostly because it is user-friendly and the basics could easily be self-taught. Every part in SolidWorks was created by making a 2D sketch of the geometry and then extruded into a 3D-model. By the use of other features, there was possible to make bends, cut holes etc. All available tools in SolidWorks make it attainable to recreate any component with high accuracy.

Measuring up chamber and parts

The chamber, in which the experiment took place, was measured to create a duplicated version in SolidWorks. The chamber makes an enclosed space, yet, with small openings to let air flow out. The chamber appoints the boundary of flow and is more or less the shell of the experiment. It measures 3,66 m long, 2,75 m wide and 2,70 m from the floor to the highest point, as seen in figure 12. The air outlets of the chamber measures 0,23 m wide and 0,10 m high. These holes are close to the floor and decisive for how air behaves in the lower part of the room as air will seek to desert the room because of pressure differences. These outlets are placed two by two on each of the four walls, making a total of eight outlets. All other detailing characteristics were left out in the drawing.

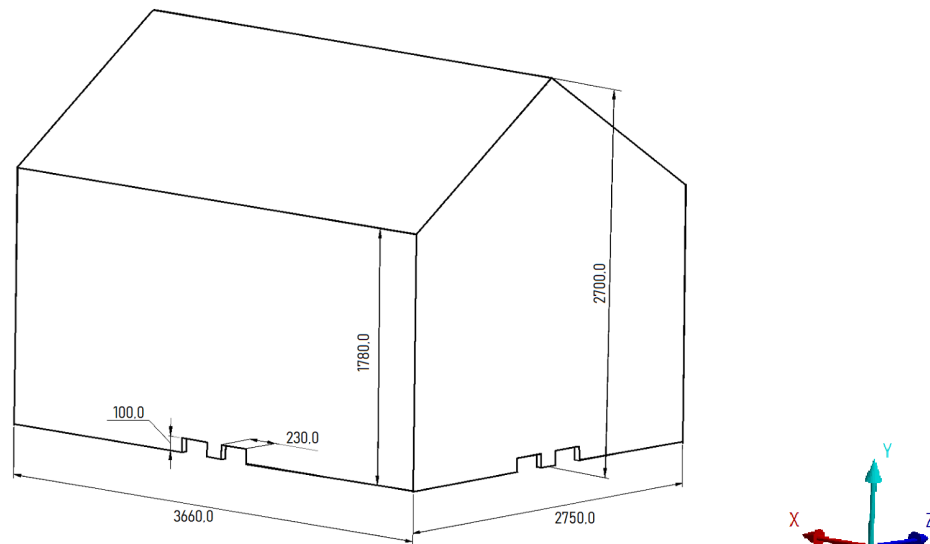


Figure 12: Three-dimensional drawing of the chamber measured in millimetres. The holes located at floor level are occurring on all four walls.

The most significant detail that was ignored was the door to enter the chamber. It was located in the middle of the facing short-sided wall seen in figure 12. Leaving this detail out was done with the assumption it would not affect the result in such extent that it would interrupt any measurements of parameters. Leaving such details out will be discussed later in chapter 6. The person that will be present during the experiment was located on the opposite side from the door to minimize possible disturbance of air around the person the door could create. Based on this, it was evaluated that this detail was insignificant enough to leave out of the drawing.

The accuracy of measuring the chamber was done down to the closest centimetre, and every detail below this was neglected. Mouldings, edges and screws were some of the details that were ignored. Both because it would be too comprehensive work and because it is unlikely such details would impact the results to a great extent. It would also simplify the process of doing the mesh later on. After all, the measurements of the chamber were done, the geometrical model was ready to be re-created in SolidWorks.

All other furniture or installations would also be measured next to be re-produced in SolidWorks. Drawings of these are shown in appendix B1-B4. These were of such size that they would likely impact the behaviour of air. Or, influence the air properties in such a way that it could not be ignored. Inside the chamber, there is a table, a laptop to work on, a chair and most importantly, a pipe which supplies the chamber with air. The inside chamber looks more or less like a simplified office cell with minimized furnishing. A view of how the chamber model looks on the inside can be seen in figure 13.

Air flow is intricate, and with furniture of such magnitude and impact, it should be included in such an assembly. These can not be ignored as the table and chair will block air flow and influence the distribution. The laptop creates heat through radiation. The pipe is decisive for the airflow because this is where the inlet of air is. When all these elements were created, they were put together in an assembly with correct positioning similar to how the experiment would look like.

Because air flow can be complex and can behave unexpectedly, a minimum of adequate details was necessary. Then it becomes more likely to achieve a lifelike scenario when simulating it in a software

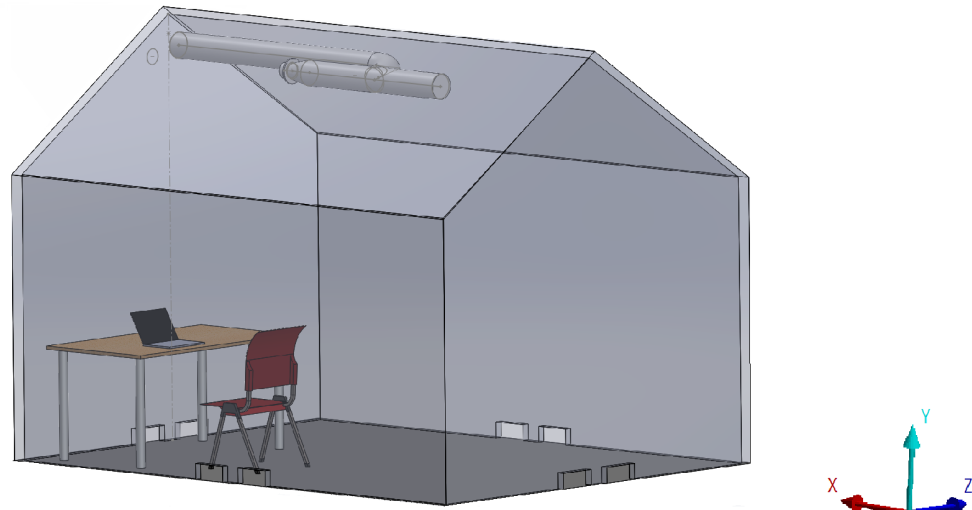


Figure 13: Transparent view of the chamber with pipe, chair, table and PC.

program. For the purpose of this, only elements that could cause the largest errors were implemented. The smaller ones were neglected. In regard to the meshing, square geometries are preferred. Choice of mesh was early decided to be hex-dominant, meaning that squared details were beneficial to make a good mesh. Minimizing the number of curved lines and drawings was, therefore, to be compiled as feasible.

4.2 Align geometry in DesignModeler

Transferring the model from SolidWorks to ANSYS was done by creating an .IGS file. Done in regard to utilising ANSYS 19.2 Academic version. For other versions, other file types may be necessary or sufficient. This chapter will continue processing the model that was designed in SolidWorks.

Carrying out two different parts in the ANSYS software was chosen because distinctive approaches were advantageous for the result. The chamber as one part, with the containing table with PC and chair, and the pipe as another part. It was attempted to have a simulation model where the pipe also belonged to the chamber, without success. A reason for why the pipe became a separate part was because it is decisive for the air distribution and therefore becomes a very crucial component. Because of its impact on air, meshing of the pipe is crucial for the result and preferably done with different settings than the chamber. Using the same mesh method also rendered some issues with the mesh. Separating them are constructive for both parts since they have dissimilar bodywork.

The chamber can vaguely be looked as box-shaped with straight lines in the outer edges. It has a ridge and furniture inside which makes it more complex than a cube. The pipe, on the other hand, is shaped like a tube with a circular body and a bend in the middle of it. Because of this, the distribution and behaviour of air would be different when conducted through the pipe first. Results would be different if the air was initiated directly into the chamber in the simulation.

The two geometries from SolidWorks is to be reassessed in ANSYS. This is due to some expedient features which could not be executed in SolidWorks but could be done in DesignModeler. An integrated program in ANSYS to modify geometry. One of those is the *Boolean Operation*. This procedure can divide the geometry into several bodies, or, merge bodies together to create singular parts. By doing so, the geometry was divided into singular zones that later could create a finer

mesh. This will be explained more detailed later in this chapter. Three cuts are made in the X-, and Y-direction and two cuts were made in the Z-direction, making it a total of 48 zones as seen in figure 14. This makes the chamber divided into several geometric shapes split into $3 \times 4 \times 4$, read in the order of X, Y, Z.

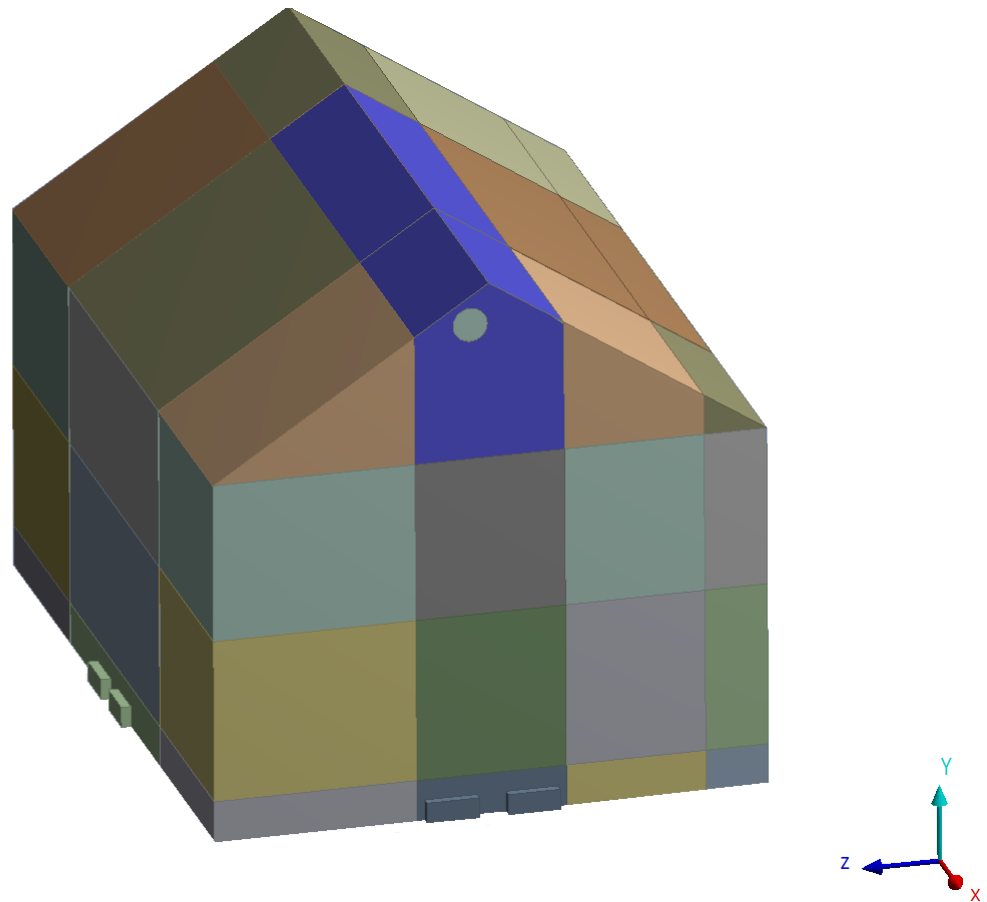


Figure 14: Display of how the chamber was cut into 48 zones with the use of a Cartesian coordinate system. Each zone is defined by different colours and separated by lines.

All zones were done with respect to what was containing and the necessity of fine mesh. The lowest horizontal separation of zones is done with regard to the outlet of air flow. The outlets can easily be observed as small pier boxes at floor level. They appear so in figure 14 because the walls are removed and only pictures air. Air movement in the chamber is driven by pressure differences as there is no external force to draw air out of the chamber. Therefore, the outlets required a finer mesh as it is decisive for the behaviour of air. Appointing outlets to be pressure-driven was applied in Fluent.

A better mesh was also easier to achieve with square boxes. The highest horizontal separation, from where the roof starts, would assure this in a larger extent. Leaving the three lowest levels of zones in Y-direction to be completely cubic. Then, the highest level ($Y=4$, in the Cartesian coordinate system) was left to be prisms in shapes of triangular, quadrilateral and pentagonal.

Also, furniture and installations should have restricted area to disturb as pure zones of air would create perfect mesh with respect to the settings. All other separations was thereby made to create as many of these zones as possible, leaving the other zones with chamber articles to have minimized volume. The vertical separations of the chamber are seen in figure 15, where the chamber is viewed from above. A complete list of all zones with coordinates and contents is shown in appendix C.

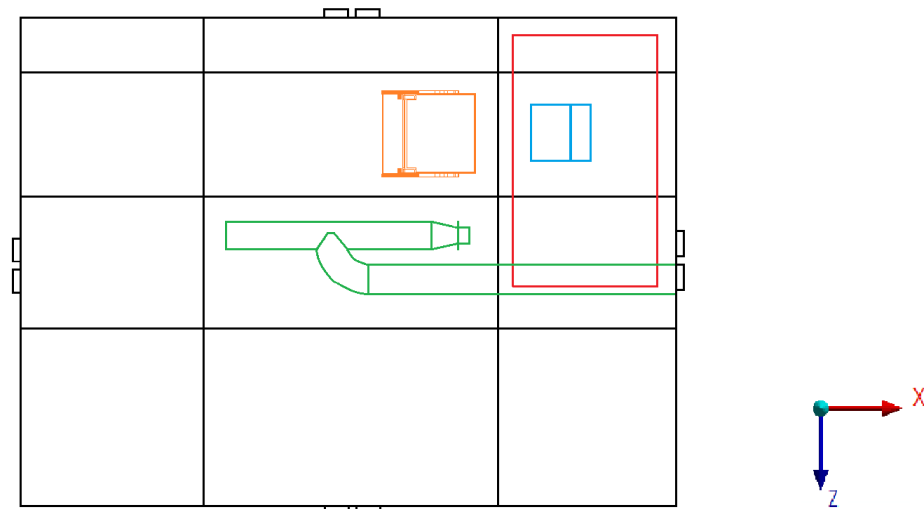


Figure 15: Section overview of zones and containing furniture article. The chair is coloured in orange, the table is red, PC is blue, and the pipe is drawn green.

Since there is air characterization that is interesting in this study, every solid object drawn in figure 15 must be cut out of the geometry. Then, the surfaces of the objects create boundaries for the air flow, the same way as a chamber wall. By using the *Frozen* function, the object is cut out of the zone and leaves the zone as expedient material containing only air. An example is shown in figure 16, which displays the zone 'Table_221' with table and PC. The zone is transparent to show what it is containing, but since the table was extruded through the whole zone, the background is visible. Table legs are not displayed as they belong to the adjacent zones in Z-direction and not in this zone. The PC is in the middle of the zone and is displayed in grey since it is surrounded by air. The rest is entirely air, shown in faded blue.

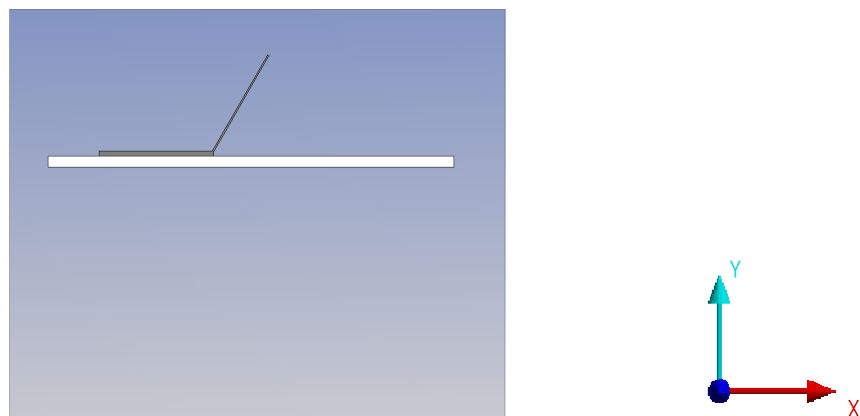


Figure 16: Transparent zone in the chamber with the table and PC cut out from the air

The example above is repeated for the other chamber articles. To simplify, each article no longer exists in the chamber, which now is entirely air. Articles are suppressed from the model and only work as boundaries for air flow. The pipe, however, is unsuppressed in another model to simulate the air flowing into the chamber. This became namely, the pipe model. The pipe was furthered separated into two parts in case different mesh methods would create finer meshing. It was separated right ahead of the nozzle to make the pipe outlet a single part, as shown in figure 17. Which also could be beneficial in case the transport of information to the chamber inlet would create issues. The other part of the pipe is, therefore, the larger share of the full pipe body.

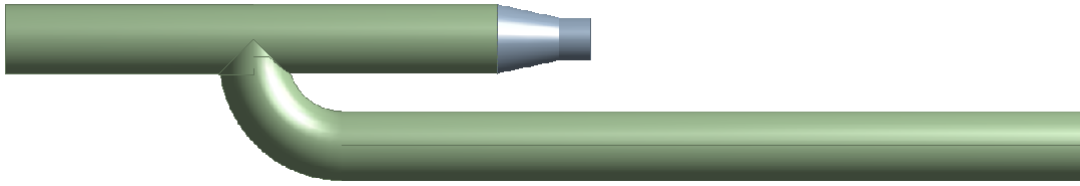


Figure 17: Pipe model divided into two zones. The grey part is the separation ahead of the nozzle, and the green part is the main part

Now the whole experiment has two geometry models; the chamber and the pipe model. They are virtually in the same space inside the chamber but separated from each other to ensure and improve quality during simulations. It is at the surface on the right side in the figure that properties of air is initiated, in terms of temperature and mass flow. By the simulation of the pipe model, there is an end result at the nozzle which will be transferred to the chamber model. This will be described more detailed later in the chapter about simulation.

4.3 Meshing in ANSYS

Meshing is a complex and crucial part of the analysis that requires years of experience to understand completely and conduct with high precision. Creating and simulate a real-life scenario requires knowledge about the driving forces that occur in real life and how to re-create it in ANSYS. What makes the mesh so complex is the number of settings that could be modified and the lack of control over the behaviour. It requires experience and knowledge about the impact each setting has in a mesh. Knowing what type of mesh that is desired for the specific problem, how to create it and deciding between the acceptable and non-acceptable mesh.

Settings put into ANSYS works only as guidelines, rules or restrictions, in which the software automatically generates the mesh. Meaning, some settings could lead the model to fail because the certain rule can not be applied to a particular geometry or part of it. Even if it does not fail, the mesh quality could still be poor and lead to end results with low accuracy. With symmetrical geometries, it is easier for the software, and the user, to create a good mesh. This is the reason for dividing the chamber into zones so each is meshed without too much influence from adjacent zones.

To mesh basically means dividing a component into a finite number of elements. In this case, the air inside the chamber is the component or components since each zone is singular. It is discretization the equations for finite volume method or finite element method, i.e. converting the differential equations to arithmetic equations [75]. With meshing, elements then become construction blocks for the chamber to build it up as a whole. Some also refer the elements as cells. The element size can be decided manually, again as a guideline, before conducting the mesh in ANSYS.

Furthermore, each element has nodes where the CFD calculation is performed to carry out results. For the purpose of this analysis, *CFD* calculation is chosen as the physics preference and *Fluent* as the solver preference. These two settings set the "default" values, so favourable settings were used. Settings can, however, be changed by individual preferences towards the mesh.

4.3.1 Elements in mesh

Elements in a 3D geometry build up the whole volume and compose it entirely. It is desired to achieve specific elements in regard to the settings and make it as refined as possible. How the elements are compound together, along with shape and size, affect the calculation later. Quality should be high and preferably reach the desirable geometry. It will in this chapter be presented how elements are formed, what is good quality elements and which settings that were applied to get sufficient quality of the mesh.

Element order and nodes

Element order is one of the settings to consider and decides the number of nodes on each element. It could either be *Linear* or *Quadratic*, and the disposal of nodes for the two settings are shown in figure 18. The picture is based on an illustration from the ANSYS handbook [75]. The vertical thick line between the square and the triangles is the separation between the elements, or cells, and becomes the body boundary. The graphic illustration on the left side is the quadratic element order. Nodes are placed on each edge and midpoint between each edge. On the right illustration, the midpoint nodes are removed, and the number of nodes is substantially reduced, and this represents linear element order. Reducing the number of midpoint nodes reduces the number of degrees of freedom [75].

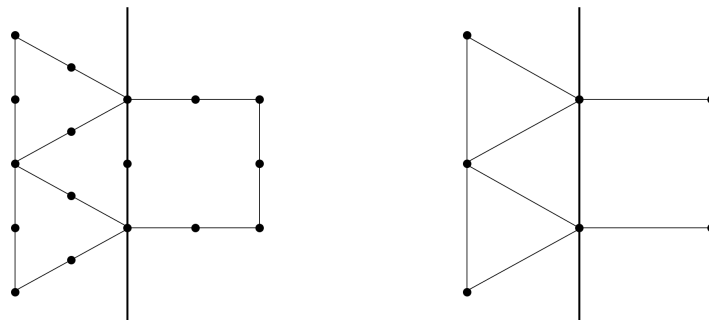


Figure 18: Two different types of element order. Quadratic element order on the left side with more nodes. The linear element order on the right side with reduced nodes. [76].

With the increasing number of nodes, the number of calculations increases analogous. It increases the accuracy but also the time the CPU uses to calculate. The simulations were performed on a stationary computer consisting of an Intel Core i7 3.20 GHz processor. A high-performance computer that allows a more profound setting without spending days or weeks to complete a calculation for an entire model. For this analysis, there were made several calculations for both the pipe and the chamber in order to find suitable settings in terms of quality and balance it up with calculation time. The decision about element order will thereby influence the time of calculation.

An element can take several shapes depending on what the CFD software find most suitable in regard to the rules set. ANSYS will, however, restrict the number of different geometries. For two-dimensional (2D) figures (read: surfaces), the two shapes appearing are either triangles or quadrilateral. ANSYS mesh creates three-dimensional (3D) element figures, which can take many shapes to fit into the total volume. Basic shapes occurring in meshing are shown in figure 19. Figures are based on ANSYS own manual [76].

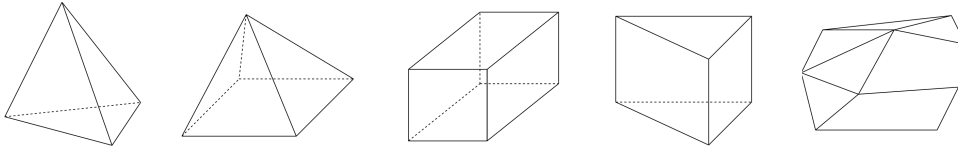


Figure 19: Geometrical 3D element shapes which appear in ANSYS meshing. From left: tetrahedron, pyramid, a prism with quadrilateral base, a prism with triangular base (wedge) and arbitrary polyhedron [76].

Element quality

Each of those shapes above has a value of mesh quality affiliated to it, called *Element Quality*. The quality metric ranges between 0 to 1 and can be calculated by using equation 13 for 2D figures and equation 14 for 3D figures. A value of 1, represents a cube or square with equal edge lengths and distances and could be considered as perfect mesh. The value of C, which is decisive for the quality as seen in the equation, is given in table 3. The shapes mentioned can be recognized in figure 19. Except for the arbitrary polyhedron, which is a composition of several various surfaces which is either triangles or quadrilateral. [76]

For 2D figures

$$Quality_{2D} = C \left[\frac{area}{\sum(Edgelen\theta)^2} \right] \tag{13}$$

For 3D figures

$$Quality_{3D} = C \left[\frac{volume}{\sqrt{\left(\sum(Edgelen\theta)^2\right)^3}} \right] \tag{14}$$

The table below shows the list of the value of C for different types of shapes.

Table 3: The value of C for each type of geometry that an element can have. [76]

Dimension	Shape	Value of C
2D	Triangle	6.93
	Quadrangle	4.0
3D	Tetrahedron	124.71
	Hexagon	41.57
	Wedge	62.35
	Pyramid	96

Aspect ratio is another parametric quantity which gives an indication for how good the mesh quality is. It measures the stretching of the cell by using the relationship between the shortest and longest distances from the centre of the element. A value of 1 corresponds to a complete regular element. The aspect ratio can more precisely be found as the ratio between the maximum distance between the centroid of the cell and the faces centroid, and the distance between the cell centroid and nodes. It is particularly important to avoid large or sudden changes in aspect ratio in areas where the field of flow have strong gradients. [76]

Skewness is a third parametric quantity to decide if the mesh has high quality or not. It is simply defined as the difference between the shape of one cell and the shape of an equilateral cell. An equilateral cell has equal lengths and angles. It calculates the value by taking the measure of the angle of each vertex point. The meshing of quadrilateral figures should have angles close to 90 degrees. Triangular figures should have angles close to 60 degrees and preferably angles less than 90 degrees. Elements with a final value above 0.95 may have convergence issues, and an average skewness below 0.4 can be considered as good mesh. [76]

Element size

Element Size specifies the size of each element, or cell, which is global for the entire model. This parameter basically sets the elements average edge length on all shapes and figures. For the chamber model, there were tested two different element sizes, 10 mm and 20 mm. Different element sizes could also be applied to different zones by setting edge size to a lower value. This manipulation should, however, be treated carefully as it could distort some elements. 10 mm was first attempted but the number of nodes as was too large and the computation would take too long.

Which is why the chamber was geometrically separated on the lowest level (the cut that separates $Z=1$ and $Z=2$). Zones near the outlets could thereby have finer mesh because they would not exceed calculation time too much, and without influencing the mesh for adjacent zones. Because this caused some stretching of cells, and 20 mm was after consulting considered as sufficient, it was decided that the chamber model should use this particular element size. The lowest horizontal cut was still kept as it benefited hex dominant mesh.

For the pipe model, 10 mm was first attempted with success. It was, however, possible to get finer mesh as the mesh reckoning only took less than a minute. The element size was then reduced to 4 mm, which was considered sufficient for the pipe. The air flow through the pipe is more turbulent than inside the chamber and it was necessary to get more accurate calculations. A reduced element size would then improve calculation precision.

A *Max Size* of the elements could also be applied to the model. Obvious by the name, this setting sets maximum edge length that can be grown in the mesh. This should not be too large, since important areas in the volume could then be overlooked in the mesh. For the chamber, this was set to 20 mm, equal to the standard size. For the pipe it was set to 6 mm due to the risk of some stretching along the boundary.

In the other end, *Defeature Size* could also be determined and basically sets the minimum size. This setting removes elements smaller than the input value. Defining this too low could mean unnecessary amount of nodes, while too high could lead the mesh to fail because it can not cover the entire volume. In the chamber model, this was set to 2 mm. In the pipe model it was set to "default", which implied 0.02 mm. [76]

After the element size was decided, there were other settings as well that were considered. One of them was *Use Adaptive Sizing*, which determines which other tools that can be activated in the settings. For both the chamber and pipe model the function was not applied. Experimenting and increase knowledge about these alternative tools could have improved the mesh somehow. It could, e.g. solved the erroneous which occurred in some of the zones.

The *Bias Factor* was a setting that was tested out to endeavour better mesh. It structures the edges of a zone with a specific pattern. By using the same bias type and the associated settings, adjacent

edges will have the same pattern and would assure a smooth transition of information from one zone to the next. Bias factor sets the size of the element from a reference location and consecutive elements will either decrease or increase in size depending on the options selected. It was attempted for the chamber model to use small element size close to each vertex. Implying that the longest element was located in the middle of an edge and from there, to both sides, decrease in size. The setting could, however, not be applied as it was not a successful operation.

Growth Rate is another setting that was considered. It decides the rate of increasing element edges length with each succeeding layer of elements. A value of 1.2 results in a size increase of 20 %. For complex geometries where there are parts with tighter areas, the growth rate smooths the transition between the cells so it does not make sudden changes in size. For the chamber model, the growth rate was set as default, which is 1,2. For the pipe model the growth rate was set to 1.1.

Other settings that were changed from default were the level of *Smoothing*, which was set to "high" for both models. This setting re-positions nodes to diminish the maximum skewness of elements in the mesh. It is also important to set the *Number of CPUs for parallel part meshing* to what is capable for the computer to handle. For each additional numeral size until reaching the computer's limit, the computational time is reduced. The amount that was chosen to use in this case was 4 CPUs.

Capturing Curvature and *Proximity* was also considered before meshing the model. Capturing curvature examines curves on edges and faces and computes element sizes on these entities such that the size will not violate the maximum size or the curvature normal angle. Which are either automatically computed by the mesh program or defined by the user. This feature was evaluated unnecessarily for the chamber model, but was considered beneficial for the pipe model. Use of proximity creates a refinement of the mesh by specifying a minimal number layer of cells in regions with "gap" in the mesh. This feature was, however, not applied to any of them. [76]

4.3.2 Mesh methods

The shape of each element is highly dependent on which mesh method is applied. It is also possible to utilise various methods by devoting a different method to another part of the model. This was e.g. done with the chamber model where the two zones, containing the pipe cutout, had the *Automatic method* instead of the *Hex Dominant method*. These two zones are highlighted in purple and located along with the ceiling in figure 14. Different methods in the same model would adjust node delegation for faces located in adjacent zones. Meaning, the bordering faces between zones has isometric face mesh and the transition would not become a problem.

The pipe model had a third type of method called *Body fitted Cartesian method*. It was separated from the chamber model and would not influence the chamber model mesh procedure. Using different methods would still produce smooth transmission of information between the two models. In this chapter, the three methods will be investigated closer and why they are selected to be explained.

Hex dominant method

Hex dominant mesh is by many CFD analysts the preferred method to mesh a component. Its main advantage is the decreased amount of elements required per volume with the same amount of vertices. [77] Compared to other methods which will create more distorted shapes. Coherently, the number of elements and nodes for the whole model are reduced but the precision of the calculation is maintained.

In CFD, it is also claimed that hexahedral meshes offer good results along with boundary layers [77]. It is also summed up in X. Gao et al. paper that a hex dominant method contain only a small number of irregular elements and in addition offers good numerical properties [78]. Quality of the element is better with hexagons as seen in table 3 about the value of C for different geometries. A cross-sectional view of two parts with hex dominant mesh of the chamber is shown in figure 20

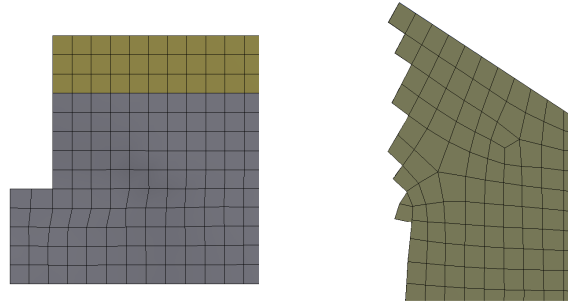


Figure 20: Generation of elements applying the hex dominant method. The part on the left is a cross section at one outlet. The part on the right is a cross-section along with the ceiling. Adjacent elements are removed.

Creating a hex dominant method consist of the geometries that are illustrated in figure 19. It implies, also in the name of the method, that not all shapes are hexagonal. Some triangular geometries are necessary to fill the whole volume, unless, the meshing will fail. Creating hexagonal shapes is thereby challenging and there is no technique that automatically creates mesh consisting exclusively of hexagons. This method is consequently more time-consuming to produce good quality mesh. The quadrilateral shape is the input and the software tries to create such elements. Hexagonal figures can also roughly be made by merging tetrahedrons to provide ideal node locations. [79]

Because adjacent faces of each element must be equal to each other, no triangular face of any shape can be directly connected to a quadrilateral face of a hexahedron. This is why the restrictions must be chosen carefully in order to fulfil this requirement. If ANSYS does not find any way to solve this, the mesh will fail and computation can not proceed. The way this can be avoided; a tetrahedron needs a pyramid to carry on with a quadrilateral face, which can continue on with a hexagon. This is, however, not desired since hexagons are preferred. By creating as many zones as possible in the chamber that are purely hexagonal, these zones will in most cases be meshed as all-hex. Which is why such zones are attempted to occupy most of the chamber.

Automatic method

The two zones with the pipe cutout, zone 'Pipe_431' and 'Pipe_432', marked with a significant purple colour in figure 14, are meshed with the automatic method which implies free mesh. Figure 21 exhibits the two zones which are meshed with automatic control. This method has no restrictions on the shape of each element and has no specific pattern affiliated. The two zones have yet completely different patterns. The olive-green elements belong to the zone where the inlet of the pipe starts, zone 'Pipe_431'. This zone is not that complex since it is just a straight pipe that goes through it. The zone with the grey element, on the other hand, have bends and contractions which makes it troublesome to create hexagonal elements. Instead, the software created a mesh where tetrahedrons are the prevailing geometry.

Note that there is not a smooth transition between nodes on the picture on the right. This is because the cross section is made diagonally through the chamber and the elements not necessarily interact with each other.

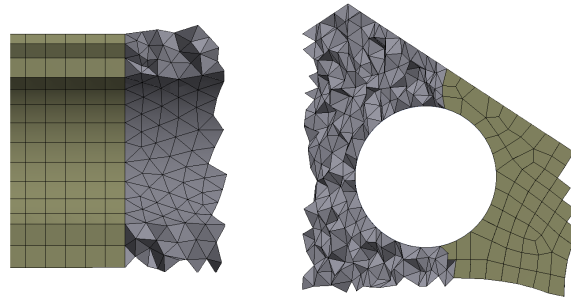


Figure 21: Generation of elements applying the automatic method. The part on the left is a cross section along the pipe. The part on the right is a cross-section where the pipe is cut out. Adjacent elements are removed.

Automatic mesh method was applied because the mesh would fail if hex dominant method was the selected option for the given element size of 20 mm. These two zones are also not so interesting as the occupant does not interact with these zones and the mesh becomes less important. The Automatic mesh also benefits from being the fastest way of meshing, using far less time than structural mesh.

Body fitted Cartesian

The body fitted Cartesian mesh method was applied to the pipe model. Hex dominant method and other accessible methods did not work that well with a rounded body. After running a few tests, it was clearly the Cartesian method gave the best solution. Compared to the hex dominant, the body fitted Cartesian method seemed to handle the geometry in the reversed direction. While the hex dominant method usually works from the boundary and inwards, Cartesian generates the interior mesh first and connect it with the boundary last. This is well illustrated in figure 22, where the fine mesh is created in the centre and the mesh along the pipe surface is less good.

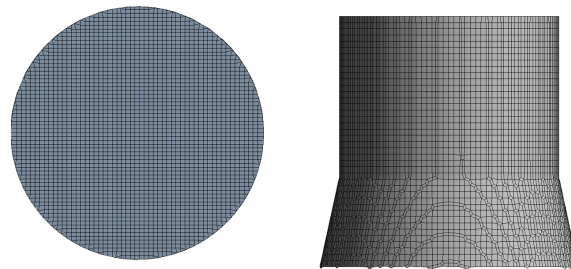


Figure 22: Generation of elements applying the body fitted Cartesian method. The part on the left is a cross section of the pipe. The part on the right is the surface of the pipe nozzle. Adjacent elements are removed.

This method was also tried applied to the chamber without any success because the mesh could not be completed properly. What is also happening close to the boundary is also far more interesting in the chamber model compared to the pipe. This is why the Cartesian method was well suited for the pipe as the mesh through the centerline is more crucial than at the boundary of the pipe.

Coda

The steps in this process are summarized in figure 23. The left column represent the coarse steps in creating the mesh for the chamber model, displayed in pink. The right column is the equivalent

step process for creating the mesh of the pipe model, displayed in blue. Separating into two models and further split into zones was done in DesignModeler. Programs used in ANSYS is shown in the top right corner of each box. Processes in DesignModeler are within the first yellow box area in the figure below and dealt with everything that concerns the geometry in ANSYS. Furthermore, the sheer geometry is then to be meshed in ANSYS own feature, represented by the bottom green box.

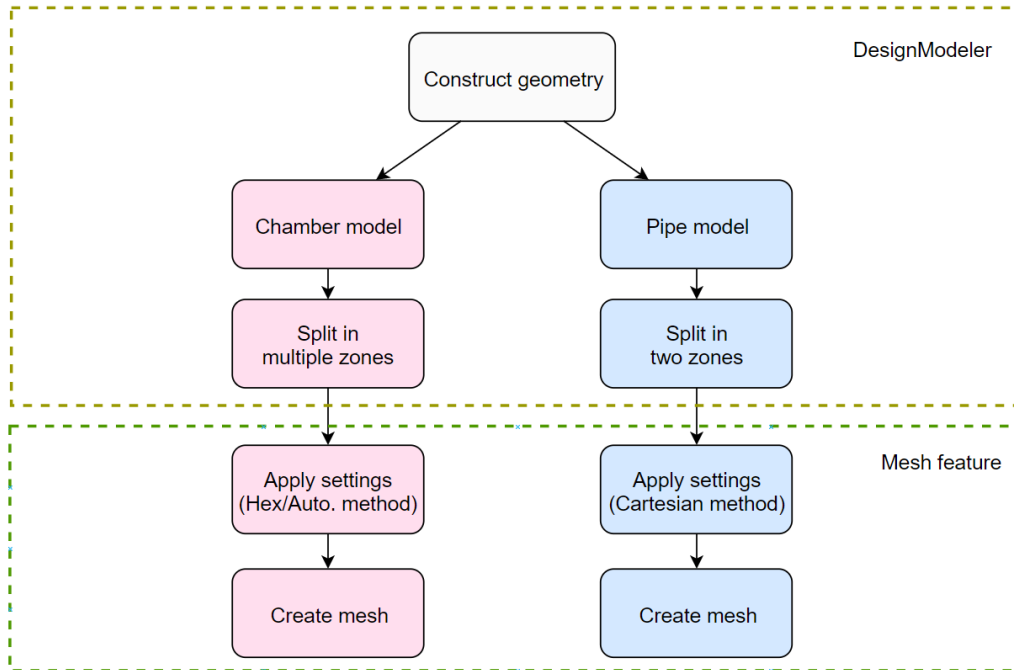


Figure 23: Steps from the SolidWorks geometry to the generation of mesh. Left pink column represent the chamber model and the right blue column the pipe model. First steps are done in DesignModeler while the last two steps were performed in ANSYS mesh feature.

The setting which was used in the ANSYS mesh feature is shown in table 4. Dissimilar methods and settings were applied to the two different geometry models before mesh was created. Because their shape and form are unlike, this was necessary in order to obtain decent results. Yet, many of the basic settings are kept the same. Those who matter significantly for the mesh are, however, different and are presented below.

Table 4: Mesh settings

Model	Pipe	Chamber
Physics and solver preference	CFD, Fluent	CFD, Fluent
Method(s)	Body fitted cartesian	Hex dominant, automatic
Element order	Quadratic	Quadratic
Free face mesh type	-	Quad/tri
Element size	4 mm	20 mm
Use adaptive sizing	No	No
Growth rate	1,1	1,2
Max size	6 mm	20 mm
Defeaturing size	0,02 mm	2 mm
Capture curvature	Yes	No
Curvature min size	1 mm	-
Curvature normal angle	18°	-
Capture proximity	No	No
Smoothing	High	High

4.4 Simulating in ANSYS

Once the meshing is completed, the model can be simulated in the ANSYS Fluent. The feature simulates flow and other physical fluid occurrences related to the model. It gives insight into the component and the behaviour of ambient circumstances. This way, the computational results should reflect how the model will work in a real-life scenario. This has great benefits in the industry because the outcome of a model could be embodied before constructing it. Evaluation performance of a component, a situation or scenario can also be useful for the developer. It can address issues with the model and pinpoint a prevailing problem. Fluent provides tools to present numerous analysis capabilities and set conditions which fit the scenario.

Setup

The tree outline starts off by giving options to the setup of the simulation. For both the chamber and the pipe model, the same setup was used in simulations which were interacting with each other. First general attributions, where gravity and general behaviour of the model were decided. It was assumed steady-state conditions, the model is pressure based and velocity is given in absolute formulation. Checking these boxes will activate these mentioned features.

Next step is to activate the *Energy Equation*. This feature is decisive for the parameters which are driving forces in the model and in addition necessary for calculating heat transfer. For instance, the energy equation controls the behaviour of temperature, pressure and kinetic energy. For the model to take deference to these parameters, the energy equation must be turned "on".

The Standard $k-\epsilon$ model was the first *Viscous Model* that was tried. It gave results that could represent the reality to some extent. Searching for another model that would match better was then to be conducted. Because the Standard model only was a reference at this point, three more options were considered to extend the study. The selections and testing of the three viscous models are based on A. Aganovic work [80]. These three are; the realizable group $k-\epsilon$, the renormalization group $k-\epsilon$ model (RNG) and the shear-stress transport $k-\omega$ (SST).

Each one of these four models utilises and solve different equations and carries out a solution to the case scenario. Meaning they can come up with diverse results. Their applicability has been studied by many analysts, and it is recommended to try experimenting with which model to use since each simulation is different from each other.

The Standard $k-\epsilon$ is the simplest, but yet a profound turbulence model which is often used in practical engineering flow calculations. It is robust, effective and has proven to engage accurate results. The k represents the equation for turbulent kinetic energy and is taken into account for all four of the examined models. The ϵ represents the equation for turbulent dissipation rate. [81]

The Realizable $k-\epsilon$ model stems, and is an alteration, from the Standard $k-\epsilon$ model. The term "realizable" means that the model fulfills mathematical constraints on the Reynolds stresses. It has improved from the Standard model by utilising a new formulation for turbulent viscosity and dissipation rate. More accurate prediction of spreading rate and good performance for flows involving rotation and close to boundary layers are other benefits from the Standard model. [81]

In resemblance to the Standard and the Realizable model, the RNG model uses the same two equations for solving expressions. The model has improved accuracy for rapidly strained flows and swirling flows. It also operates with a formula for effective viscosity that accounts for lower Reynolds

number. It is claimed that $k-\epsilon$ models performs better when simulating the distribution of flow far from boundaries. The three models mentioned here, are said to be robust and has a wide spectrum of application for different scenarios. However, it is also claimed the $k-\epsilon$ models lack some sensitivity to adverse pressure gradients and performs poorly with strong streamline curvature. [76, 81]

The shear-stress transport $k-\omega$ model (SST) is a variant from the Standard $k-\omega$ model. The ω represents the specific dissipation rate, sometimes referred to as turbulence frequency. The SST model tries to mix the free-stream independence of the $k-\epsilon$ model and the formulation of the $k-\omega$ in regions near boundaries. The SST model should, therefore, have a versatile range of application which suits most scenarios. It is also claimed that the model works better with low Reynolds number and is more appropriate for separated flows. [81]

After selecting one model to test its performance, the boundary conditions were considered next. Here, the existing zones and parts of the model are available for adjustments which can be specified for the case in question. Since the scenario for the topical simulation starts with the pipe, it is natural to begin here. More precisely, the air induced into the pipe is the starting point of the whole scenario. It was chosen to use *mass flow* as a reference unit for the inlet of the pipe, given in kg/s. The reason was that the actual fan that provides ventilation to the chamber, measured the input in litre per second.

Four mass flows were chosen to be initiated at the pipe inlet; 0.0167, 0.0333, 0.0500 and 0.0667 kg/s. By knowing the physical properties of air, the volume flow could easily be converted to mass flow by using the value of air density. The thermal properties that were bestowed the air were 293 kelvin [K] for all the simulations, based on Y. He's experiment conducted in the same chamber done just weeks before this study [82]. This temperature was also appointed upon all the exterior surfaces as well.

The outlets, at the floor, displace air out of the chamber to maintain mass conservation and was set to be driven by pressure. Pressure is chosen as the driving force at the outlet for both the chamber and pipe model. It is beneficial as it exhibits deference towards temperature, velocity, conservation of mass etc.

Because the first few simulations caused some improper results, it was attempted to change other settings to debug the problem. One of them that was tried adjusted was the *Hydraulic Diameter*. This setting is usually modified when the cross-section is non-circular and purposely create realistic physical properties for the model. It was set to 0.16 m, equal to the pipe outlet diameter. Unfortunately, this did not solve the problem. The issue was, however, that the computer probably had trouble with separating simulation from each other and causing some overwriting inputs and outputs and lead to false results. It was solved by rebooting the computer and restart ANSYS. The hydraulic diameter was later tested under virtuous conditions and found to have no impact on the results.

Initialization

Before running the calculation, the initial conditions must be implemented into the boundary of the model. By running the *Hybrid Initialization*, the predetermined values of velocity, pressure, temperature and turbulence are being used as information to set the initial conditions. The reason it is called a hybrid, is because it uses this information to interpolate these parameters, together with the solution of Laplace equation to produce a velocity and pressure field that conforms to the geometry domain. Other parameters were directly applied to the geometry. [76]

Calculation

The model is now ready to be calculated. Based on the time that was obtainable to complete this study, the *Number of Iterations* was set to "1000". Because the mass flow rate is specified, Fluent needs to calculate the pressure gradient, denoted as β . The number of iterations set the number of sub-iterations performed to correct β in the pressure correction equation. What is defined is not explicitly precisely and balanced. Therefore, numerous iterations must be performed until what is defined is achieved in the computational model. This is only final when the quantities of the simulation converge. Figure 24 shows a simulation that reached convergence after approximately 600 iterations. Judging the graph by how stable the outputs are, information can be gathered about the complexity of the scenario.

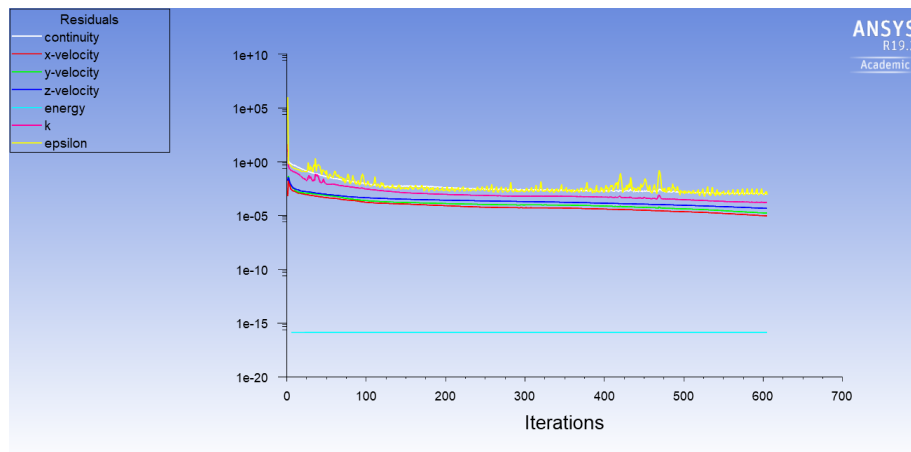


Figure 24: Simulation residuals for the pipe at 0.0167 kg/s with the Realizable model. The simulation was set to 1000 iterations but stopped at roughly 600 because of convergence.

To transfer the result from the simulation of the pipe, the output must be written and saved. By doing so, the parametric quantities that occur at the pipe outlet, can be transferred to the chamber model. The parameters were chosen to 'write' was the *Velocity Magnitude* and *Total Temperature*. The stationary conditions that take place in the pipe outlet, was then printed to the equivalent surface in the chamber. When simulating the chamber model, the same profile is to be 'read' and the scenario from the pipe model continues.

Coda

Settings in the chamber model are first to be set up before continuing to run the simulation. These are equal to the corresponding settings in the pipe model. Since there were run four different mass flow rates and all with the four different turbulence model, there was a need to run sixteen simulations for the pipe and an equal number for the chamber model. Which means that a pipe model and a chamber model with a matching setup would become a pair and represent one scenario. A flowchart of the process in Fluent is shown in figure 25.

Distinctive settings that were applied in Fluent is shown in table 5. The remaining settings were kept as default in the 19.2 version of ANSYS. Note that the viscous models have even more detailed settings than rendered here.

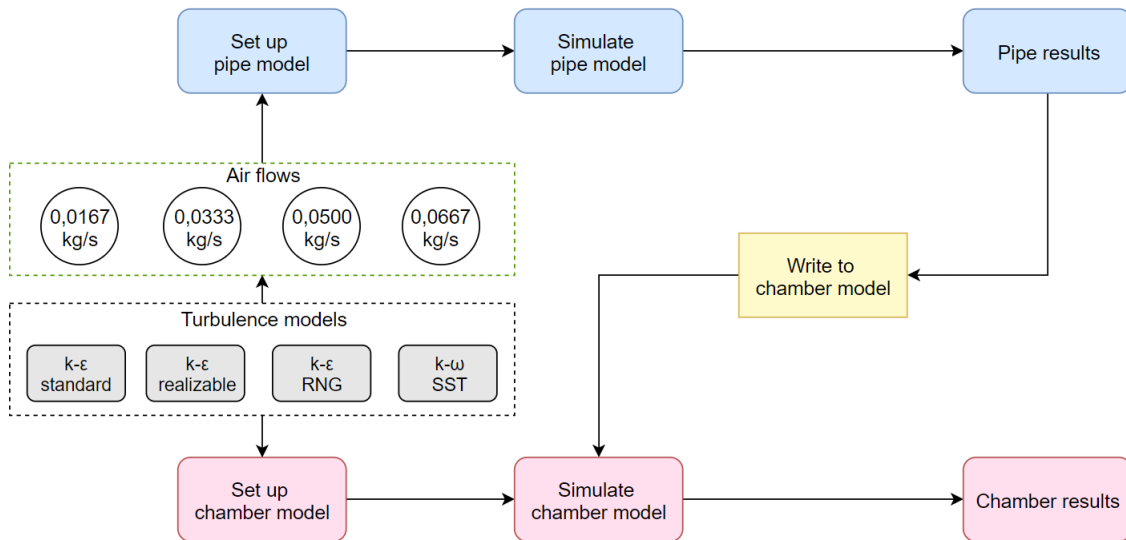


Figure 25: Flowchart of the working process in ANSYS Fluent. Four turbulence models were examined along with a combination of four levels of mass flow.

Table 5: Fluent settings

General	Type	Pressure-based
	Velocity	Absolute
	Time	Steady
	Gravity	Y: -9.81 m/s ²
Models	Energy	On
	Viscous	Standard, Realizable, RNG, SST
Boundary	Exterior surfaces	293 K
	PC surface	318 K
	Inlet pipe	293 K
	Outlet pipe	0.0167, 0.0333, 0.0500, 0.0667 kg/s
	Inlet chamber	Pressure
	Outlet chamber	Velocity/temp profile from pipe Hydraulic diameter 0.16 m
Initialization	Method	Hybrid
Calculations	Iterations	1000

4.4.1 Validation of simulation

Since each turbulence model and various mass flow rates gave diverse results in the Fluent simulation, these had to be tested and compared to what it looked like in real life. By to determine how the behaviour of air actually is, a model can be chosen to be the best representative match compared to the real-life scenario. Results from the validation can later be used for authorising the model for this particular case.

Selecting locations of measuring points

The chamber was first set up, equally to the model drawn in SolidWorks and simulated in ANSYS. Then, several locations inside the chamber and in the model were chosen for comparison. Because the location of the measuring points should be compared, accuracy is important for a valid representative model. When the furniture and installation are used as references in the measurements, they should

preferably also be placed accordingly to the drawn model because they are also referenced points in the model.

There were used two instruments to measure the velocity in the chamber; the TSI VelociCalc 8388-M-GB and the TSI Transducer 8475-300, both described in chapter 3.6 about supplementary instruments. VelociCalc was used for locations where the expected velocity of air exceeded 1 m/s. While the Transducer was used where the air velocity was likely to be below 1 m/s.

Five measuring points were selected inside the chamber. Various sampling was chosen to provide information about different zones of the chamber and where the velocity is eminent. It was also done with the intention to test locations close to where the person would sit since particularly this area is of importance in this study. Other locations were chosen due to the expectancy of higher velocity gradients compared to other parts of the chamber. List of the five measuring points and which instrument that was applied is shown in table 6

Table 6: The five locations in the chamber and in the model that was compared against each other. Type of instrument is described in the right column.

Location	Instrument
1. Middle of pipe outlet	VelociCalc 8388
2. 50 cm in front of pipe outlet	VelociCalc 8388
3. Middle of chamber	Transducer 8475
4. Between chair and table	Transducer 8475
5. Chamber outlet	Transducer 8475

In figure 26, the probing points are marked with a cross. The red crosses represent the measuring points that were measured with the VelociCalc and the green crosses are measured with the Transducer.

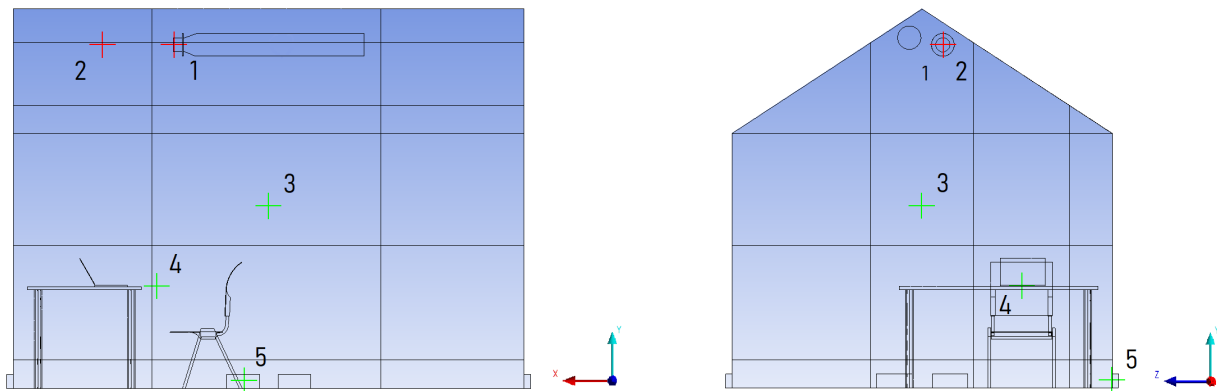


Figure 26: Measuring locations in the chamber as viewed from X-direction. This was the probing points used in Fluent.

Adjusting and setting air flow

The different flow rates were changed by adjusting the opening or closing of three valves. The fan supplying the chamber with air was cited a CKS 355 and is closer described in chapter 3.6. The fan provides two chambers with air. Meaning that adjusting the valve to the chamber not in use, would also affect the chamber which was used in this work. There is a main valve that conforms the

mass flow for both of the chambers. Each valve has a flap to be adjusted which represents a certain number and is denoted as \mathbf{k} . Along with the pressure difference over the valve, the volume flow, \mathbf{q} , could be calculated given by the unit l/s. Equation 15 shows this correlation.

$$q = k\sqrt{p_I} \quad (15)$$

By selecting an appropriate value of \mathbf{k} , it could be calculated what value of p_I necessary to obtain the desired volume flow in the topical chamber. p_I could be measure by the use of a micromanometer, described in chapter 3.6. Air density, ρ , is required to know when calculating from mass flow to volume flow. Air density was set to 1.204 kg/m^3 , based on J. H. Keenan findings on air properties for various parameters [83]. The value set is based on the chamber temperature of $20 \text{ }^\circ\text{C}$. With each of the four already defined mass flows, denoted as \dot{m} , the required volume flow can be calculated from equation 16.

$$q = \frac{\dot{m}}{\rho} * 10^3 \frac{l}{m^3} \quad (16)$$

With each mass flow simulated in the model, it is possible to find a combination of \mathbf{k} and p_I in equation 15 that will yield exactly desired volume flow for the topical chamber. The value \mathbf{k} could be determined by adjusting the valve that controls the flow into the chamber. The desired p_I could be prescribed by adjusting the main valve and the valve to the opposite chamber. Then, measuring the velocity inside the chamber could be carried out.

Measuring air velocity

VelociCalc and Transducer are two different instruments, utilising both to do measurements for the same case are not optional. But since they both had their restraints in terms of accuracy and range, it was the best option. It was, however, developed a method to try equating and compensate for this issue. The velocity from the chamber was not directly compared to the model. Instead, it was measured a range between a certain time frame. This was also done because the velocity seldom would be stable and a scale would be a better presentation.

After the volume flow induces into the pipe was chosen and the chamber was set up like the model, there was given a time frame of approximately one minute for the room to settle. This would be the initial conditions. The highest and the lowest value in the next sixty seconds was then noted. The Transducer only gave values momentarily. The VelociCalc could be given time constant up to twenty seconds, which then could display the average velocity in that time frame. Since this would render more stable results and possibly ignore erroneous measurements, this option was chosen to be exploited.

Between each measurement, the chamber was yet again to be settled for initial conditions before the measuring would start over again. This was due to some exaggerated body movements which would be uncommon in the actual scenario. The measurements done with the VelociCalc was done hand held and was another reason the time constant was utilised since this could also cause some erroneous. Measurements in mid air were done by anchoring the device to a tripod. To make sure it was done in the exact same location, marking spots were used on the floor. False results were kept to a minimum by having a distance between the person and the measuring location.

4.4.2 Sensitivity analysis of the Standard and RNG model

By testing the four turbulence models for each of the four flows and at five different location points, the Standard and the RNG model were selected for further analysis. Both showed good performance under the given circumstances and a more thorough investigation was required. Lack of accuracy by the Realizable and the SST model entailed these two were not followed up any further.

Standard k- ϵ model

The Standard k- ϵ model is a semi-empirical model, and the derivation of the model equations relies on phenomenological considerations and empiricism. The equation for turbulence kinetic energy, k , is derived from the exact equation. While the equation for dissipation rate, ϵ , was obtained using physical arguments. Derivation of the k- ϵ model assumes fully turbulent flow and the effects of molecular viscosity negligible. The expressions for transport for the Standard model is shown in equation 17 and 18.

$$\frac{\delta}{\delta t}(\rho k) + \frac{\delta}{\delta x_i}(\rho k u_i) = \frac{\delta}{\delta x_j} \left[\left(\mu + \frac{\mu_t}{\sigma_k} \right) \frac{\delta k}{\delta x_j} \right] + G_k + G_b - \rho \epsilon - Y_M + S_k \quad (17)$$

and

$$\frac{\delta}{\delta t}(\rho \epsilon) + \frac{\delta}{\delta x_i}(\rho \epsilon u_i) = \frac{\delta}{\delta x_j} \left[\left(\mu + \frac{\mu_t}{\sigma_\epsilon} \right) \frac{\delta \epsilon}{\delta x_j} \right] + C_{1\epsilon} \frac{\epsilon}{k} (G_k + C_{3\epsilon} G_b) - C_{2\epsilon} \rho \frac{\epsilon^2}{k} + S_\epsilon \quad (18)$$

RNG k- ϵ model

The RNG (renormalisation group) k- ϵ model is a further derived model from the Standard k- ϵ model. RNG has a different equation for turbulent viscosity and in addition puts a maximum limit for Reynolds number, R_ϵ . This adds to a different ϵ equation where an extra term is included, compared to the Standard model. As a result, rapidly strained flows yields a lower turbulent viscosity in the RNG model. Meaning it responds better to streamline curvature and the effects of rapid strain. The RNG k- ϵ transport formulations are shown in equation 19 and 20. [81]

$$\frac{\delta}{\delta t}(\rho k) + \frac{\delta}{\delta x_i}(\rho k u_i) = \frac{\delta}{\delta x_j} \left(\alpha_k \mu_{eff} \frac{\delta k}{\delta x_j} \right) + G_k + G_b - \rho \epsilon - Y_M + S_k \quad (19)$$

and

$$\frac{\delta}{\delta t}(\rho \epsilon) + \frac{\delta}{\delta x_i}(\rho \epsilon u_i) = \frac{\delta}{\delta x_j} \left(\alpha_\epsilon \mu_{eff} \frac{\delta \epsilon}{\delta x_j} \right) + C_{1\epsilon} \frac{\epsilon}{k} (G_k + C_{3\epsilon} G_b) - C_{2\epsilon} \rho \frac{\epsilon^2}{k} - R_\epsilon + S_\epsilon \quad (20)$$

The principal difference between the RNG and the Standard k- ϵ models is as mentioned in the additional term in the equation for ϵ , presented in equation 21.

$$R_\epsilon = \frac{C_\mu \rho \eta^3 (1 - \eta/\eta_0)}{1 + \beta \eta^3} \frac{\epsilon^2}{k} \quad (21)$$

By equation 21, the term \mathbf{R}_ϵ makes a positive contribution when $\eta < \eta_0$. This renders results close to the Standard model and appears tenuous to moderately strained flows. In regions where $\eta > \eta_0$, the \mathbf{R}_ϵ term makes a negative contribution. ϵ will strengthen, reducing \mathbf{k} , and as a cause also the effective viscosity. This results in a lower turbulent viscosity in rapidly strained flows compared to the Standard model. List of all variables included in the equations above are shown below:

t	time
ρ	density
k	turbulence kinetic energy
x_{ij}	vector of direction
u	velocity parallel to the wall
α	inverse effective Prandtl number
μ	turbulent viscosity (effective)
G_k	generation of turbulence kinetic energy due to the mean velocity gradients
G_b	generation of turbulence kinetic energy due to buoyancy
Y_M	fluctuating dilatation in compressible turbulence to the dissipation rate
S	user-defined source terms
σ_ϵ	turbulent Prandtl number for epsilon
C	constant
Re_ϵ	Reynolds-number
η	strain rate
β	constant

Each of the variables in the equations can be further derived in to their own separate equation in which together compiles the transport equations presented. Each model has a distinct amount of variables, and equations can vary based on application. In Fluent, constants that would influence the transport equation can be adjusted to the specific case. The Standard and the RNG model showed promising results but still not completely accurate to the measurements inside the chamber. Adjusting the settings of the two models was thereby the next step to create a model similar to the actual movements inside the chamber. This includes adjusting several settings which comprise applying *Full buoyancy effect* and *Curvature correction*, constants like C_{μ} , C_1 - and C_2 -epsilon were also resolved.

A sensitivity analysis of each of these was conducted to discover how they would influence the air distribution and velocity inside the chamber. Other settings could also be considered, but by getting knowledge about their behaviour it was decided to try adjusting those who were most likely to have an impact on the air flow. Each of the settings, for both of the two models, were tested with an air flow of 0.0667 kg/s This is due to larger fluctuations through the room in terms of air velocity compared to minor air flows.

Full buoyancy effect

First setting evaluated was the full buoyancy effect, which generates turbulence due to buoyancy. The effect of the phenomena is given in equation 22. Where β is the coefficient of thermal expansion, Pr_t is the Prandtl number for energy and \mathbf{g}_i is the component of the gravitational vector. As long as the gravity field is not zero, it should be automatically activated already. By applying it anyway, it could be confirmed that gravity was present in the model. [76]

$$G_b = \beta g_i \frac{\mu_t}{Pr_t} \frac{\delta T}{\delta x_j} \quad (22)$$

Curvature correction

Curvature correction should only be considered depending on the scenario of simulation as it works to complete the model if it is not entirely accurate. The k- ϵ models already include expressions for swirl and rotational effects. Large changes were therefore not expected by activating this feature. K. J. Elliott et al. investigated the performance and functionality of the curvature correction and studied the effects [84]. Their findings conclude that appropriate streamline curves and velocity profiles are achieved by activating this feature.

C μ

C μ is sometimes referred to as C_μ and the expression is given in equation 23. It is a function of mean strain and rotation rates, denoted as \mathbf{A} , the angular velocity of the system rotation, denoted as \hat{U} , and the turbulence fields (\mathbf{k} and ϵ). The value of C μ is part of the equation for turbulent viscosity, μ . An increase of C μ will increase the turbulent viscosity parallel. The value of C μ is standardised for the RNG model to be 0.0845. It was therefore tested out to double this value to 0.169. This would increase viscosity as it was assumed this would be beneficial for the model air flow. [81]

$$C_\mu = \frac{1}{A_0 + A_s \frac{k\hat{U}}{\epsilon}} \quad (23)$$

C1- and C2-epsilon

C1- and C2-epsilon are empirical constants in the transport expression presented in equation 20 earlier. They can not be further derived and their default values have been determined from past experiments done by analysts. An original RNG model has the values of 1.68 and 1.42 for C1 and C2 respectively. For the original Standard model the values are 1.44 for C1 and 1.92 for C2. They have been found to represent most scenarios well but can be modified depending on the case. It was determined to experiment with these numbers for the sake of research and accuracy of the model. [81]

Based on other previous experiments by other analysts, an increased value of C1 will lead to less mixing of air, lower shear and a smaller change in pressure. The opposite is claimed to happen when C2 increases, with more mixing, more shear and greater change in pressure. Equation 24 and 25 shows the variables that affects C1- and C2-epsilon. To watch their effects, both of their default values were doubled. [85]

$$C_1 = C_0 \frac{\eta \left(1 - \frac{\eta}{\eta_0}\right)}{1 + \beta \eta^3} \quad (24)$$

and

$$C_2 = \left[1, 0 - 0, 3 \exp(-R_t^2) \right] \quad (25)$$

Mixed settings

After all five model characteristics were tested individually for each of the two models, the RNG continued the sensitive analysis by mixing the settings and values. Not all of the tuned settings lead to any rough changes of air flow in the model. Some of them, however, had much impact on the model. Interpreting the consequences each of them had was carried out. Then, the previous analysis of the delicate characteristics was evaluated against the measured values to find an adequate weighing between them. This implied testing two or more model characteristics to watch their impact together on the model. A total of four combinations between the numeral settings and features were tested before reaching a satisfying solution.

4.4.3 Appending radiator inside the chamber

For the extension of this work conducted so far, a radiator was placed inside the chamber to check how the subject would respond to this and potentially report different. This extended the scope and gave some answers consequently of temperature differences and also exclusively. Radiators are common in many buildings in northern countries and gives the experiment another element to take into regard. In addition to provide heat, the radiator also produces noise and could lead to worse air quality because of the release of air contaminants. It has also the psychological effect of making the subject expect the chamber to be heated up.

The previous steps from earlier are followed in the same order. The radiator was cut out from the two zones; 'Air_123' and 'Air_223', showed in appendix C. The type that was used was a floor oven from Siemens, described in chapter 3.6. It was placed close to the entrance door, behind the back of the person inside the chamber. Kept away from the outlets to reduce the amount of lost energy and increase the impact on the ambient air inside the chamber. The model was then to be re-created in DesignModeler and further meshed with the same techniques as described earlier.

Because the simulations developed some erroneous results in temperature throughout the chamber, zone 'Chair_222' had to be meshed differently. This was due to some excessive production of heat that originated from nowhere. It was experimented with how the automatic mesh would solve this issue, instead of the hex dominant, and it gave a better temperature solution in the zone. The automatic mesh method was thereby appointed to this zone for these scenarios.

The radiator was only tested at the two air flows; 0.0500 kg/s and 0.0667 kg/s. This was done because the mixture of air would be better with these two air flows. The radiator also had a fan attached to spread heat throughout the chamber. This was set at a constant speed at 4/6 notches and rendered approximately 1 m/s. This was measured using the VelociCalc with a time constant, as applied earlier.

The temperature applied to the radiator was set based on measurements also made with the VelociCalc. This temperature was also engaged to the air the fan induced. It was also run tests by applying heat flux. But with a basis in the inaccuracy and uncertainty of measuring heat flux and the results it rendered, these simulations were scrapped. With no heat generation the fan air was bestowed a temperature of 293 K. The temperature of the air when heat on the radiator was turned up one

notch was 325 K. Second notch meant the temperature was 337 K and maximum heat generation entails that the air coming out from the fan had a temperature of 353 K.

The first scenario was without any specific heat generated with only the fan running. This would cause the air movement in the chamber to increase with tenuous heat generation. Then, the heat generated from the radiator was increased for each scenario, all with an air flow of 0.0667 kg/s. Afterwards, the air flow was reduced to 0.0500 kg/s and heat generated from the radiator was first set to 4/4, and lastly 3/4 notches. Work of flow were equal to the other previous simulations, presented in figure 25. The list of the six scenarios is shown in table 7.

Table 7: The six scenarios which were conducted in the chamber. Two different air flows were tested together with different radiator settings.

Scenario	Air flow	Heat and fan power
V	0.0667 kg/s	0 and IIII
VI		1 and IIII
VII		2 and IIII
VIII		3 and IIII
IX		2 and IIII
X	0.0500 kg/s	2 and IIII

The scenarios were carried out in the same order as presented in the table. Increasing the temperature gradually was done to examine how the evaluating would change accordingly. By reducing the heat again to replicate a previous scenario, it is possible to analyse a possible adaption towards the thermal environment. The effect of air flow could also be closer investigated by reducing it to 0.0500 kg/s.

4.5 Design of experiment

The experiment is the final step to collect valuable data before the work can be compiled as a whole. This chapter will explain how this experiment was executed in the test chamber on NTNU Gløshaugen. First a brief explanation is presented of how it was set up and how the experiment was initiated. Then comes information about each parameter which is to be evaluated and how. This include which scale is used and how the index is applied in the evaluation.

4.5.1 Setting up and initiate the experiment

Every scenario is endeavoured to be equally set up and initiated to elude errors in the evaluation and establishment inside the chamber. Following a fixed procedure at each scenario would ensure this and creates equal initial conditions. This procedure has of course some digressions which is indispensable but was within acceptable frames so it was not leading to false results. If any occurrences were to happen, it was noted in the evaluation form. This includes visitors inside the chamber, breaks or other occurrences.

The scenarios lasted a full day and the duration varied within a certain range. The participant spent approximately 8 hours or more inside the chamber for each scenario. Seeing trends and how the evaluation changes throughout the day could thereby be analysed over a long time span. The set up

inside the chamber was equal each day with the same equipment and furniture located in the same place.

The experiment was initiated in the morning hours between 8.00 - 8.30 AM. The door to the chamber has then been left open before the experiment starts to have similar conditions as the hall, which surrounds the chamber. The ventilation inside the chamber was turned off the day before. This way, the initiate condition inside the chamber would more or less be equal for each scenario. The ventilation in the hall run all night and consequently the air inside the chamber was changed before a new scenario could start. Electric equipment that could have an impact was turned off as well the day before.

Air flow was decided in advance and set up immediately as the subject entered the chamber. Appointing air flow was done in similar a fashion as when validating the model described in chapter 4.4.1. As each air flow had specific valve positions, these were replicated to render the same air flow. Then, the air flow was validated at the pipe outlet so that air velocity matched with the measurements carried out earlier. Next, the subject entered the chamber and made sure the door was closed and that the outlet openings were free. Kinect device was set up in advance and started recording behaviour.

4.5.2 Evaluation

The evaluation contains several parameters and chosen to narrow the number of uncertainties which could affect the result. To find possible coherence between thermal comfort and surrounding parameters, it is important to consider other factors which could impact the evaluation. It is, therefore, in this evaluation included psychological, personal, and ambient parameters inside and outside the chamber. Occurrences and other details outside of this were registered in the form. Presentation of each of the segments follows below.

Segments were evaluated every half hour as long as the subjective was inside the chamber. The evaluation was a representation of the current state and at that moment. But it was also a representation of the last half hour. This only concerns body positioning and movement. This was done because at the present moment the subjective was evaluating, the body's heat accumulation could be affected by former body motions. The heat produced earlier by any activity, should express the present heat accumulation conditions in an attempt to equalise activity level with the duration since it occurred. Then, how long ago the body repositioning took place was considered along with the activity level.

Psychological parameters

Psychological parameters represents those factors that can not be measured and which are related to the condition of mind. These parameters are completely individual to evaluate and can vary greatly from person to person. Psychological parameters are often overseen in many studies due to the lack of knowledge about their influence, but could definitely influence the sensation of thermal comfort. The psychological factors to be considered in this study concerns vaguely basic feelings and emotions that often occurs in a typical work place. Such psychological factors do have an impact of the perception of thermal comfort and are therefore to do be assessed.

Stress

Stress is rated from a scale from 1-5, where 3 represents normal stress. Stress could have many causes and could be affected by factors like work pressure, problematic relationships to other people or other influencing factors that contributes to stress. Stress can make the body sweat uncontrollably and the adrenaline is usually pumped up. This causes the body to heat up as a reaction because the brain becomes overactive.

The score of 1 is not stressed at all, which implies a calm mind and not feeling the anxiety of deadlines or the urge that something must be done. The score of 2, some stress, is the feeling that something must be done, but does not have any rush of doing it now. 3 is a normal stress level at work and should somewhat represent the average level of stress. 4 is the feeling of stress, which implies a little bit of tension in the body and that the work task requires a lot of effort in a short time. 5 is the feeling of being overwhelmed by work and that this task can even hardly be accomplished before the deadline.

Tiredness

Tiredness is rated from a scale from 1-5, and is correlated to energy level and the feeling of being sleepy or not. The score of 1, not tired, represents the feeling of being fully awake and that the body and brain are full of energy. 2 is sort of the typical level of tiredness where the person does not feel fully energized and not feeling tired either. In a normal day, this is the level the subjective is expected to be most of the time. 3 is the feeling of being tired and that the subject has the sensation of being a little bit exhausted. Typically the feeling a person has at the end of a good day's work. 4, very tired, is when the subjective feels almost completely out of energy and it is hard to concentrate on the work. 5 is extremely tired and it is the feeling that the subjective can hardly stay awake. Meaning that the subjective starts to nod and eyes shut uncontrollably for a few seconds or longer.

Excitement

Excitement is closely related to both of the previous two parameters but is included as it does not necessarily represent the opposite or similar, to both or one of them. Excitement is the feeling that the work task is somehow thrilling and gives the person motivation and energy to complete it. The feeling could also occur if something exciting is happening later that day or in the future, bear in mind that the level of excitement not necessarily has to be correlated to the present task, but it should describe the excitement the subjective is feeling in that present moment. Excitement is rated from a scale to 1-5.

The score of 1, not excited, is the sensation of being very bored by what the subjective is doing and nothing special to look forward to. 2, some excitement, meaning that what the subjective is doing is a little bit boring or could feel some excitement towards a future event. 3 is normal excitement which is a sort of the neutral state, which is neither particular bored or feel particular excitement. The score of 4 is the feeling of excitement and describes a feeling of having a positive mindset and feels motivated. 5, very excited, is the feeling of being very motivated and that the subjective has high energy levels and a positive mind towards the task or future event.

Hunger/Thirst

Hunger or thirst are related to the energy levels of the subjective. The heat produced by the body is a product of calories in food. Being full often means that the body was to work and heat is therefore produced. While it is the opposite when being hungry. Then, the processes that happen inside the

body is less intense and produce less heat. Hunger or thirst is rated on a scale from 1-5. Being so full that it is past satisfaction and the subjective feels physical uncomfortable with it represent the evaluation value 1. 2, satisfying full, is the feeling of being full, but does not feel any discomfort with it. 3 is the sensation of neither being full or feel any hunger. For the score of 1, 2 and 3 the subjective is not thirsty. 4, hungry/thirsty, is when the body starts to give a signal that it craves food or something to drink. The energy level starts to drop a little as a cause of this. 5, beyond hungry, is when the body and mind are being irritated by the lack of food or something to drink. The energy level is very low and the subjective can easily lose concentration or become dizzy.

Personal parameters

Personal parameters represents factors that can be adjusted by the person itself. These can vary greatly from person to person, and can easily be adjusted momentarily. The personal parameters can be roughly be estimated the same way like the psychological parameters and some are hard to estimate precisely and can also be viewed objectively. Some are, however, possible to measure accurately because it is physical parameters.

Clothing

Clothing is the amount of insulation the clothes provide to protect the body against the environment and to maintain satisfying thermal conditions. A low level of clothing implies very little thermal protection towards the environment where zero represents the subjective to be naked. For reference, summer clothing normally could vary from 0,2-0,8 on a warm day. While winter clothing based on Norwegian conditions could vary from 0,8 indoor to 3,0 or higher when outdoor. Calculating clo is done by using the table provided by Engineering Toolbox [86] The value is given by the unit *clo* and a more detailed description is given in chapter 2.3 about clothing.

Wet clothing

Wet clothing is given in percentage from 0 to 100

Because wet clothes, and consequently skin, increases the heat loss, this is an important parameter to be considered. As a guideline, if an area is fully soaked, that area could contribute all of its areas. If, however, that area could only be considered as clammy, that area could be divided by a factor of two. Sweat also contributes to clammy clothes in typical areas like pelvis and along the back. Clothes then become moist when sweating and are being taken into consideration here.

Body positioning

Body positioning should give a representation of the body posture and how comfortable that position is. The scale some sort of represents how much of the muscular system that is under stress and goes from 1-5. An evaluation value of 1 represents a completely comfortable body positioning without any stress in the muscular system. The score of 2, little odd positioning, is where a small limb is not in a comfortable position, like wrist or foot. 3, odd positioning, is where a larger limb is uncomfortable, could be the arm, a leg or that the whole-body posture is a little out of its comfortable position. 4, very odd positioning, is where a larger part of the body is in an uncomfortable position, similar to light stretching of big body parts. 5 is where the whole body is in a stressful position and the body is in a really uncomfortable position. This is often where the subjective can barely stay for a long period of time or maintain.

Body movement

Body movement is related to the activity level and how much the subjective creates movement or moves around the room. The scale goes from 1-5, where 1 is being stationary or that the subjective has no movement. The score of 2, small movement, implies that the subjective tends to move arms or legs occasionally. 3, some activity, means that the subjective makes larger movements that can be felt by some small heat generation. 4, active, is around equal to the heat generated by walking. Could be large movements similar to that, or quick movements made by arms or legs. 5 is where the subjective is very active and generates a lot of heat or become a little sweaty in indoor conditions.

Sweat rate

Sweat is the body's system of cooling down the skin to increase heat loss. It correlates to the activity level and the temperature surrounding the subjective. The scale ranges from 1-5, where 1 is no sweating. 2, some sweating, implies that the subjective can be clammy in the armpits, back or other places. The subjective feels slightly too warm compared to the environment. 3 is where the subjective is sweating and the forehead seems wet and the subjective is uncomfortably warm. 4, much sweating, is where the sweat start to go through the back of a t-shirt and it is very uncomfortable. 5, heavily sweating, is where droplets start to fall from the face of the subjective and larger area of the clothing is soaked by sweat.

Ambient parameters

The ambient parameters are factors that mainly is coordinated by the HVAC-system, and could either be fixed settings, or adjusted manually. The parameters can also change by doing interference with the building envelope, like opening windows or doors or block out the sun. The rating given for these parameters is the perception of actual ambient values. Same ambient values can be perceived differently and vary from person to person. The ambient values can however be measured accurately by instruments, yet, subjectives can react differently to them. The psychological and personal parameters are what affects the perception of the ambient parameters and could be seen as the cause of the thermal sensation.

Core/hand/feet thermal comfort

The thermal comfort of core, hand and feet share the same scale and description and therefore chosen to be depicted together. It is based on the 7-point scale that was presented for the first time by Fanger. For this evaluation, the same terms are also been used to avoid confusion.

The score of -3, cold, is the sensation that the subjective need to take action to move towards neutrality as it is really uncomfortable. -2, cool, is the sensation of being cold, but it is bearable for a period. -1, slightly cool, is when it feels a bit chilly and it is just past the limit of being comfortable. 0 is when it is neutral for the subjective to stay in these conditions, and feels either being slightly too cold or slightly too warm. +1, slightly warm, when it is just past the limit of being comfortable and measure is considered by the subjective. +2, warm, is bearable for a short period, but the subjective wants to take measures if it endures. +3, hot, is really uncomfortable and the subjective needs to take measure immediately.

Air humidity

Air humidity is something most do not reflect upon as it usually is between comfortable limits. It could, however, affect the subjective if the air humidity level exceeds those outer limits. The scale

ranges from 1-5, where 1 is dry air, which usually means that eyes feel dry and irritation occurs. 2, little dry air, is when these symptoms occur in a less degree and it is only slightly uncomfortable. 3, normal air, when the relative humidity has no effect on the subjective. 4, little moist air, is when the sensation of air is not neutral and is slightly moist. 5, moist air, is when the sensation of moist air is really strong and the air could smell.

Air quality

Air quality can be related to gases that are in the air as well as particles. Air quality can be measured by taking into account several aspects, which include; CO₂-levels, particles or certain smell. These factors are not directly connected to the sensation of thermal comfort, but with poor air quality the perception of general comfort decreases and could affect the sensation of thermal comfort.

The scale goes from 1-5, where 1 is very bad air and the subjective feels that it affects the mental health, loses concentration and can barely stay in the environment. The score of 2 is bad air, and it represents that it is uncomfortable for the subjective, but the subjective is able to work there and it can occasionally be ignored. 3, normal air, when the subjective does not perceive the air as either bad or particular good. 4, good air, when the air in the environment gives the feeling of being particularly good or well above an average indoor environment. 5, refreshing air, is when the air feels like outdoor air and the subjective slightly feels energy levels rising as a cause of it.

Draught, includes towards neck and feet

Draught is strongly connected to the perception of thermal comfort as it vastly affects the heat loss from the skin. Draught can be local or general depending on the air distribution of the room and type of ventilation system. Therefore, draught is divided into three categories where one is general, and the other two is evaluated based on the draught around face and feet as these are two common places to feel a draught. It is important to note that comfortable draught is dependable on the air temperature. Here, the level of draught should therefore only be evaluated based upon what would be comfortable if the air temperature was optimal.

The scale ranges from 1-5, where 1 is still air and no air movement is felt at all by the subjective. The score of 2, some draught, means that there is some air moving, but not sufficient to be fully comfortable. 3 is comfortable draught, and is not recognized by the subjective as it is ideal. 4 is little too much draught, and the subjective feels the draught as a bit uncomfortable. The subjective can feel it as a small breeze. 5, is way too much draught and the subjective is uncomfortable with it as it is almost like a strong breeze. Typically occurs when the subjective is placed in front of the air inlet.

Other measurements

These measurements are quantities that are being measured with instruments. This is what separates these segments from the other as they are not perceptions. They are evaluated as a substantiate part of the experiment and should be included as they set the state for surrounding conditions. The segments to be evaluated is the outdoor and hall temperature and pulse. The first two are ambient parameters that are being measured and pulse can be denoted as a personal parameter measured by the use of Garmin Forerunner 235.

Before the experiment officially starts, the temperature outside was measured with the VelociCalc. As this device conforms with the surroundings rather slow, the temperature displayed had to be stable for at least half a minute. The measurement was done with a rounding error down to 0,5

°C. Then, the temperature inside the hall, right outside the chamber, was also measured the same way. New measures at these two locations was carried out after the lunch and noted down. This is because the surrounding temperature could influence the chamber. It also affects the subjective as that concerning person may be outside for a few minutes.

Occurrences and headphones

Anything that was to happen outside the regular behaviour inside the chamber was to be noted. Especially when other persons are entering the chamber as they will be recorded by the Kinect. Other occurrences that also could be a disturbance for the subjective was also noted. Such events affect the subjective mental state and could influence the perception of thermal comfort. It was not necessarily affecting thermal comfort directly but could be a cause of improper evaluation. Disturbance from noise or physical illness is typical factors.

Headphones protect the ear and insulate them, and consequently lead to less heat loss. Wearing them also protects somewhat against draught around the head as ears are very much an exposed part of the body. Because of their impact on thermal comfort, it should be noted if they were in use.

4.6 Data processing

The gathered information is now to be compiled and summarized. This chapter will explain how all data assembled together will form this study and make it as a whole. A full investigation of thermal comfort and behaviour can then be examined in detail. There is a lot of processes involved and these will be endured here.

The first thing that had to be done was to process all the data from the Kinect in order to capture the behaviour of the participant which was present during the experiment. Because the Kinect is not yet calibrated in terms of the chamber geometry this had to be done first. By locating each of the chamber's corners and the position of the Kinect, it is possible to estimate the participant pattern inside the chamber by high precision. As the participant only had a small room to move inside, it is easy to illustrate a reproduction of the pattern in the chamber, which usually was between the chair and towards the door.

The Kinect has data from all the movements inside the chamber and also recordings outside the chamber. It is not certain that the Kinect picks up the correct location on the participant body so there is a lot of misrepresented data. Processing such data was done by the use of MATLAB. Each recorded data is found in a table containing precise positions of each of the 25 joint locations in the 'X-, Y- and Z-positioning'. These are enumerated in figure 8 in chapter 3.5. Positions of the occupant are later implemented into ANSYS to create a map which shows each of these locations. An example is shown in figure 27.

This is where the importance of having a proper CFD simulation comes effectuated. Each of these location points corresponds to a certain property of the air at a given scenario. Each day-to-day recording done by the Kinect, is then to be applied to the corresponding simulation carried out, i.e. recordings of behaviour the 13.05.19 is applied to the simulation with an induced air flow of 0.0167 kg/s. Location nodes are then connected to a specific 'temperature' and 'air velocity' calculated by the Fluent software.

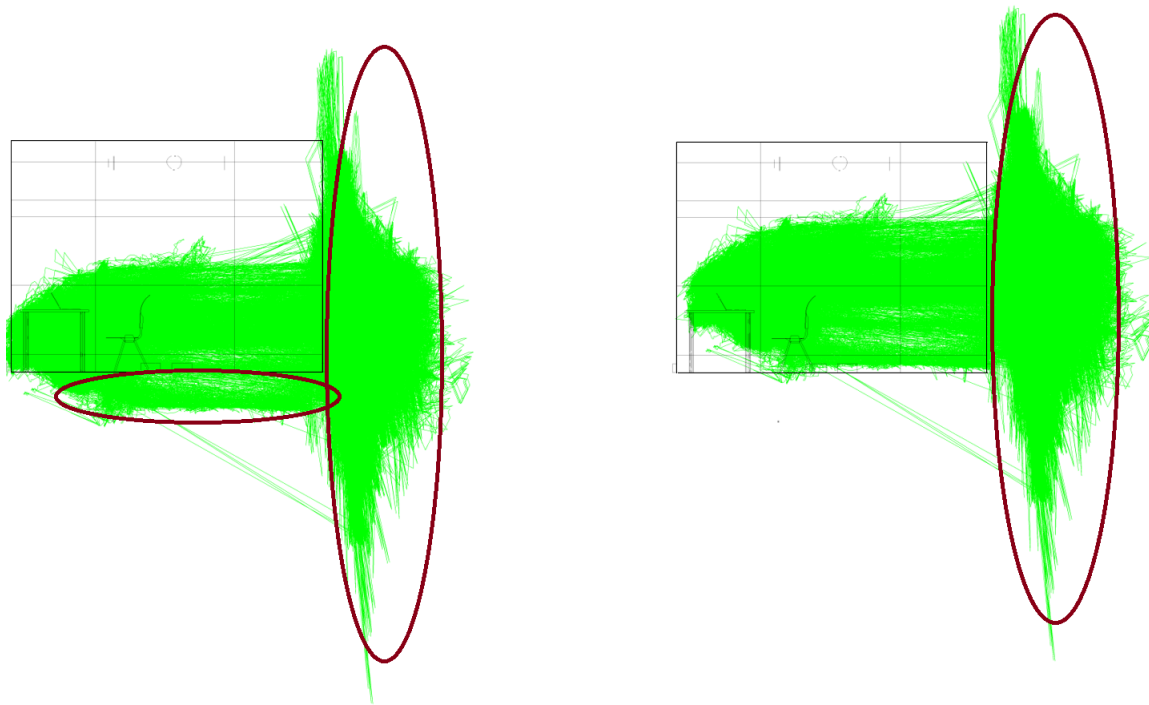


Figure 27: Polyline displaying the recordings of the participant inside the chamber carried out by the Kinect. Right illustration is an adjustment of the polyline.

There was now a file containing both the exact location points of each recording, and a corresponding value of temperature and air velocity. The Kinect also recorded behaviour with deference to time of occurrence. This implements the experimental variable 'time' into the equation. As each recording of point locations are also labelled with a specific time and date. The data are, yet again, processed in MATLAB to create strings of information about time of occurrences and the air properties.

Data outside the geometry were removed as they could be seen as erroneous recordings. The boundary of the experiment was also set at the chamber walls and door so information about the air parameters are also absent. The red circles in figure 27 represent these recordings, which does not have any thermal attributes attached. As the recordings were still intact, these values were set to zero. It was also chosen to leave out recordings when there were two or more persons present during the experiment. This was due to double reading values at the time step and then becomes a source of false information.

The air properties, temperature and velocity, were then plotted accumulative to see the exposure development of each of the 25 joint locations on the participant's body. Each point have a colour attached, which could again be found in the graph. The graphs could also represent several other joint locations. If the Kinect did not receive any information, either because that particular location was blocked or any other fallacies, the value became zero. Equal to the recordings outside the chamber.

Importance of having an accumulative plot is shown in figure 28. There is still possible to see the exposure of temperatures linearly but it represent exposure to an uncertain amount of heat. Over time, the quantity of high temperature or velocity have an uncertain affect on the participant. Seeing the accumulative plot displays the history that of which the specific joint location was exposed to. Thermal sensation is not only momentarily but also represent exposure to previous conditions. Note that the figure is only an illustration of the two methods and does not represent any results.

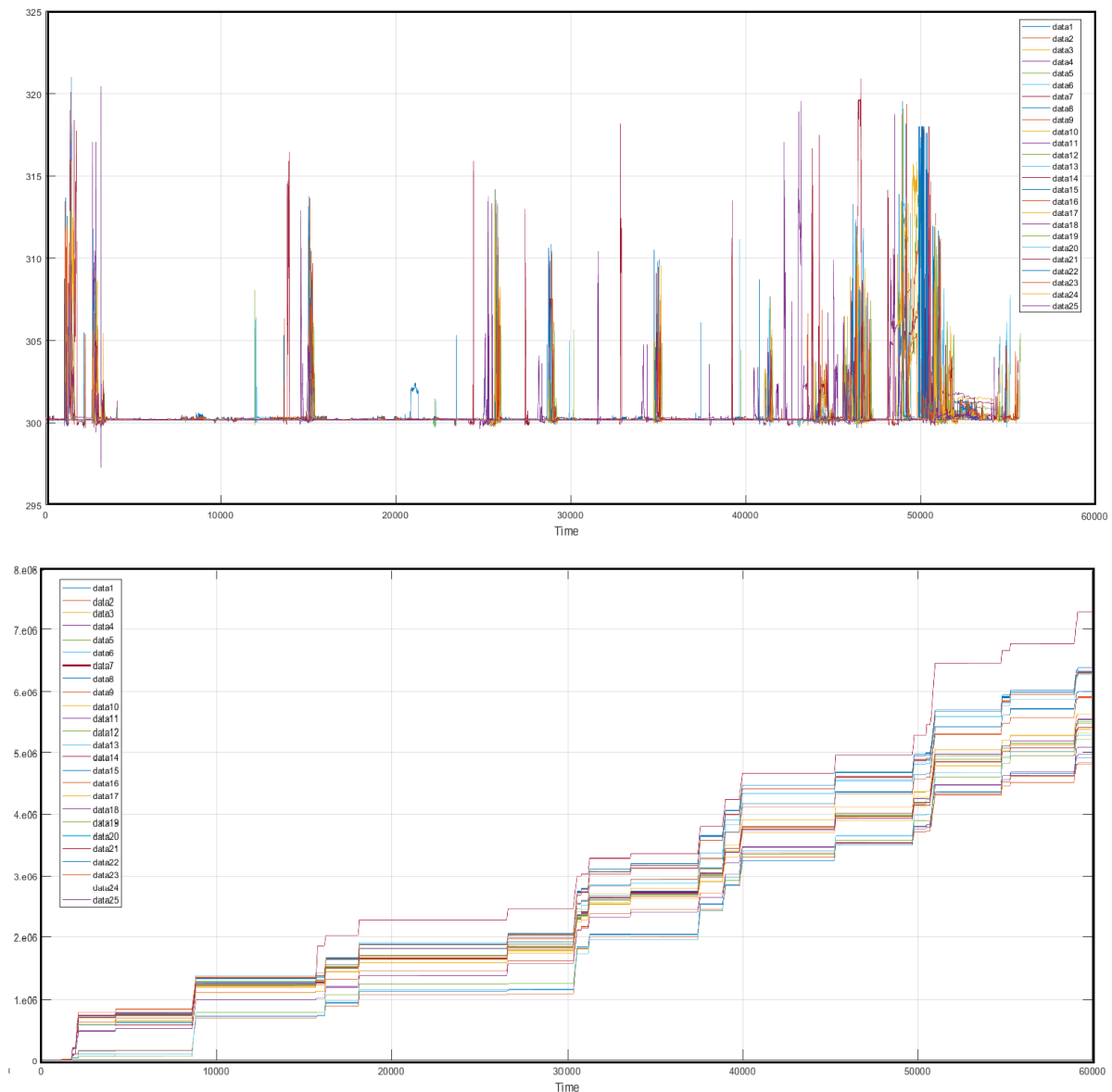


Figure 28: Linear plot of temperature of 25 joint location points compared to accumulative plot.

By the use of accumulative plot it is possible to watch the trend development of exposure to certain conditions, either temperature or air velocity for this case. These quantitative data were directly compared to the evaluation of the participant for further interpretation, the qualitative data. Watching the reported evaluation, and with regard of the exposed air properties, gave the study fundamental information about the thermal sensation and the behaviour of the occupant.

5 Results

Results are presented in chronological order as the methodology in the previous chapter. They can be seen in connection with the study objectives presented in chapter 1.1. Results will endeavour to answer those questions and give clarity on why this study is carried out. These are important to continuing the further work of developing models which would alter relevant industries. This includes topics about CFD models, thermal comfort and behaviour and the response of a subject under a given indoor environment.

Many of the results descend from the work conducted in ANSYS. This includes the mesh, and the solutions from the simulations. Validation was done by the use of several tools, instruments and computational programs. Validation gives the study the reliability of the results and is thereby included in the study. Comparison between different settings and features used are also included in determining the impact they had. Lastly, evaluations from the scenarios put into action are presented. Syndicating these final result will eventually lead to a discussion and a final conclusion.

5.1 Meshing

Meshing is the first step of creating a solid and valid CFD model with an already built geometry. It sets the basis for further development and is decisive for the results. Possible erroneous should be kept at a minimum already here to minimize sequel inaccuracies. Results from the mesh are presented in this chapter and indicate the robustness of the model. Note that the radiator is left out from geometry in this section and does not affect the meshing. Zone 'Chair_222' is also appointed the hex dominant method for the presented results.

Since there are two models, both of them endured an inspection of quality to check for improvement before moving on to the next step which is simulating the model. Certain values should be of minimum, or maximum, to be ratified as acceptable mesh. The models were evaluated by three characteristics; 'element quality', 'aspect ratio' and 'skewness'. These are closer described in chapter 4.3. A brief repetition of the benchmarks for what is acceptable mesh or not, will also be presented here.

5.1.1 Quality of pipe mesh

The simulation starts with air initiated at the inlet of the pipe and is naturally assessed first. Behaviour of air through the pipe is decisive for how air behaves when entering the chamber. To elude continuous errors, the pipe mesh is crucial for the advancing steps to come. The quality is here evaluated to ensure the properties for further simulations.

Element quality

The desirable value of element quality is the value of 1. It means that all edges and lengths have the same proportions to each other. Type of shape is also an important matter to consider, previously described in the methodology. The element quality of the pipe mesh is presented in figure 29. Number of elements (height on the columns) appear for some distinct element qualities to be insignificant to the scale on the y-axis. The amount is therefore presented on top of the column. The x-axis describes the element quality from 0 to 1.

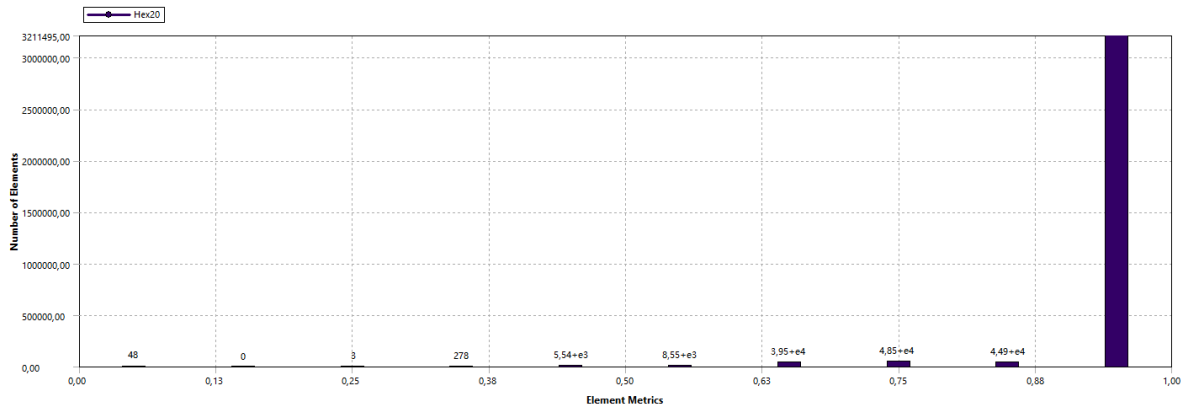


Figure 29: Element quality of pipe mesh. Displaying volume (*y-axis*), the shape of the element and the quality of elements (*x-axis*).

The result shows there is a total of $3.36 \cdot 10^6$ elements in the pipe model and they are all hexagonal. Most cells had a value above 0.88, which indicates most elements is close to the desired value. Very few of them has poor quality as seen from the quantities of cells on the left side of the diagram. The average quality of the cell is 0.9711 and a standard deviation of $5.7688e-2$. These values are provided by the mesh feature in ANSYS and are only roughly displayed here.

Aspect ratio

Aspect ratio describes the relationship between the distance from the face to the centroid of the cell, and the distance from the node to the centroid of the cell. Implying that the value of 1 is a regular element in terms of the element geometry. The pipe model aspect ratio quality is shown in figure 30, where the x-axis represents quality.

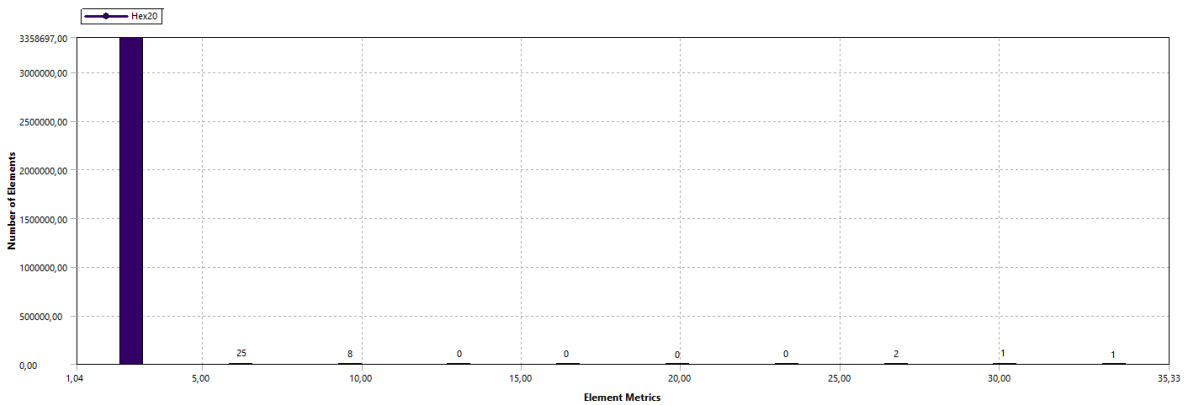


Figure 30: Aspect ratio of pipe mesh. Displaying volume (*y-axis*), the shape of the element and the quality of elements (*x-axis*).

The result shows that nearly every cell has low values when it concern aspect ratio. There is only a few of them that is very crooked. This implies that most of them had shapes which are more or less symmetrical. The average aspect ratio is 1.2148 and has a standard deviation of 0.1489.

Skewness

Skewness is the difference between the shape of an element compared to shape of a cell with equal lengths and angles. A value of 0 means a complete equilateral geometry and is the preferred shape. High values mean the shape is skewed. Such geometries can have trouble with convergence. An average value below 0.4 is considered as good mesh. The skewness of the mesh elements in the pipe is shown in figure 31.

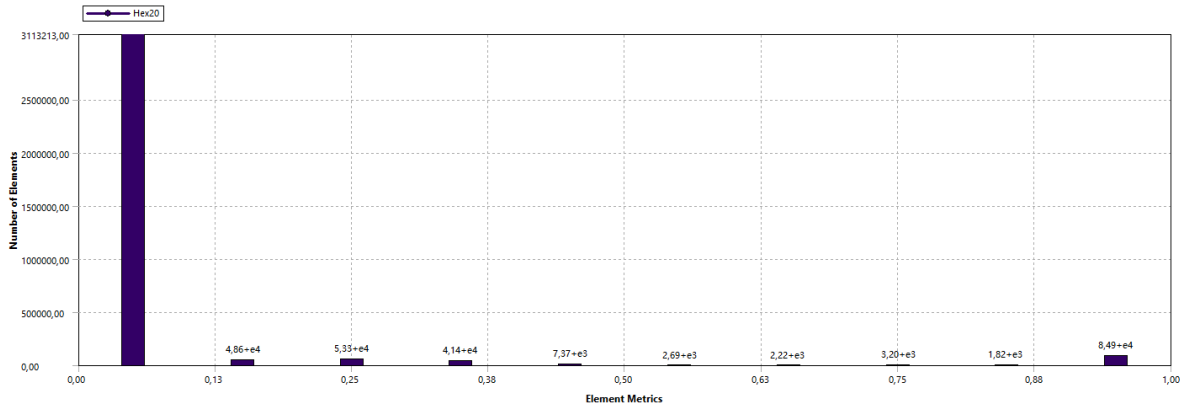


Figure 31: Skewness of pipe mesh. Displaying volume (*y-axis*), the shape of element and quality of elements (*x-axis*).

The result shows that most elements have low skewness. A few had very high skewness and some elements have moderate values. The average value is $3.779e-2$ and a standard deviation of 0.16034 .

5.1.2 Quality of chamber mesh

After the air has passed through the pipe it enters the chamber. This is where the experiment takes place and is thereby another crucial part of the CFD. Creating a model close to the reality commences with a good quality mesh. If the chamber is not well meshed, it is challenging to know if it matches reality. Result of mesh quality of the chamber model will be presented in this chapter.

Element quality

For the convenience of comparing the pipe and the chamber, it is here presented in a similar fashion. Element quality of the chamber mesh is shown in figure 32. Since some quantities become small, it is also chosen to carry out a table to present all of the values. This is shown in the first table in appendix D.

The number of hexagons with high quality is large as seen from the figure. The quality of some of the undesired geometries is also considerably high as they find themselves on the right side of the diagram where the quality is considerably good. The average value is 0.95152 with a standard deviation of 0.11952 .

There is some volume of tetrahedrons in the mesh but very few wedges and pyramids. Evaluation of the four different 3D geometries was presented earlier in table 3 in chapter 4.3. Most of the geometry elements that are not assessed as high quality, stem from zone 'Pipe_432' which was meshed with the automatic method. This zone was almost exclusively meshed by using tetrahedrons and reduces the mesh quality of the model as a whole.

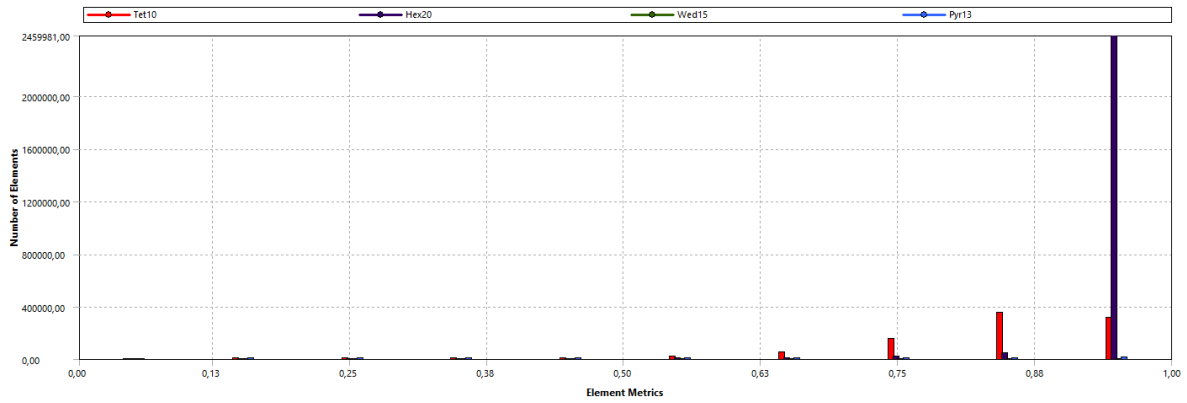


Figure 32: Element quality of pipe mesh. Displaying volume (*y-axis*), shape of the element and the quality of elements (*x-axis*).

There is a total of $3,53 \cdot 10^6$ elements in the chamber model which is almost equal to the amount in the pipe model. This means the mesh produced a number of $11,75 \cdot 10^6$ nodes using the quadratic element order. The linear element order would produce only $2,78 \cdot 10^6$ nodes and was disfavoured because of less accuracy. With an reduced element size of 10 mm, the number of nodes became $84.60 \cdot 10^6$. This was too large and the computational time would be too extensive.

Aspect ratio

The aspect ratio for the chamber model is shown in figure 33. A more detailing description of the quantities is shown in the second table in appendix D.

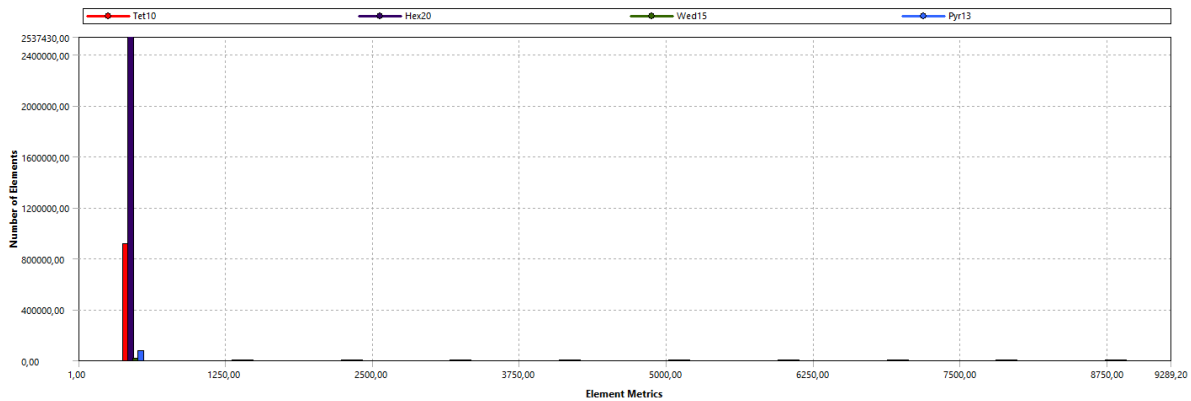


Figure 33: Aspect ratio of chamber mesh. Displaying volume (*y-axis*), the shape of the element and the quality of elements (*x-axis*).

There is a broad range in the aspect ratio since some had a ratio over several thousand and the *y-axis* becomes indistinctly. The cause of this is the maximum aspect ratio of 9289, which is extremely stretched geometry. By taking a closer look at it, every geometry over the value of 40, is either a tetrahedron or pyramid. These are geometries to fill some remaining volume to improve the general quality. This was discussed earlier in chapter 4.3 about hex dominant mesh. The number of such geometries is, however, insignificant.

More interesting is the average value of 1.3998, which is a better measure of the actual aspect ratio. The standard deviation is 7.6617, which also confirms the variety in the ratio. The average value is approximately the same as the pipe model.

Skewness

The skewness of the elements in the chamber model is shown in figure 34. Profound values of the element metrics that hardly can be seen in the figure are enumerated in the third table in appendix D.

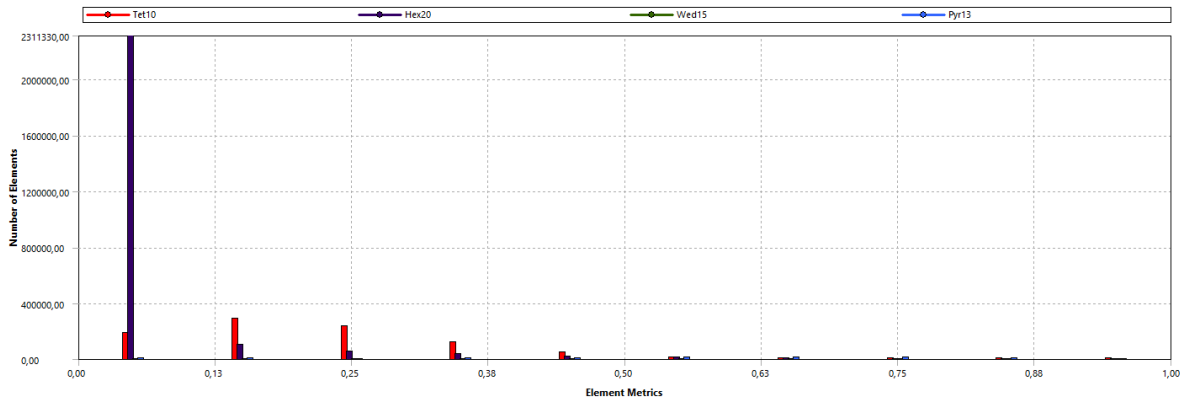


Figure 34

As the benchmark for acceptable skewness by the ANSYS handbook is set to 0.4, nearly every element in the chamber model is within this criterion. Most are also at the lower part of the scale, which is substantiated by the average value of $9.3085e-2$. This average has a standard deviation of 0.15292.

5.2 Simulation

Simulation is the final step in the CFD progression and sums up the work from creating an element to calculating its performance. The results are functions of model precision, mesh and settings chosen and shows the end product from the work conducted until this point. From the outcome of the simulation, the evaluation and interpretation of settings could commence. By running such analysis, features and settings applied could be furthered assessed.

It is at this stage, the erroneous from previous steps arises if not discovered earlier. Reporting these errors is a step towards further development for such models and are of value for other analysts. The results from the models should preferably represent how the component would perform in real life and this should be the basis for the evaluation. Equal states and conditions between the computational simulation and the lifelike scenario are desired for this case. Then, what is an acceptable solution for the CFD would be discussed later. The results, and comparison between models and reality is carried out in this chapter.

5.2.1 Pipe model

The four air flows; 0.0167, 0.0333, 0.0500 and 0.0667 kg/s, were all initiated at the pipe model. Air flow through the pipe and continuously in to the chamber would make a whole case, but is for now separated and the pipe model could be analysed solely. This was done by effectuating all the four turbulence models; the 'Standard', 'Realizable', 'RNG' and the 'SST' model.

For the cause of finding the optimal model, these are now compared towards each other. Performance that would be considered as unacceptable would leave them out for further simulations as it would

be unnecessary to carry out completely with the assigned turbulence model. Results from the cross-section of the four models are shown in figure 35. As it exists sixteen different presentations, only the air flow of 0.0667 kg/s is displayed here. Behaviour of air for different air flow was roughly the same. The black surface divides the pipe in half so only one half is exposed.

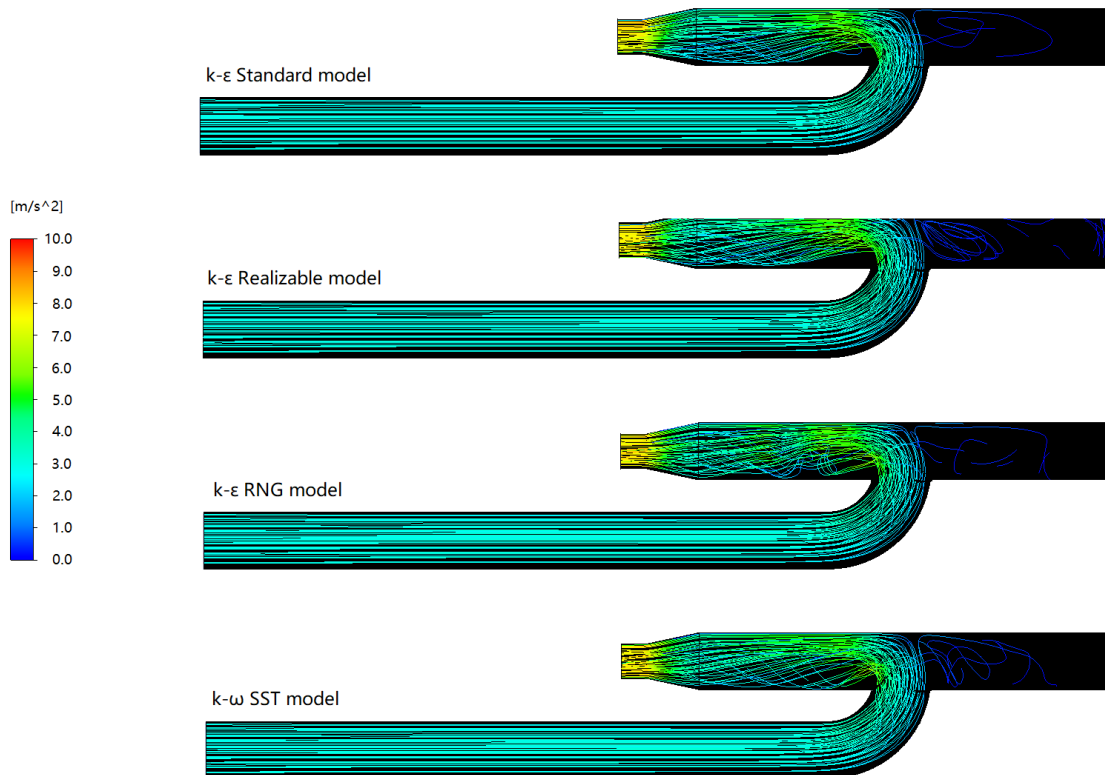


Figure 35: Cross-sectional view of the pipe showing streamlines from the inlet to the outlet. Range of colours represents the variety of air velocities through the pipe.

The figure displays the streamline from the inlet on the left side of the pipe to the outlet. Various air velocities through the pipe are displayed by different colours presented on the colour scale. It ranges from 0 to 10 m/s but confines usually to only the middle part of the scale. The velocity at the inlet is close to 3 m/s and at the outlet the velocity has increased to almost 8 m/s. This applies to all four of the models and their behaviour is nearly equal.

The main difference between them is in the inner area when entering the exiting part of the pipe around the bend. This, however, does not affect the result at the outlet, which they are all more or less similar to each other. Which model is more correct than the other could not be determined as measurements inside the pipe could not take place. Validation could only happen at the outlet.

A more precise evaluation could be performed looking more closely at the cross-section at the outlet, shown in figure 36. The four topmost turbulence models shown, corresponds to the pipes shown in figure 35. The four at the bottom is the cross-sectional look of the chamber inlet, equivalent to the pipe outlet.

Looking at the pipe outlet, the values of air velocities have small deviations from each other. The differences are, however, too small to be validated by doing measurements and all turbulence models were kept for further simulation in the chamber model.

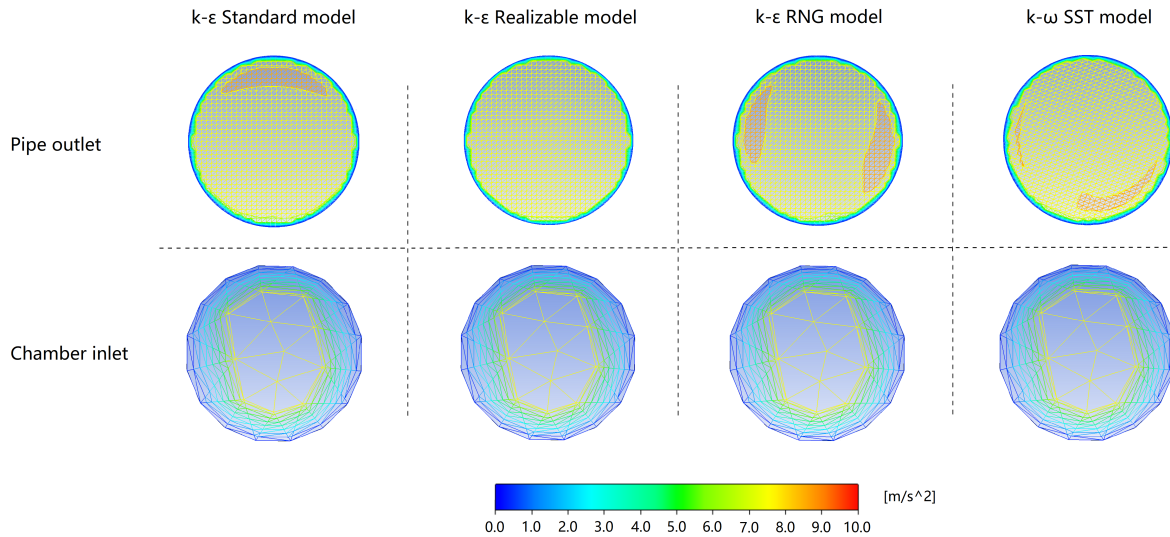


Figure 36: Cross-sectional view of the outlet of the pipe for the four turbulence models. The face was then transferred to the chamber inlet which is in a different geometry model.

Figure 36 also displays the difference when the face of the pipe outlet is transferred to the chamber inlet. Both, the top four and the bottom four, are presented equally in Fluent - using the same scale and equal settings to project the result. The structured lines, which forms a net, each represent a certain value of velocity. As the middle masks have become bigger, the exactness has decreased through the transportation of velocity quantities between the pipe and the chamber model. This has lead to four, apparently equal, chamber inlets regardless of turbulence model.

Assuring their equality were tested by utilising a certain turbulence model for the pipe and simulate it with a different turbulence model in the chamber. As the simulation in the chamber rendered exact same results as with equal turbulence models for the pipe, the distinction between turbulence models seem not to influence any results after the transfer.

5.2.2 Chamber model

The physical parameters from the pipe outlets are then copied over to the chamber inlet. Equal turbulence models are paired up for the pipe and the chamber model. Results from the chamber model are the conclusion of the CFD study, and is the designed product used for creating an analytical tool for thermal sensation. The model should thereby be as precise to the reality as feasible.

The four turbulence models are, yet again, compared against each other to confirm their applicability in later analysis. Cross-section of the chamber displaying air velocities is shown in figure 37. The pink, vertical line represent the cross-section on the corresponding adjacent illustration. The air flow demonstrated is 0.0667 kg/s, equal to the previously presented pipe results.

The figure displays contours of the air velocities up to 10 m/s, as shown in the legend underneath in the figure. The two k-ε models, Standard and RNG, stand out as they have a consistent air flow perpendicular from the pipe, which eventually hits the wall before spreading down the wall. Air movement in rest of the chamber is then reduced to > 1.0 m/s.

The Realizable k-ε and the k-ω SST model has no particular straight streamline from the chamber inlet. Instead, analysis of streamlines shows air flowing directly in the Z-direction. In the Standard

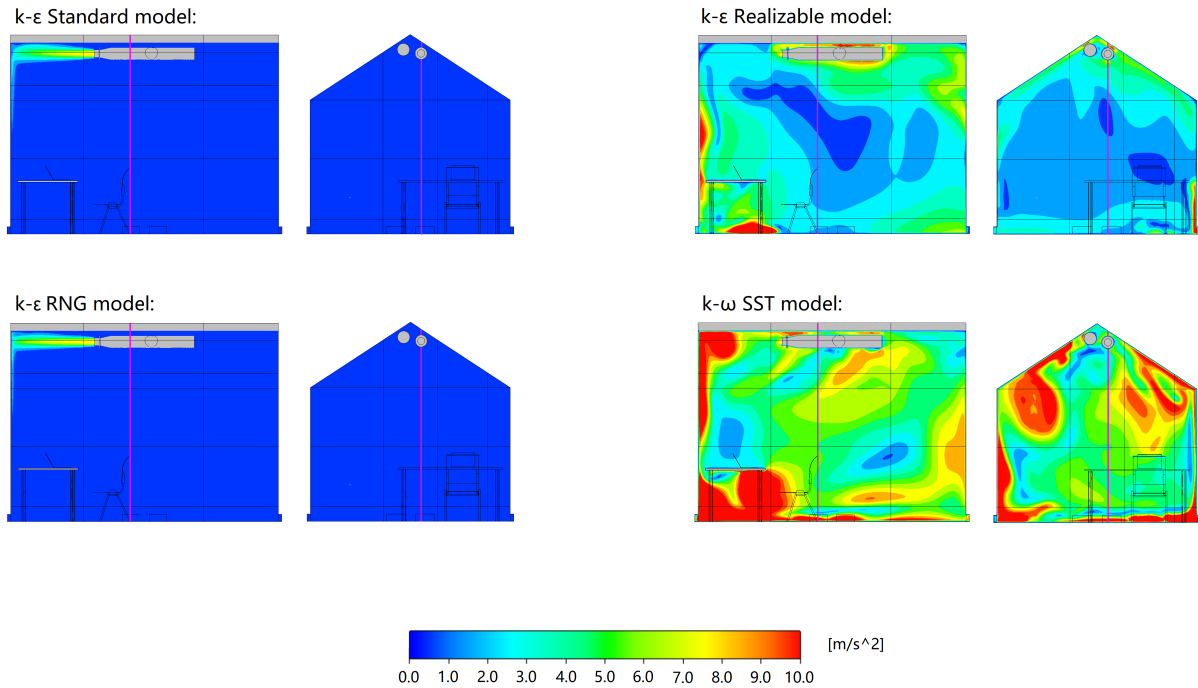


Figure 37: Cross-sectional view illustrating the movement of air in the chamber. The vertical, pink line represent the adjacent cross-section. Contours ranging from 0 to 10 m/s for all four turbulence models.

and the RNG model, the air flow continues in the originated X-direction as seen from the figure. The cross-section, normal to the chamber inlet and the right picture of the illustrations, is behind the chamber inlet. The curvature streamlines in the Realizable and the SST model are therefore not shown here but can be seen in appendix H.

Particularly the Realizable model overstates the air flow close to boundaries at some areas compared to other sections of the room. Areas further away from boundaries are more stable and velocities less than 3 m/s are more common. The SST model seem to evolve some very turbulent velocities at some areas in the chamber. Especially under the table and close to the chamber vertices.

The four different viscous models all renders various results. Temperature for all of them was stable around 293 K in the whole chamber as there are no substantial heat sources. Results from temperature gradients across the room is not interesting yet for these scenarios as they are all virtually equal. Before choosing which model to implement with occupant behaviour, further testing is required. This is carried out by taking measurements from the chamber and compare them to the four models presented.

5.3 Validation

The four turbulence models are now to go through a more extensively analysis where they will be compared against reality. The ventilation system was set to accurately provide the inside chamber with the four air flows, in which the models were evaluated towards all of them. Figure 38 shows the results from the measurements along with the computational calculation of air velocities for all scenarios including the four turbulence models.

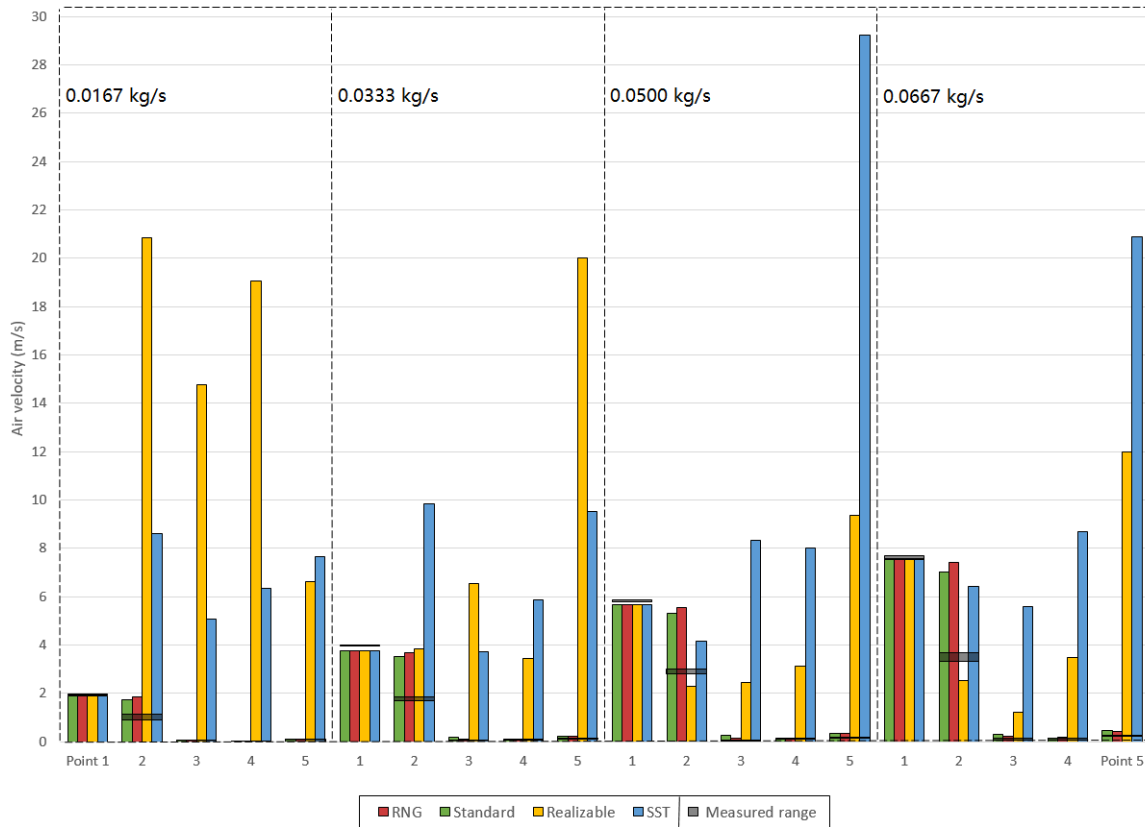


Figure 38: Measures of air velocities for five locations points inside the chamber. Grey, transparent boxes represents the actual measurements. The coloured columns represent each of the turbulence models.

The graphical illustration of air velocities inside the chamber equate to figure 37, but this engages more depth in the analysis. Turbulence models to write off and which to examine further is now attainable. For conveniences, the five measuring points are repeated below:

1. Middle of the chamber inlet
2. 50 cm in front of the chamber inlet
3. Middle of chamber
4. Between chair and table
5. Chamber outlet

In coherence with the findings at the chamber inlet presented in figure 36, the velocity is equal in point 1 for all turbulence model and for all air flows. The differences become, however, extensively larger for the other chamber locations. Here, it is chosen to show the full scale for all findings. Detailing values for the measurements are shown in appendix E. A closer look at the quantities with low values for relevant turbulence models will also be shown later in this chapter. This in particular location 3 to 5 where velocities are close to 0 m/s.

By comparing the measured range, displayed by the grey boxes in figure 38, to the velocities in the simulated models it is eminent what models that are far from reality. The Realizable model responds in a strange way too low mass flows rates as it renders higher velocities for 0.0167 kg/s than higher mass flows. Besides that, accuracy at point 2 can be said to be acceptable for this model when simulating higher mass flows. Overall, the Realizable model seems to overestimate the velocities appearing in the chamber. Further analysis of the Realizable model will not be carried out.

The SST model also overestimates the velocities and does not produce an accurate solution to the scenarios. The model also responds differently to a mass flow of 0.0500 kg/s, as it has exaggerated values at the chamber outlet. This diagram confirms the suspicion that this model is furthest away from reality with a basis in the findings from figure 37. This is mostly due to high air velocities throughout the whole chamber. In resemblance to the Realizable mode, the SST model also embodies some exceedingly high values at some locations. Extensive research on the SST model is chosen not to be conducted.

The two $k-\epsilon$ models, Standard and RNG, are giving solutions close to each other and looks to be almost identical. From the diagram, it is also clearly they mostly provide results near reality as well. It is, however, hard to separate between which one is better than the other and further inquiring of the two are necessary to be conducted.

5.4 Modifying the Standard and RNG model

By taking a more thorough investigation of the two models, the most accurate model will be used as an implementation in the analytical tool. For the benefit of a reliable end product, having a simulation model that presents the reality as close as possible is fundamental. Work conducted here takes the viscous models a step further by tuning the characteristics of the two models.

A sensitivity analysis of different features and model qualities were conducted for both the Standard and the RNG model. The features; full buoyancy effect (FBE) and curvature correction (CC) was first tested. Then, the magnitude of $C1$ - and $C2$ -epsilon along with C_{mu} were adjusted. These three numbering values were theoretically analysed before it was chosen to double their proportions individually.

The sensitivity analysis of these mentioned characteristics and their effect on the two models are shown in figure 39. The grey bar is still the measurement inside the chamber and represents the range of desired air velocity. The Standard and the RNG model are here more closely examined. The first columns on the y-axis, "normal", constitute a model without modifications and is equal to the established columns in figure 38. Accordingly followed by each of the settings which were modified. Note that this analysis does not look for suitable and distinct values, but rather alter the air velocity in the correct direction.

Changing the settings of the model, evidently influence the behaviour of air in great extent as can be seen in the diagram. Some have more impact than others and it can easily be seen where in the chamber the change is significant compared to the original. For example, the full buoyancy effect has absolutely no impact on the results, which also confirm the existence of the gravitational effect.

The curvature correction only has small adjustments to provide the two turbulence models. It has a positive impact in point 3 and 5, where it forces the air to act more accordingly to the reality. Unfortunately, it does not give any correct values, except for the Standard model in point 4, between chair and table. For the RNG model, this area decreased its precision with curvature correction.

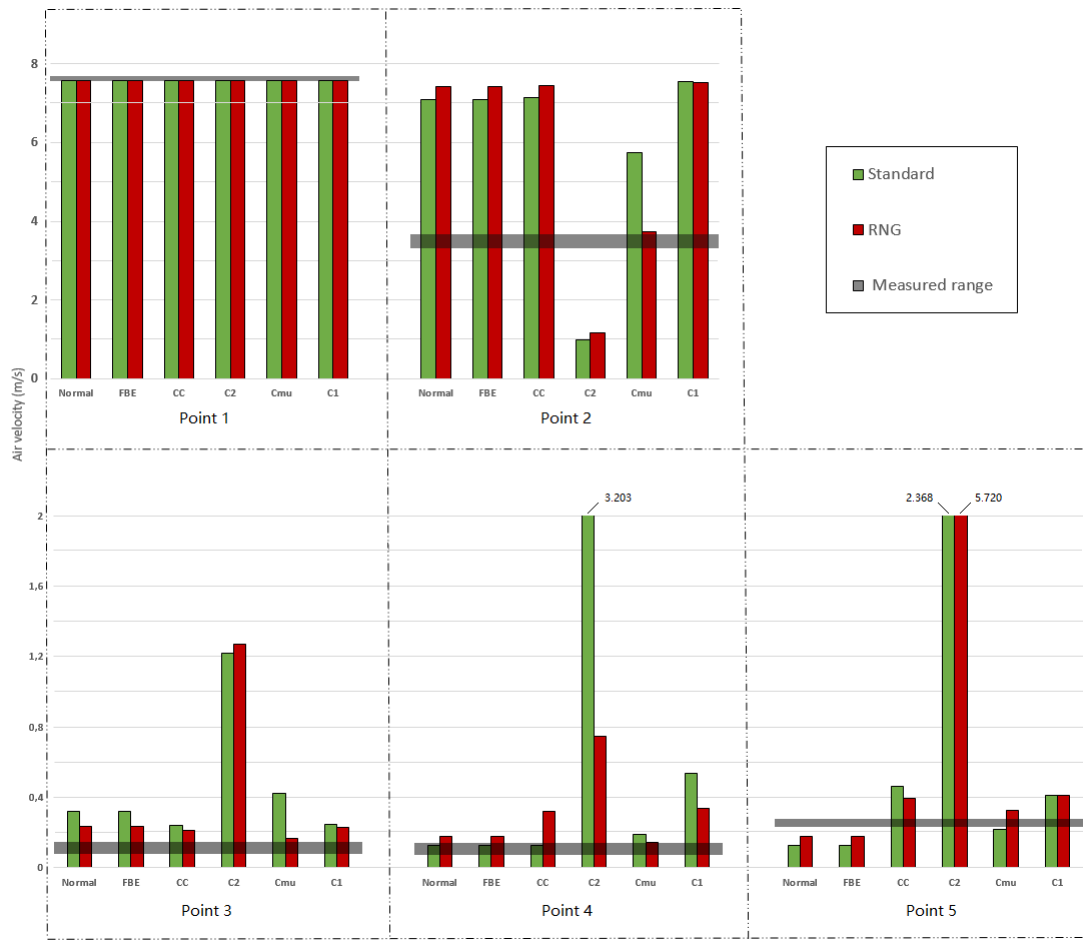


Figure 39: Comparison of air velocity between the Standard and the RNG model for the five locations in chamber. Including a sensitivity analysis of features and model characteristics for both turbulence models.

C2-epsilon was doubled, and had the most impact on the total air movement across the chamber. It had a negative affect on all measured regions far from the chamber inlet, hence point 3-5. This also happened accordingly to the theory, where an increased value of C2 claimed to lead to more mixing of air. Velocity throughout the room has now become more even as a consequence. This is also acknowledged by the drastically reduced velocity in front of the pipe, point 2. C2-epsilon also handle the turbulence models differently. It renders bad precision in point 4 and 5 for the Standard model and for the RNG model it gave values slightly off in location 4 and had really bad influence near the outlet, point 5.

Doubling the Cmu seemed in general to provide better results than the original model. It reduces the velocity in point 2, and also had a positive impact on location 4 and 5. It also corrects the velocity for the RNG model in point 3, but slightly worsen the results for the Standard model.

Lastly, the C1-epsilon was tested by doubling its value. It did not render any drastic adjustments for point 1-3. For point 4, the precision of the model decreased by generating slightly too much air movement. It had, however, positive impact near the outlet by increasing air velocity.

Based on these results, it was evaluated whom of the model characteristics that would benefit further modifications of any of the two turbulence models. The RNG model was selected to proceed with the process of further development. This with a basis in generally improved performance of the modifications and slightly better precision in the original model.

Further analysis of the RNG model

The modifications of the RNG model is carried out to find the balance between the turbulence model characteristics. Based on figure 39, a proper weighting between them is required to reach a precise turbulence model.

Full buoyancy effect was not kept as it was redundant. Curvature correction was kept. Increasing C2 was necessary to adjust velocities in point 2 but should be handled with care because of the great impact in other areas. Increased value of Cmu increased the accuracy of the model and was thereby kept. C1-epsilon did not, singularly, improved the performance to a great extent and was found not necessary to be carried out any further.

Three different variations of model characteristics were carried out by mixing the values of Cmu and C2 with the inclusion of curvature correction. The colours in the parenthesis represents the columns in figure 40. The different tests of mixing model characteristics are listed below:

Table 8: The original RNG model and experiments with model characteristics, values and activated feature.

Try	Curvature correction	Cmu	C2
0. (red)	No	0.0845	1.68
1. (purple)	Yes	0.2535	0.84
2. (yellow)	Yes	0.21	1.3
3. (blue)	Yes	0.2	1.4

The results from the examinations of different RNG model characteristics are shown in figure 40. The values chosen are with a basis in the sensitivity analysis conducted. There were carried out three tests, all with 0.0667 kg/s as an initial condition, before reaching a satisfying solution

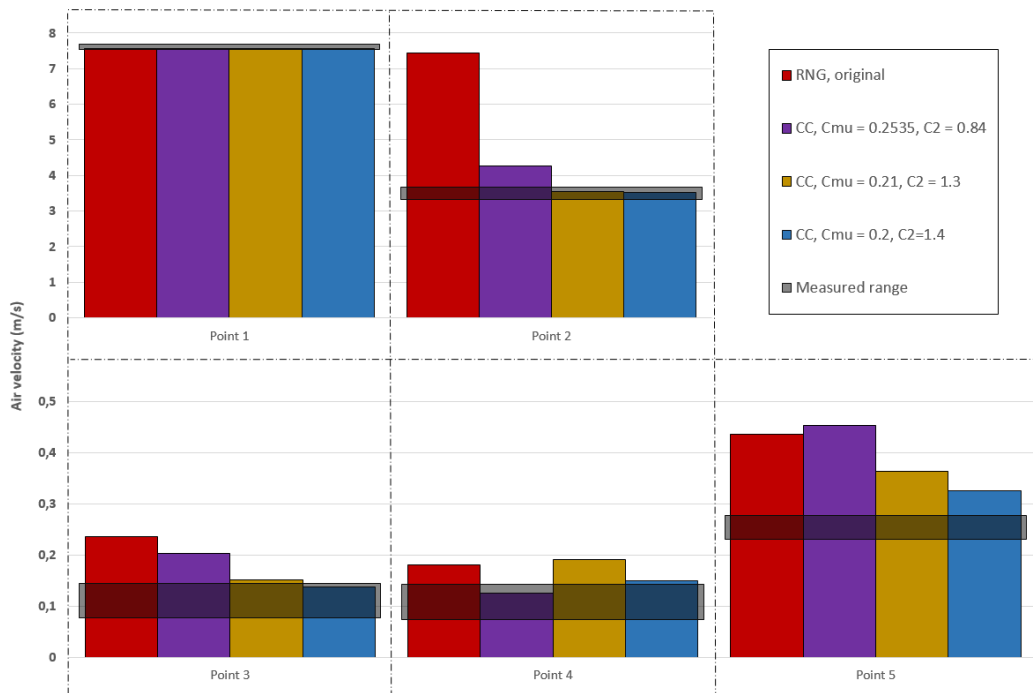


Figure 40: Comparison of air velocity when experimenting with RNG model characteristics at five locations in the chamber.

The experiments of the turbulence model settings show all of them improved from the original. As the value characteristics are mostly based on what is assumed to function and previous results, they behave in a predictable way. Each test altered increased performance and more accurate solutions were produced. The blue column provides very precise results with the basis of the measurements conducted in the chamber. This test applied curvature correction, Cmu was set to 0.2 and C2 was 1.4.

Results from the best performance RNG model for all four air flows are shown in table 9. Values are given in m/s. These can be compared against the measured values presented in appendix E for a thoroughgoing examination. Appendix F1 and F2 shows the cross-sectional view of air velocities for all air flows. Appendix G shows the streamlines at a plane for the air flow of 0.0067 kg/s.

Table 9: *Fluent settings*

	0.0167 kg/s	0.0333 kg/s	0.0500 kg/s	0.0667 kg/s
Point 1	1.894	3.777	5.672	7.566
Point 2	0.865	1.683	2.645	3.533
Point 3	0.033	0.106	0.109	0.138
Point 4	0.047	0.102	0.108	0.149
Point 5	0.074	0.173	0.251	0.325

5.5 Radiator

A radiator was placed inside the chamber to extend the research around other environmental thermal conditions. The radiator had three levels of heat generation and also offered the alternative to just have the fan running. All these scenarios with different heat generations were simulated with constant fan speed and at two different air flows. The fan provided an air speed of 1 m/s right at the exit. Every scenario was run with the air flow of 0.0667 kg/s and one scenario with a reduced air flow of 0.0500 kg/s. In total there were carried out five simulations as seen in figure 41.

The first scenario was just with the fan running with a bestowed temperature of 20 °C, or 293 K. In the result of this simulation was equal to the simulations carried out earlier in terms of temperature but with a slight increase of air movement inside the chamber. Result from this simulation is pictured in the top left corner with a significantly even blue colour which implies approximately 293 K evenly distributed.

With the radiator turned up one notch, the air coming out from the fan had a temperature of 325 K right at the exit. The temperature throughout the chamber then ranges from 297 to 299 K around the area where the participant mostly is. This is represented by the illustration in the top right corner. The effect on the bestowed surface temperature of 318 K on the PC is also visible here.

Turning the heat on the radiator up another notch will make the temperature in the same area rise to 299 to 301 K. Temperature of air coming out from the radiator is now 337 kelvin. Simulation of this is the mid left of the five scenarios illustrated. This scenario was also experimented with two times in the evaluation.

Reducing the air flow to 0.0500 kg/s increases the temperature to be around 303 K, or 30 °C. In the occupant area, this is the warmest scenario of the five which were simulated. It is the mid right illustration and temperature of the fan air is for this case 337 K.

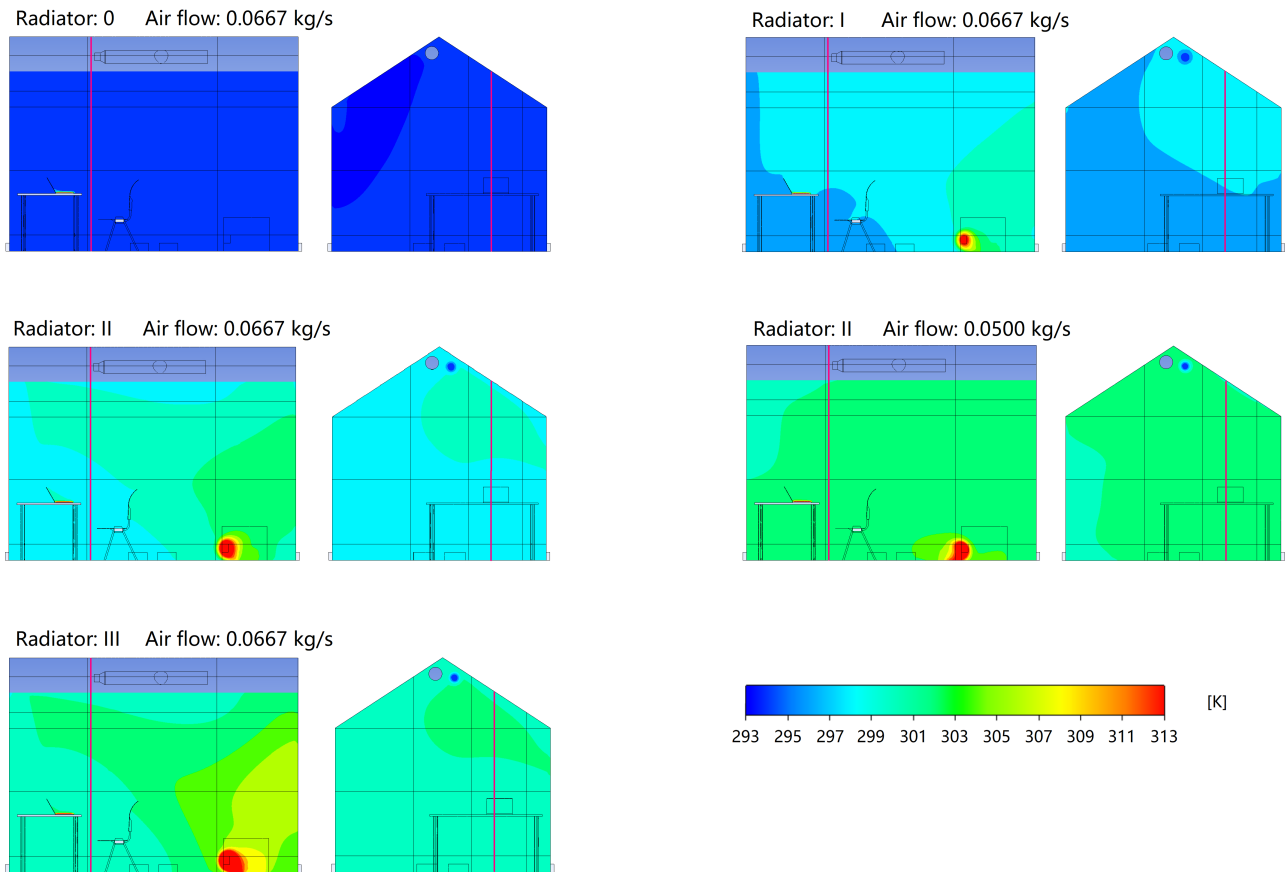


Figure 41: Cross-sectional view illustrating the temperature of the air in the chamber. The vertical, pink line represent the adjacent cross-section. Contours are ranging from 293 to 313 Kelvin for all simulations.

Heat generated from the radiator is then put to maximum load, which implies a fan temperature of 353 K. Air flow is also increased to 0.0667 kg/s for this scenario and is displayed in the bottom left in figure 41. The temperature around where the occupant is sitting is 301 K and close to 303 K in the near area. Temperature close to the door and in that part of the room is up to 307 K in this case.

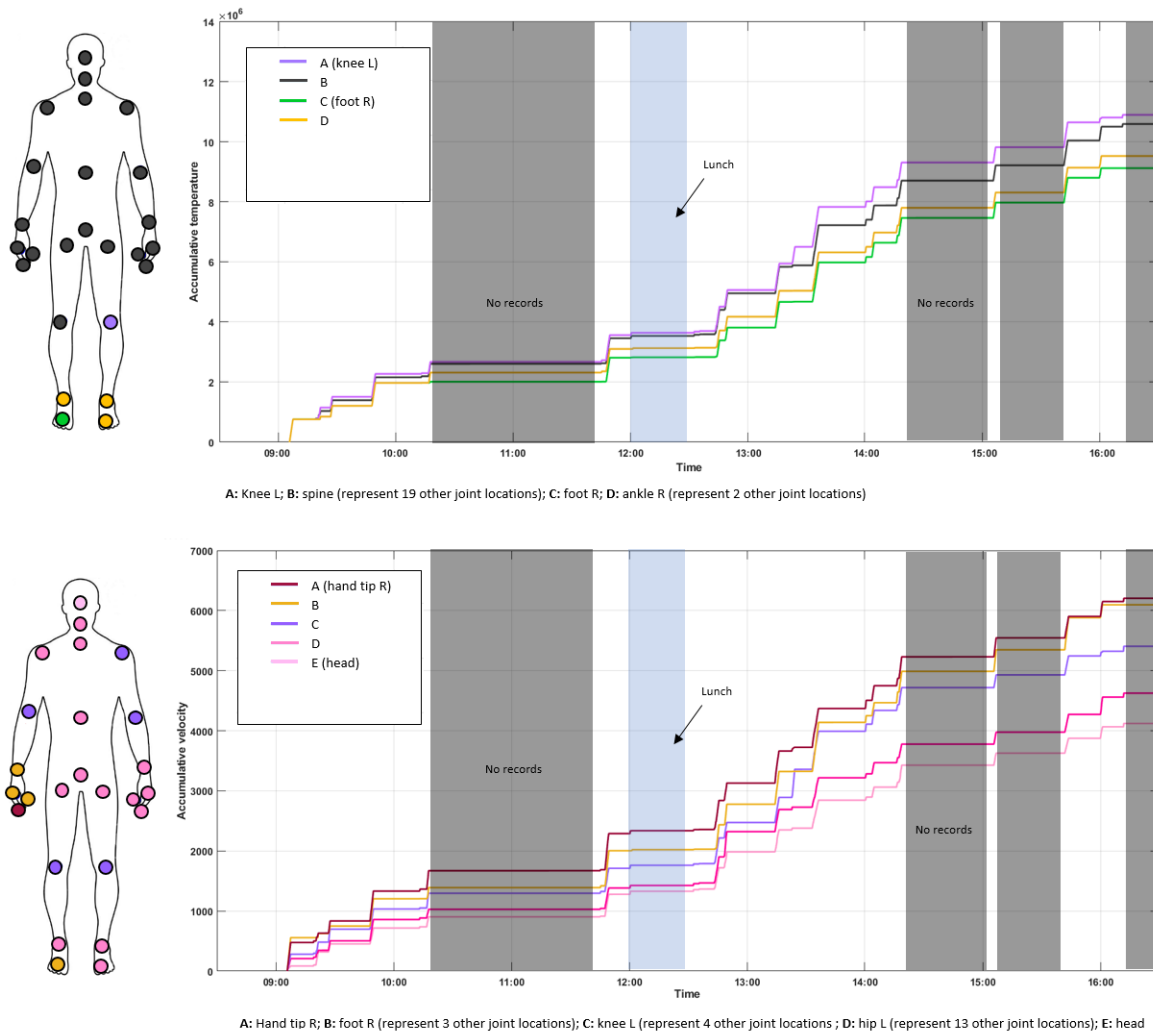
5.6 Evaluation

The subject gave report on the thermal environment every half hour during the experiment. It includes giving report on psychological, personal and ambient parameters inside the test chamber. Other measurements, like outside temperature and temperature inside the hall was measured in the beginning of the experiment and in the middle. Evaluation of the thermal environment is subjectively and represent the one participant which was present. These are the qualitative data from the study.

The quantitative data from this work stems from the simulations conducted in ANSYS. The k- ϵ RNG model was the preferred turbulence model as seen previously, and information about the air properties in each simulation was collected. Data from the Kinect, which tracked the movement of the subject, were compiled together with the data from the simulation to the corresponding day the experiment occurred. The Kinect was able to track 25 joint locations on the body and collect information about each point.

The location points are displayed on the left side in figure 42 and figure 43 with different colour. Each colour represent a graphical illustration of the development of the exposed conditions, hence temperature and air velocity and can represent several joint locations. The properties of air are shown accumulative to display history and quantity of exposure. The grey transparent boxes represent no recordings, which either mean the recorded data was improper, or the participant could be outside the defined geometry. The blue section at 12:00 expresses the lunch break and does not have any recording attached as the subject was outside the chamber.

Data from the 23.05 are shown in figure 42, which displays both temperature and air velocity, respectively. Underneath follows the most important evaluation segments. The scenario for both these are an air flow of 0.0667 kg/s and heater having an effect of II/III notches. The full evaluation conducted by the subject for every segment could be seen in appendix J7.



Core thermal comfort (1-7)	5	5	5	5	5	5	5		5	5	5	5	5	6	5	5
Hand thermal comfort (1-7)	4	4	4	4	4	4	4		4	4	4	4	4	4	4	4
Feet thermal comfort (1-7)	4	4	4	4	4	4	4		4	4	4	5	5	4	4	5
Body movement (1-5)	2	2	1	2	1	1	2		1	2	1	1	1	1	1	2
Sweat rate (1-5)	3	2	2	2	2	2	2		2	2	3	3	2	3	3	2
Pulse (-)	64	63	62	63	60	44	54		62	64	63	64	63	64	61	62

Figure 42: Accumulative exposure of temperature and air velocity at segregated locations on the participant's body. Results from 23.05 with the heater on (II/III) and an air flow of 0.0667 kg/s.

Data from the 28.05 are shown in figure 43, which displays the equal information as in figure 42. These two were particularly interesting because of they display the exact the environmental conditions, i.e. they share the same simulation. The evaluation, behaviour and recordings are however different. The subject's full evaluation of this scenario is shown in appendix J9.

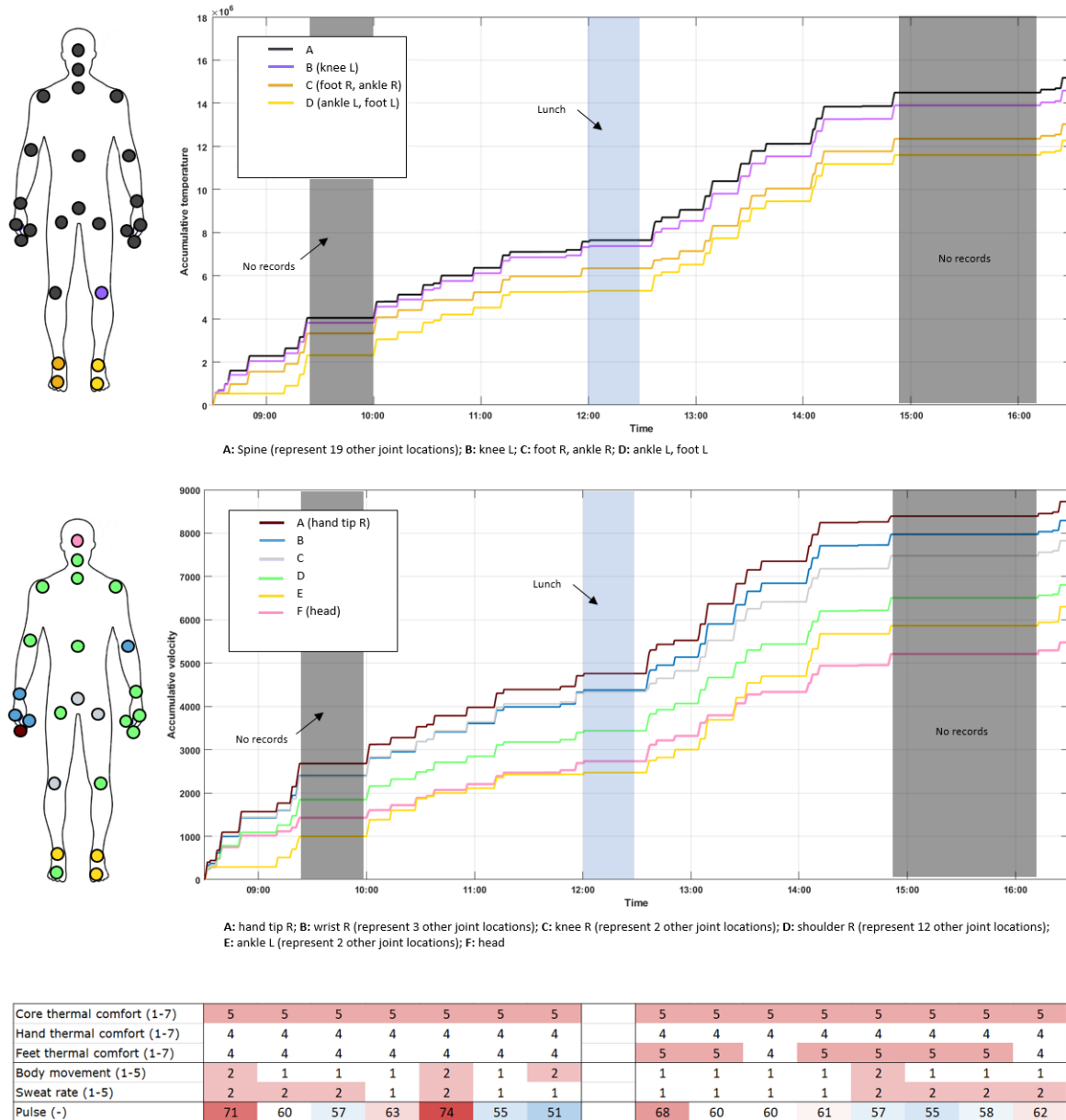


Figure 43: Accumulative exposure of temperature and air velocity at segregated locations on the participant's body. Results from 28.05 with the heater on (II/III) and an air flow of 0.0667 kg/s.

The time of exposure is different and the accumulative values on the y-axis could not be compared against each other. This is due to the amount of 'no recordings'. Only the most significant joint location are pictured in these two figures and a representative average is created to narrow the number of graphs.

By examine temperature development on the 23.05 it can be seen that the four location points at feet level was exposed to less heat and the subject reported 'neutral' thermal conditions. The 'sweat rate' is relatively high during the whole even though the 'body movement' is very low. The 'pulse' stable mostly around 63. It can also be seen that the right side of the body seemed to be exposed to slightly more air movement, while draught around the head is less compared to other locations.

Comparing towards the scenario conducted the 28.05, the feet were, yet again, exposed to less heat compared to other parts of the body and the subject report this body area as 'neutral'. The head and feet are also exposed to less velocities compared to other parts of the body and the right side is more exposed. There are only minor changes when comparing the exposure of different properties.

The most interesting finding when comparing these two scenarios are the change of report, the evaluation of the subject. The thermal comfort is reported more or less equally. Body movement is the approximately the same but the most significant change is the reported 'sweat rate'. This has been significantly reduced for the scenario conducted 28.05. Besides some fluctuating values of pulse, the average pulse has seemed to lower during period the in between the scenarios.

Equal graphs and illustrations for the other eight scenarios can be found in appendix K1-K8.

6 Discussion

With such a comprehensive field of study there are enough discussion points to grab into. There is a significant number of erroneous which could occur during the process of creating the CFD model. There are many steps and processes conducted in this work and each has a possible false input which could affect the end result. These will be discussed here. There will also be presented a few topics around the matter as a whole.

Meshing

Meshing the chamber was carried out by using the preferred method for this type of component, namely the hex dominant method. By running simulations which included the radiator, the temperature gradient increased. Erroneous solutions occurred at some locations in the chamber as a cause of this and were solved by changing the mesh method. Appendix I shows accumulation of heat at a certain location where there is no source of heat and the radiator was not yet been installed. The magnitude of the area increased greatly during the simulations with the radiator included. This pinpoints the importance of having an appropriate mesh with good quality.

It raises the question of how the mesh could affect the results in any other way. This in particularly the two zones with the parts of the pipe. These zones are not interesting areas for the sensation of the subject, but are well influencing the distribution of air in the rest of the chamber. Because in front of the chamber inlet, there is an area that is meshed with the automatic method. If meshed differently, it could impact the distribution of air differently for the rest of the chamber.

The behaviour of initiated air into the chamber in the Realizable and SST model strengthens this suspicion. The streamlines of the air took an unexpected shift in direction before reaching the adjacent zone in front of the chamber inlet as displayed in appendix H. How this only could happen to these two turbulence models, and not the Standard and RNG model is still uncertain. It does not remove the possible uncertainty that the mesh method could have an impact.

It still proves how the results are influenced by the mesh, which again is primarily decided by the geometry. For the hex dominant method, square components are beneficial and make it easier to create a fine mesh. When curved geometries are present, the mesh can produce some vicious mesh and consequently improper results in these areas. This was proven in the zone containing the chair, where an odd phenomenon regarding temperature occurred as mentioned. With the intention of using the hex dominant method, square drawings are preferable to be carried out instead of too many details and bends. Such mouldings make it impossible to create mesh entirely made by hexagonal elements.

The investigation of the mesh quality, in terms of skewness, aspect ratio and element quality, shows that the quality is in general good. However, the quality should be discussed in the two zones containing the pipe, and eventually zone 'Chair_222' when meshed with the automatic method. The rest of the elements are mostly hexagonal, which was desired and also accomplished. The body fitted Cartesian method, applied to the pipe model, worked well as it only rendered hexagonal shapes and generally very high quality as well. The chamber model could also be said have a good mesh, but contains a lot of undesired geometries due to the automatic mesh.

Excluded details

In conflict of what is just discussed about being too accurate in the drawings, other details that were left out of the drawing could impact the end result. This in particularly details along the walls which could affect the behaviour of air. Most relevant is where the induced air from the pipe hits the facing wall as relatively high velocities appear at this place.

Physical properties at the wall could act differently in the simulations and in real life. It is questioned if the simulations would produce the same result if the exterior was equal to reality. Fluent assumes there is 'no slip' at the wall, and how much this affects the simulations is an unanswered question. As the wall, opposite to the entrance door, affect the distribution of air in large degree, the more detailed surface would increase the precision of the simulation. There is no recorded data on friction, shear stress or any other obstacles blocking the air in the simulation. The consequences of leaving out these small details in important areas are not presented in this study.

During the simulation, when including the radiator, there was induced some heat which circulated the room. The modeled chamber is considered to have no outlets other than those small openings at floor level. These openings are the only places air could leave the room and any exchange of heat of any kind is only present here. There is no heat loss through the walls in the simulations, and considering the chamber is only made of thin plastic, some heat is transferred through the wall in reality. There are also small gaps along the floor and at the door, which probably also contributes to infiltration loss or a pressure drop in real life as these are not completely airtight. There was no reckoning for this in the simulations.

Lay out of the actual scenario also does not match completely the scenarios simulated. Most significant, a monitor placed on top of the table in front of the present person. Seemingly, this object blocks air at a critical location in the chamber. By touching the monitor, it was also clearly the monitor also accumulated some heat which as was not calculated for in the simulation. The Kinect device and another small monitor was also present but they were not considered to make a significant impact because of their size and location.

More fundamental is the person who is not included in the simulations. The person would not create any boundary for the air movement and does not disturb the behaviour of air. Any joint locations on the skeleton recorded by the Kinect that is somehow blocked by other body parts are not affected by this in the simulations as air movement is not influenced in any way. Exposed body parts in the front will render precise results, but anything behind obstacles which is not included in the mesh will be inaccurate. The person also generates heat to the chamber which is not been reckoning for.

The problem with this, is the person's movement. A stationary mannequin of any kind implemented in the geometry would create empty space without data. Because the person is dynamic in the chamber, the appliance of a geometric shape of a person also needs to be dynamic. This does not only take the computational process to a whole new level but also requires some computational power beyond many computers today.

Fluent simulation

Change of profile when transferring data from the pipe model to the chamber is another source that somehow could influence the end results of the simulations. As seen in figure 36, all turbulence profiles from the pipe applied to their respective chamber have become equal during the transfer of information. This is not the case in each of the pipe models which is the "proper" solution of the

turbulence models. The effect of the applied turbulence model in the pipe is thereby obliterated. It is, however, evaluated that the results of simulating air through the pipe with different viscous models, was of such equality it did not impact the behaviour of air in the chamber to any great extent.

The cause of this is the transformation between models with different element sizes set for the mesh. Within the same surface area the number of nodes is less dense and this decreases accuracy accordingly. Because the pipe model had 4 mm element size and the chamber 20 mm, accuracy of calculation within an area or volume will decrease as a cause. Selection of element size was a crucial part of in the step of creating a CFD model. More accurate solutions could be rendered with smaller elements. Weighting this alternative for the cost of being able to run less simulations, the decision of keeping the values could be considered as good. However, the chamber inlet surface could have a more fine mesh to create a better transition between the two models.

The four turbulence models did show their differences when simulating the behaviour of air inside the chamber. While the Standard and the RNG model rendered equal and precise solutions in resemblance with to reality. The Realizable and SST model did not match with the reality at all for this case. The Realizable could seem to calculate somehow correctly far away from boundaries. This is highlighted by air velocities below 1 m/s far away from obstacles. Along boundaries, the Realizable overestimates the air velocity and also creates some accumulative areas with very high values. It is also worth mentioning the model gave solutions in contrary to the air flow induced. The lowest induced air flow rendered the highest air velocities. This was doubled checked but still gave the same results. It rises the question if the Realizable model is far more suitable in turbulent flows.

The SST model performed worst of the four turbulence models. This turbulence model were expected to actually work best for these scenarios as it has been used in similar projects before with success [87, 88]. It produced velocities with very high velocities and was already before validations written off as a useful model. In resemblance to the Realizable model, the SST model also produced some equal or higher velocities when air flow was reduced. Testing other turbulence models could also be considered as these two gave improper results right at the beginning. The four viscous models were based on A. Aganovic work but gathering more information about other potential models should also be carried out.

Temperature appointed the air was set with the basis of Y. He's experiment conducted just a few weeks before. It was assumed that nothing was changed or adjusted in which could have made the temperature change from the 20° which was set.

The measurements of velocity inside the chamber is very important for setting the benchmark for what is acceptable and non-acceptable velocities in the simulations. There are no doubt the Standard and the RNG was closest anyhow but when tuning the detailing characteristics of them, the precision of measurements also become important. Point 1 and 2 could be said to have such a range it did not affect the benchmark in large degree. Point 3-5, on the other hand, had very small margins and could be influenced by the smallest occurrence. The Transducer was also not calibrated before use and could give some false results. Using different devices is also not beneficial but were necessary as the differences in velocity were too large. Utilising the Transducer also increased the amount of significant numbers when measuring low air speeds.

Continuously, the adjustments made to the characteristics are also affected by it. There should also be considered that the sensitive analyses was only conducted by doubling the values. Even if it was done with basis of theory, how the turbulence models would behave if the values of C1-, C2-epsilon and Cmu were halved is not exposed. The Standard model responded less good to doubled values

compared to the RNG model. If the sensitivity analysis was taken further, the results could look different and another conclusion could be made.

It was also assessed that increasing the C2-epsilon was necessary for reducing air velocity in front of the pipe, point 2. Because the Standard model had particularly bad accuracy in the important area between chair and table when C2 increased, finding the correct alteration of model characteristic seemed to be more comprehensive work. The basis of continuing with the RNG model was based on the shortest route to the best solution and not the potential of the models. This could be conducted by going deeper into the mathematical construction of the models as knowledge about the inside processes increases.

The effect of the model characteristics is also not mapped when doing a single test by doubling their values. The assumption was based on more or less a linear, or proportional, impact when doubling the value. The sensitivity analysis is only based on two recordings. One with the "normal", or original, model and another with adjusted settings. The behaviour of properties inside the chamber could only be determined if more analysis were made to assure the values more or less was working linearly. In worst-case scenario, the equation is solved with a variable in second exponentiation or more. This will lead the calculation values to eventually turn at one point and go in the opposite direction. It could also be beneficial to test the turbulence models at different air flows and not just 0.0667 kg/s.

Validation

Only the most significant locations in the chamber were also examined for the validation of simulations. These five location points sort of makes a representation of the whole turbulence model. Preferably, every area of the chamber should be examined and compared against the simulations. It is stated that point 4 is maybe the most important location investigated and there should more measures around the area where the person is sitting. Values in other places inside the chamber are less important as other areas are more interesting from a CFD perspective and not an occupant sensation perspective. The precision of the measurements done in the chamber could also be questioned in terms of measuring at the right spot compared to the coordinates applied in Fluent. It was carefully measured up by the use of reference distances but could not be ascertained in any way.

Air flow coming out of the pipe was measured before every experiment to make sure correct velocity was actually induced into the chamber. This was easily adjusted by using the written down notes about valve positions. Even if the valves had fixed positions they could still render various velocities at the pipe outlet. This variety is not present in the simulations as it is fixed for such calculations. Velocities throughout the room could, however, vary even if it is claimed the mass flow was set to 0.0667 kg/s. Which also does not mention the deviation. Position of valves was therefore sometimes different from each other to reach the desired air velocity. Air velocity could thereby fluctuate more than what was measured in the chamber.

The scenarios which included the radiator was just briefly validated during the experiments. The temperature at the fan was thoroughly measured although the displayed value would fluctuate some, which is naturally because of the magnitude of temperature and turbulent air. The input temperature in the simulation could, however, be said to be within 1 K of the measured values. As this only sets the temperature at the fan, temperature throughout the chamber will even out and the differences become minimized. Measurements with the VelociCalc was carried out next to the table and close to the participant to validate the simulation at some degree. Values provided was close enough to

what the simulations rendered for the different scenarios and they could be said to be acceptable. For more validated results, the measurements should be done more thorough and the temperature precision of the simulations could increase.

Experiment

This study was prepared by one person and also carried out and executed by the same person. Evaluation is then maybe biased by desired results for the purpose of the study. The person inside the chamber also know that being exposed to these conditions are done with the purpose of the study and the degree of accepting the thermal environment could be larger. The environment then becomes unnatural for the subject and could somehow affect the evaluation.

This is why such an investigation should contain several persons to compare with. Or, at least have participants without any relation to the study. The environment becomes more natural and the participants are more focused on the sensation. Rather than reporting desired results and a wanted evaluation for easy interpretation. This is why there should be at least two groups present in any experiment conducted. One is the control group which make sure there is nothing external or anything outside the experiment affecting the results. For these scenarios, the control group could be tested by exposing them to a natural thermal environment but tell them differently. It examines whether or not the experiment is influenced by the placebo effect. While the experimental group would actually be tested to the environmental conditions set. They will be tested against the variables in the experiment and will render the result of the study while the control group is used for validation of the study. An experiment done by a psychologist with name Rohles did a study on this and confirmed the importance of having a control group in studies like these [19].

As the experiment was carried out by one person. Every scenario was set up by the person that also was the participant in the survey. It means the air flow was known and the heat on the radiator was known. Expectancy was present for the participant and is hard to come by the fact that the participant could be affected by this.

Persons react to thermal environments different based on previous experiences, physical properties, daily mood etc. In addition to comparing the participant in the study to other persons, the participant should also be mapped in terms of sensation to other conditions. The basic idea is to map out what each person in such an experiment would like to have as reference, e.g. temperature, where the participant has a completely neutral sensation. Then, the evaluation of each specific person in a specific scenario could be compared against what would be the average reference temperature.

The level of acceptance towards the thermal environment is higher when the conditions are fixed compared to an adjustable environment. It is easier to accept something that is decided by yourself and in which can not be changed. For this experiment, there were no actions made to feel more thermal neutral or be more comfortable. There was not allowed during the experiment to leave the door open for periods, turn off the radiator or adjust air flow to change conditions. The participant just had to tolerate the environment as it was and this influence the psychology of that person to just accept the conditions as they are.

Many previous studies looks directly upon the interaction the occupant has towards the building [3, 4, 26, 57]. What were the actions the participants made? These actions were then noted down and compared against the evaluation they gave on the thermal environment. The building is an active part of the study in that case when the occupant actively changes the building. This could be opening windows, sun shading or change set point temperature. Some studies also look upon the

effective use of energy and what measure people take to feel comfortable [3, 26, 61]. Again, this could be analysed opposed to the energy consumption of the building. Many studies prove the fact that fixed conditions lead to less satisfaction with the indoor thermal environment, but are more energy efficient. On the other hand, buildings which let the occupants control and manage in a larger degree has more satisfying consumers but also higher energy consumption.

In this study, the occupant is the only active component. The participant is operating in the building and not with the building. There is no interaction between the occupant and the exterior building in this study after the experiment has started. As mentioned, the building is a fixed element in the study and can not be engaged with. The occupant is not looked through the building's perspective but through a behaviour perspective.

During the experiment the person was exposed to many exterior factors outside those in the chamber. This is mainly why the outdoor temperature was recorded as the weather outside affects our sensation indoor. Hence, 'the Adaptive model' uses outdoor temperature as the only parameter for calculating limits for discomfort. Sun affects persons in that way they feel more comfortable when exposed to sunshine when feeling cold [89]. Or, the sun could affect the indoor climate directly by heating space up because of the solar radiation. This was present occasionally during the experiment as there is a glass ceiling in the hall where the chamber is located. Which is why the hall temperature also was measured.

The participant could probably also be biased by the prediction of what other people sense and act as the person wants to be similar to other groups of people. If everyone around is sitting with a t-shirt, the participant assumes the thermal conditions are warmer than assumed individually. The participant could be drawn towards the expectancy, not just its own expectancy, but also according to what other people expect and think. Seeing other people with e.g. less clothes would send signals to others to think it is warmer than they feel.

Evaluation

Evaluation of thermal sensation is almost an endless discussion many analysts still can not end. With the inclusion of physiology, psychology, history and behaviour, occupants sensation becomes a composition of many factors and result in a very complex field of study. It is fair to say the evaluation conducted in this study also rises the question about influencing factors. A profound thermal model is yet to be found. In the meantime, each study must thoroughly evaluate possible of sources which makes an impact on the evaluation.

The evaluation parameters are all qualitative data which is the subjective opinion of the participant in the study. Which implies a lot of uncertainties attached to the evaluation. It is fair to say, based on the discussion about the experiment, that evaluation is not reliable data. No one can predict another person's perception of the thermal environment and no one can with certainty know exactly how a neutral condition of that person is. This evoke the term 'thermal alliesthesia' back. Where the sudden exposure of, e.g. warmer conditions could be reported as 'neutral' for a person who has been exposed to a cold environment. While the same environment could be reported differently by another person who is already in 'neutral' state. As the experiment had only one participant present, the uncertainty around that person's perception is big.

Thermal alliesthesia can also be said to be an impact of the outdoor conditions and pinpoint the importance of measuring the outdoor temperature. The first evaluation in the morning and after the lunch break, when exposed to the outdoor weather, is often different from other periods as seen in

the evaluations in appendix J1 to J10. This is mostly due to the level of activity and the thermal conditions. Going into a warm building is completely different in winter time and in the summer time. If heat is already accumulated in the body, exposure to colder conditions is a lot more pleasant for the subject.

Thermal comfort was thoroughly evaluated in this study and a few interesting data were discovered. From the results of the evaluation it is clear that the participant felt more satisfaction when being exposed to the same scenario over again with the radiator on. The sweat rate also decreased throughout the experiment as a cause of being exposed to heat over several days. It is just not about the acceptance of the thermal environment but the response was also physically and uncontrollably by the mind. This pinpoints the importance of knowing what circumstances the participants have been exposed to before the experiments. Adaption seems to have a big impact on thermal sensation and previous experiences thereby become important.

Based on the evaluation from the 23.05 and 28.05 it is eminent that the subject adapted to the thermal environment. If this is mainly an effect of psychological or physiological factors is uncertain. Over several days of being exposed to very hot conditions the sweat rate is reduced as a cause and slightly pulse likewise. Sweat rate is a physical reaction to the conditions and can not be said to be a subjective opinion as with the evaluation of the ambient parameters.

The experiment was run over a period of over two weeks with involuntarily gaps or breaks in between. The effect of adaption is thereby uncertain in this case. A few days break could have a drawback on the adaption and probably would change the evaluation in some degree, especially during the scenarios with the radiator. The experiment should, therefore, preferably have a consistent schedule for when the experiments took place so the phenomena of adaption could be properly examined. Either by excluding the variable with adaption and long fixed breaks between or have a day-to-day experiment where adaption would be included as a parameter.

Adaption is not an uncommon phenomenon when discussing thermal comfort. Persons adapt to other people, the weather and the environment around. This in particularly the thermal environment around. A sudden change in temperature could make the participant feel uncomfortable and it is not necessarily decided by the temperature being exposed to. It is rather the temperature change in which the participant is used to. By being exposed to a certain temperature, a person's neutral state will move towards the desire to always experience this temperature. History of the participant in the experiment should, therefore, be reported to have knowledge of what conditions it has been exposed to earlier. This was particularly present during the scenarios with the radiator. The participant seemed to start adapting, both physically and psychologically, to the environment.

Evaluated parameters

There are also several other things that could influence the result of the evaluation. The term 'clo' does not say anything about the distribution of clothing on the body and could affect the feelings of draught on limbs or other parts. This in particular the sensation of 'draught around neck/head' or 'draught around feet'. A better description of clothing should rather be enumerated to different parts of the body, e.g. divide the term to apply to the upper and the lower body. For this study where joint locations are examined precisely, this is particularly important. By the use of the applied calculator it could also be considered to enumerate clothing in this study by the precise number and not with a resolution of 0.2. It does, however, represent the value with some uncertainty with this resolution. It was also done with the thought of maybe run scenarios where the participant overdid

the 'clo' and the range would be much larger. Headphones were an accessory with many aspects around the experiment attached. It is first and foremost not a consistent wearing throughout the experiment and it had to be reported if it was a utilised subject or not. This is because it adds to being a clothing and an insulating layer. The 'clo' value is uncertain and not a part of the table used for calculating clothing. What amplifies this subject's importance is the location of it, as the head is claimed to contribute to most of the human body's heat loss. Another interesting thing is the noise protection it provides and benefits from making the participant more comfortable with the surrounding, especially the acoustic environment.

Headphones were an accessory with many aspects around the experiment attached. It is first and foremost not a consistent wearing throughout the experiment and it had to be reported if it was an utilised subject or not. This is because it add to being a clothing and an insulating layer. The 'clo' value is uncertain and not a part of the table used for calculating clothing. What amplifies this subject's importance is the location of it, as the head is claimed to contribute to most of the human body's heat loss. Another interesting thing is the noise protection it provides and benefit from making the participant more comfortable with the surrounding, especially the acoustic environment.

Pulse was measured by the use of Garmin Forerunner 235. The accuracy of the pulse measuring device is not stated but could display value that did not reflect the reality occasionally. Because it measures pulse momentarily, the displayed value could jump up to fifteen beats within seconds. Pulse was read without caution of this and could in some cases not represent the beating of the heart. In general it could still be said it rendered stable results which are probably a good envision of the reality. However, it did render some values that seem to not represent reality. The lowest pulse was measured to be "37". Measured in case I as seen in appendix J1.

Based on the evaluation, some parameters were found unnecessary. The reported 'Psychological parameters' are indeed interesting in terms of what is happening to the participant. But as the participant was not exposed to any intense strains of any kind, the parameters were mostly stable. It could be assumed they only have created consequences when the participant is exposed to more extreme conditions. Like being under a lot of pressure or in an environment where the excitement level is high. Psychological parameters should still be kept as a tool for observing the participant.

The personal parameters tracks mostly the participant's physically appearance. Most of them proved to be valuable regarding the sensation of thermal comfort. Some of them had also a strong correlation with the sensation as well where the evaluation had some coherency. It could, however, be questioned if the 'body positioning' was necessary to report as the participant mostly was comfortably seated.

The sensation of ambient parameters provided various information where some are essential and some unnecessary. The sensation around feet is one of those who was not particularly interesting. This applies to both the 'feet thermal comfort' and the 'draught around feet'. Wearing trousers and shoes prevent any verdicts in the evaluation of draught around them. The same applies to the parameter 'feet thermal comfort' as it was mostly stable in this case. This is due to the fact the participant was indoor and the conditions were good to keep them comfortable.

Draught elsewhere where also not that interesting as the air flow was too low to have any eruption in the experiment. The maximum load of air flow in this study could barely be felt. It could also be discussed if the sensation of draught is biased by the fact that this was the maximum air speed that was provided as the participant knew this. Just the slightest sense of air movement would then be reported in that case. Regardless of that, the parameters of evaluating draught should be kept for a similar experiment with higher air velocities.

'Air quality' and 'air humidity' is not easy to give an evaluation on unless the participant is exposed to any reference levels. This is because these two parameters are easily to adapt to. Air quality could almost only be evaluated by walking in and out of the chamber to really have the sensation of it. Air humidity is also unnoticed most of the time unless exposed to extreme values. The radiator gave some verdicts on these parameters but exposure to "normal" conditions could be found unnecessary to report. Equivalent to some of the psychological parameters, air quality and humidity should only be reported if there is an experiment which is conducted with the purpose of testing these parameters exclusively.

The 'core thermal comfort' is the most weighty parameter in this experiment as it sort of is the accumulation of all other parameters. It is also the represent the sensation which is easiest to report as it is a feeling with constant reminders, i.e. the body send signals of core thermal comfort quite frequently and is hard to ignore [6, 90]. The 'hand thermal comfort' is more like a supporting part of the overall sensation of thermal comfort. It could deviate from the core thermal comfort and could often be just an indication of being cold. This is due to the fact that blood flows to the core when the environment start to feel cold.

The temperatures measured outdoor and inside the hall worked for this experiment as control parameters. Especially the outdoor temperature is more a psychological effect than a direct effect on thermal comfort. Exposure to warm conditions over a longer period could lead to some heat accumulation during the time the exposure lasted. This was, however, not the incident in any scenarios.

Processing of data

All the data from the Kinect was transferred to MATLAB to carry out strings of data about the participant's movement through every scenario. These are quantitative data from the simulation and are trustworthy to the degree of the precision of the model. This emphasises the importance of conducting a reliable and accurate model.

The geometrical model was used for calibration points to print the behaviour inside the chamber. Each corner, and the Kinect device itself, provided coordinates which was applied to the cloud of information. It was assumed that the coordinates were the same for each scenario. If the camera was touched or moved, the calibration location points could be different from that point in time. Which implies a disturbance towards the joint locations for the other simulations and the behaviour pattern could be slightly tilted.

From figure 27 in chapter 4.6, there is possible to see how the polyline does not match completely the chamber as there are some recordings below ground level. Processing the data should preferably be validated directly in the geometrical model once again before further processing. This way, the calibration could with certainty be more correct.

This could also explain why is was commonly that the accumulative temperature or velocity at feet level was below all other location points on the participant's body. A cause could be the lack of data as recordings outside the chamber geometry had to be put to zero.

When the subject reported visitors, the data from this time period had also had to be set to zero. This was due to double reading values for that time step and would cause improper results. The visitors was only present during a short period of time but caused some lack of data during that period. Erasing one person from all the strings of data when two or more was present was in this study seen as to comprehensive work and was not conducted.

The Kinect also had its weakness that it does not record information when the joint location is blocked or hidden somehow. Placement of the Kinect must be done carefully and without interrupting behaviour and also without being moved as explained. This limits the range of area it could record to some degree. More beneficial for developing such tools could be having such an installation which could be placed on the ceiling instead at floor level. This would ensure a bigger range and without being disturbed.

A depth analysis of exact behaviour could for further analysis be conducted. Hence, it would be a replacement for reporting 'body position' and 'body movement' in the evaluation. The recordings show exact location for 25 joint location points and creating a time line with each position would reproduce the behaviour of the subject. Then, validating the report of activity could be conducted and also without the subjective opinion. The Kinect could also mismatch some location point and exchange the data between two points, as stated by a study done by Dziedzic et al. of the "depth registration camera" [91].

7 Conclusion

Background for this work was to design a three-dimensional CFD model to conduct field measurements in given thermal indoor environments. Results from the gathered information are later processed to derive an investigation of thermal comfort. The literature demonstrated the complexity of carrying out reliable data with a broad diversity of parameters to consider. Existing strategies can in many cases be found to give an inaccurate presentation, which is emphasized with a vast number of thermal comfort models.

Achieving thermal comfort should be balanced with the thought of energy consumption as many countries have agreed upon reducing the emission of green house gases. The behaviour of occupants is thereby one of the first steps toward understanding the fundamental causes of discomfort. A Microsoft Kinect device monitored 25 joint location points on the subject in the experiment to trace position and movement inside a test chamber which represented a conventional office cell.

Together with the recording from the Kinect, the participant gave reports every half hour of different parametric quantities. Concerning psychological, personal and ambient parameters along with other occurrences. They were later compared against the thermal conditions the CFD simulation from ANSYS provided. Rendering a model which represent the reality is thereby important to procure reliable quantitative data.

The geometry of the chamber and containing elements were drawn in detail and with regard to the mesh method. The were created two geometrical models, the pipe model and the chamber model for the purpose of producing the fine mesh. The 'body fitted Cartesian' method was applied to the pipe model and the 'hex dominant' method for the chamber model. Quality of the mesh for both models was found to be generally very good by utilising these methods to the established geometries.

Four turbulence models were applied to the geometrical models to investigate how operable they would be in the circumstances. After tuning model characterisation, the k- RNG model was found to provide a good representation of the actuality and was selected to be the applicable viscous model. There were accomplished ten scenarios in total. Four different air flows were tested, ranging from 0.0167 to 0.0667 kg/s, and in addition to the presence of a radiator with different effects.

The qualitative reported data from the participant showed that variety of the air flows was too low and reported insignificant differences. When the radiator was positioned inside the chamber, exposure of air temperatures up to 30°C leads to adaption over time, both psychologically and physically. The participant was exposed to a fixed environment. Where no measures during the experiment could be made, and is an important factor to consider as a cause of the acceptance the participant experienced.

The qualitative data from the participant's report is directly compared against the quantitative data from the Kinect and the simulations. Showing the accumulative growth of temperature and air velocity for each of the 25 joint location points could unveil the potential of sensing discomfort with the thermal environment. It also reveals the potential of experiencing temperature gradients as well as the thermal history of the subject.

With the complexity of estimating thermal comfort for given environmental conditions, developing depth analytically tools are necessary. The industry would benefit from this by knowing exactly where to allocate the building's energy consumption to provide good solutions. This, in regard to provide a satisfying thermal environment for the occupants.

8 Further Work

This study involves many aspects where each could be closer examined. This chapter will propose some ideas for how this study, and the industry in general, could improve and continue the development. There are many variables to consider and the question of increasing or decreasing them is still present. With an extensive number of factors to consider, future work in this field should put up a well organised study. It must be thoroughly conducted to minimize the quantity of erroneous and ensure reliable results.

The experiment was conducted throughout a period of over two weeks, which means there is some gaps between the scenarios. Adaption towards the indoor climate was one of the most interesting findings in this study but to what extent is still uncertain. Comparing day-to-day scenarios to one scenario a week would to a certain degree find the effect of adaption.

It was also just one participant present during the experiment and that person had a history of coping with indoor conditions different from other persons. Comparing with other subjects would render more reliable qualitative results. Involving a large group of people in a bigger space would make it possible to compare more subjective data of the thermal environment.

A representation of different genders and people within a certain age could be closer examined. Other factors to consider are running experiments at a different time of the year. The adaptive model put weight on the outdoor temperature as the only representative parameter needed. Equal indoor conditions in comparison to different outdoor climate could be closer studied to validate the comfort model.

In this experiment, the environment was fixed, i.e. the participant could not change any indoor parameters or personal parameter, e.g. level of clothing. These restrictions ensures there are less variables in the study and make the results easier to interpret with less possible sources of improper conclusions. It could, however, be interesting to see what measures the participant would make if exposed to conditions beyond the level of comfort.

Phenomena that occurs could be interesting for the purpose of studying the energy consumption. If the exposure of a certain thermal environment would lead to less or more energy consumption, results could be valuable findings towards a suitable indoor climate with regard to energy use. Saving energy should not be on the cost of the indoor conditions. If participants take measures to change the environment which leads to higher energy consumption, the two relations needs a proper weighting. Constant awareness of the energy consumption could also be closer studied along with provided information about features of the building and recommended measures.

Temperature was only adjusted by implementation of a radiator which led to an increased heat production. For further investigations it could also be interesting to see the effect of reducing the temperature of the chamber. Exposing the participant of what could be considered as a cold thermal environment could later be compared with the findings from the warm conditions.

Reported parameters with no significant changes could be narrowed down and other parameters excluded. They do not have the fundamental impact on thermal sensation but can not be excluded as factors to consider.

Creating CFD models are precision work and does not necessary provide good solutions as seen. Continuing the development of such models are essential for providing reliable results in a study like this. Having a dynamic mesh would also benefit the calculation accuracy.

References

- [1] K. Bramslev M. Lie. Arnstadutvalget, energieffektivisering av bygg. Technical report, Arnstadutvalget, 2010.
- [2] Benedicte Langseth. Analyse av energibruk i yrkesbygg. Technical report, NVE, 2016.
- [3] J. Pfafferott D. Kalz. *Thermal Comfort and Energy - Efficient Cooling of Nonresidential Buildings*. Springer, 2014.
- [4] G. Brager et al. Evolving opportunities for providing thermal comfort. Technical report, UC Berkeley, 2015.
- [5] D. Enescu. A review of thermal comfort models and indicators for indoor environments. Technical report, Valahia University of Targoviste, 2017.
- [6] Ken Parsons. *Human Thermal Environments*. Taylor and Francis, 2014.
- [7] B. Grinden N. Feilber. Ny kunnskap om fordeling av strømforbruket. Technical report, SINTEF, 2006.
- [8] R. A. Gaggioli. *Thermodynamics: second law analysis : based on a symposium*. American Chemical Society, 1980.
- [9] P. S. Ghoshdastidar. *Heat transfer*. Oxford University Press, 2012.
- [10] R. De Dear et al. Convective and radiative heat transfer coefficients for individual human body segments. Technical report, Macquarie University, Sydney, 1997.
- [11] M. Bahrami. Forced convection heat transfer. Technical report, Simon Fraiser University, 2011.
- [12] The Physics Classroom. Methods of heat transfer. <https://www.physicsclassroom.com/class/thermalP/Lesson-1/Methods-of-Heat-Transfer>, Cited 01.11.2018.
- [13] OK-FIRST project. Heat transfer. <https://okfirst.mesonet.org/train/meteorology/HeatTransfer.html>, Cited 01.11.2018.
- [14] C.-E. A. Winslow A.P. Gagge. Influence of physical work on physiological reactions to the thermal environment. Technical report, John B. Pierce Laboratory of Hygiene, 1941.
- [15] S. Tanabe et al. Indoor temperature, productivity, and fatigue in office tasks. Technical report, Part of HVAC&R Research, 2007.
- [16] Norsk Standard. Ergonomics of thermal environment - analytical determination and interpretation of thermal comfort using calculation of the pmv and ppd indices and local thermal comfort criteria (iso 7730:2005). Technical report, European Committee for Standardization, 2005.
- [17] Y. Cheng et al. Thermal comfort models: A review and numerical investigation. Technical report, Hong Kong Polytechnic University, 2011.
- [18] B.T. Chew Y.H. Yau. A review on predicted mean vote and adaptive thermal comfort models. Technical report, The Chartered Institution of Building Service Engineers, 2014.
- [19] F. H. Rohles. Temperature and temperment - a psychologist looks at comfort. Technical report, ASHRAE journal, 2007.

- [20] J. L. M. Hensen J. van Hoof. Thermal comfort and older adults. Technical report, Eindhoven University of Technology, 2006.
- [21] S. Karjalainen. Thermal comfort and gender: a literature review. Technical report, VTT Technical Research Centre of Finland, 2011.
- [22] N. Hashiguchi et al. Gender differences in thermal comfort and mental performance at different vertical air temperatures. Technical report, Kyushu University, 2010.
- [23] M. Uth et al. Body core temperature sensing: Challenges and new sensor technologies. Technical report, Drägerwerk, 2016.
- [24] M. Taleghani et al. A review into thermal comfort in buildings. Technical report, Delft University of Technology, 2013.
- [25] R. De Dear T. Parkinson. Revisiting an old hypothesis of human thermal perception: alliesthesia. Technical report, University of Sydney, 2011.
- [26] F. Nicol. The limits of thermal comfort: avoiding overheating in european buildings. Technical report, Oxford Brookes University, 2013.
- [27] F. d’Ambrosio et al. Thermal comfort: Design and assessment for energy saving. Technical report, Università di Salerno, 2014.
- [28] M. Cabanac. Physiological role of pleasure. Technical report, Science, Vol.173(4002), pp.1103-7, 1971.
- [29] R. De Dear T. Parkinson. Thermal pleasure in built environment: Physiology of alliesthesia. Technical report, University of Sydney, 2015.
- [30] C. Du et al. Quantifying the cooling efficiency of air velocity by heat loss from skin surface in warm and hot environments. Technical report, Chongqing University, 2018.
- [31] G. D. Mower. Perceived intensity of peripheral thermal stimuli is independent of internal body temperature. Technical report, Brown University, 1976.
- [32] H. Hensel. *Thermoreception and temperature regulation*. Academic Press, 1981.
- [33] K. Ivanov et al. Thermoreceptor distribution in different skin layers and its significance for thermoregulation. Technical report, Pavlov Institute of Physiology, 1986.
- [34] C. Traylor et al. Utilizing modulating-temperature setpoints to save energy and maintain alliesthesia-based comfort. Technical report, University of North Texas, 2017.
- [35] Q. Deng et al. Human thermal sensation and comfort in a non-uniform environment with personalized heating. Technical report, Central South University, Changsha, 2017.
- [36] D. Ackerknecht P. Gut. *Climate responsive building*. SKAT, 1993.
- [37] C. Gao F. Wang. Protective clothing. Technical report, The Textile Institute, 2014.
- [38] OpenStax College. *Biology*. OpenStax College Cnx Biology, 2016.
- [39] Health and Safety Executive. The six basic factors. <http://www.hse.gov.uk/temperature/thermal/factors.htm>, Cited 16.10.2018.
- [40] M. Luo et al. Human metabolic rate and thermal comfort in buildings: The problem and challenge. Technical report, UC Berkeley, 2018.

- [41] Norsk Standard. Ergonomics of the thermal environment - instruments for measuring physical quantities (iso 7726:1998). Technical report, European Committee for Standardization, 2001.
- [42] Eurotherm. The definition of comfort. https://www.eurotherm.info/ww/guida_al_comfort/The_main_parameters, Cited 18.10.2018.
- [43] Z. Lian Y. Wang. A study on the thermal comfort under non-uniform thermal environment. Technical report, Shanghai Jiao Tong University, 2017.
- [44] H. Zhu et al. Experimental study on the human thermal comfort based on the heart rate variability (hrv) analysis under different environments. Technical report, University of South China, 2018.
- [45] P. Ravindran. Diffusion and fick's law. Technical report, Central University of Tamil Nadu, 2014.
- [46] M. J. Hancock. The 1-d heat equation. Technical report, Massachusetts Institute of Technology, 2006.
- [47] Arbeidstilsynet. Klima og luftkvalitet på arbeidsplassen. Technical report, Arbeidstilsynet, 2016.
- [48] F. E. S. Levy. Luftfuktighet. <https://sml.snل.no/luftfuktighet>, Cited 16.10.2018.
- [49] Norges Astma og Allergiforbundet. Tørr luft. luftfuktighet (rf) inne. <http://www.inneklima.com/index.asp?key=RF>, Cited 16.10.2018.
- [50] P. O. Fanger. *Thermal comfort: analysis and applications in environmental engineering*. McGraw-Hill Book Company, 1970.
- [51] D. Markov. Practical evaluation of the thermal comfort parameters. Technical report, Technical University of Sofia, 2002.
- [52] J. van Hoof E. Halawa. The adaptive approach to thermal comfort: A critical review. Technical report, Fontys University of Applied Sciences, 2012.
- [53] J. L. M. Hensen J. van Hoof. Quantifying the relevance of adaptive thermal comfort models in moderate thermal climate zones. Technical report, Technische Universiteit Eindhoven, 2005.
- [54] S. Carlucci et al. Review of adaptive thermal comfort models in built environmental regulatory documents. Technical report, Xi'an University of Architecture & Technology, 2018.
- [55] R. Castano-Costa et al. A novel index of vulnerable homes: Findings from application in spain. Technical report, Universidad de Sevilla, 2018.
- [56] N. Djongyang et al. Thermal comfort: A review paper. Technical report, University of Yaounde, 2010.
- [57] K. Le V. Tam, L. Almeida. Energy-related occupant behaviour and its implications in energy use: A chronological review. Technical report, Western Sydney University, 2018.
- [58] F. Nicol. Comfort and energy use in buildings - getting them right. Technical report, London Metropolitan University, 2007.
- [59] Z. Deme Belafi et al. A critical review on questionnaire surveys in the field of energy-related occupant behaviour. Technical report, UC Berkeley, 2018.

- [60] A. Zani et al. Occupancy profile variation analyzed through generative modelling to control building energy behavior. Technical report, Politecnico di Milano, 2017.
- [61] B. Dong et al. An investigation on energy-related occupancy behavior for low-income residential buildings. Technical report, University of Texas, 2015.
- [62] NTNU. Energy and indoor environment laboratory. https://www.ntnu.edu/ept/laboratories/energy_indoor, Cited 20.11.2018.
- [63] Scan2CAD Andy. Cad software compared: Autocad vs solidworks. <https://www.scan2cad.com/cad/autocad-vs-solidworks/>, Cited 19.11.2018.
- [64] The University of Arizona. Ansys simulation software. <https://softwarelicense.arizona.edu/ansys-simulation-software-0>, Cited 19.11.2018.
- [65] Figes. What is ansys. <http://www.figes.com.tr/english/ansys/ansys.php>, Cited 19.11.2018.
- [66] Comsol. The finite element method (fem). <https://www.comsol.com/multiphysics/finite-element-method>, Cited 19.11.2018.
- [67] MathWorks. What is matlab? <https://se.mathworks.com/discovery/what-is-matlab.html>, Cited 19.11.2018.
- [68] University of Wisconsin-Madison. Introduction - what is matlab? <https://cimss.ssec.wisc.edu/wxwise/class/aos340/spr00/whatismatlab.htm>, Cited 19.11.2018.
- [69] J. W. Dziedzic et al. Indoor occupant behaviour monitoring with the use of a depth registration camera. Technical report, Norwegian University of Science and Technology, 2018.
- [70] E. Naone. Microsoft kinect. Technical report, Cambridge, 2011.
- [71] S. Motiian et al. Automated extraction and validation of children's gait parameters with the kinect. Technical report, West Virginia University, 2015.
- [72] A. S. Morris. *Measurement and Instrumentation (Second Edition)*. Academic Press Inc, 2015.
- [73] Systemair. Cks3553 radialvifte sw.out. <https://www.systemair.com/no/Norge/Produktkatalog/unpublished/CKS-355-3-Centrifugal-Fan/>, Cited 08.05.2019.
- [74] Elektroskandia. Elektrovarme og termostater. Technical report, Elektroskandia, 2010.
- [75] Inc. ANSYS. Release notes (ansys user guide). Technical report, ANSYS, Inc., 2017.
- [76] SHARCNET. Meshing user's guide. https://www.sharcnet.ca/Software/Ansys/16.2.3/en-us/help/wb_msh/msh_book_wb.html, Cited 29.04.2019.
- [77] P. Bernard et al. Hex-dominant meshing approach based on frame field smoothness. Technical report, Université catholique de Louvain, 2014.
- [78] X. Gao et al. Robust hex-dominant mesh generation using field-guided polyhedral agglomeration. Technical report, New York University, 2017.
- [79] K. Shimada. S. Yamakawa. Hex-dominant mesh generation with directionality control via packing rectangular solid cells. Technical report, Carnegie Mellon University, 2002.
- [80] Amar Aganovic. Airflow distribution for minimizing human exposure to airborne contaminants in healthcare facilities. Technical report, Norwegian University of Science and Technology, 2019.

- [81] Fluent Inc. Fluent 6.1 user's guide. Technical report, Fluent Inc., 2003.
- [82] Y. He. The experimental research on the movable personalized ventilation. Technical report, Norwegian University of Science and Technology, 2019.
- [83] J. H. Keenan. Thermodynamic properties of air. Technical report, New York Wiley, 1948.
- [84] K. J. Elliot et al. Analysis of a curvature corrected turbulence model using a 90 degree curved geometry modelled after a centrifugal compressor impeller. Technical report, University of Western Ontario, 2012.
- [85] Autodesk. Autodesk smoke user guide. Technical report, Autodesk, Inc., 2017.
- [86] Engineering Toolbox. Clo - clothing and thermal insulation. https://www.engineeringtoolbox.com/clo-clothing-thermal-insulation-d_732.html, Cited 14.05.2019.
- [87] J. Thé H. Yu. Simulation of gaseous pollutant dispersion around an isolated building using the k-w sst (shear stress transport) turbulence model. *Air and Waste Management Association*, 67(5):517–536, 2017.
- [88] Peter Hlbocan. Comparison of k- ϵ and sst turbulence models in cfd simulation of the flow in a mixed-flow pump. Technical report, Slovak University of Technology in Bratislava, 2011.
- [89] T. Law. *The Future of Thermal Comfort in an Energy- Constrained World*. Springer, 2013.
- [90] E. T. Rolls et al. Warm pleasant feelings in the brain. Technical report, University of Oxford, 2008.
- [91] J. W. Dziejczak et al. Occupant migration monitoring in residential buildings with the use of a depth registration camera. Technical report, Norwegian University of Science and Technology, 2017.

Appendix

Appendix A: Calibration data for TSI VelociCalc 8388-M-GB

Appendix B1: Drawing of table

Appendix B2: Drawing of chair

Appendix B3: Drawing of PC

Appendix B4: Drawing of pipe

Appendix C: Cartesian coordinates over zones in chamber model

Appendix D: Quality of elements in chamber mesh

Appendix E: Air velocities [m/s] in chamber and in simulations

Appendix F1: Cross-sectional view of chamber displaying air velocities for induced air flow of 0.0167 and 0.0333 kg/s

Appendix F2: Cross-sectional view of chamber displaying air velocities for induced air flow of 0.0500 and 0.0667 kg/s

Appendix G: Cross-sectional view of streamlines for the RNG model with air flow of 0.0667 kg/s and display of velocity magnitude and direction

Appendix H: Streamlines of the Realizable and SST models with air flow of 0.0667 kg/s and displaying velocity magnitude

Appendix I: Accumulation of heat in zone 'Chair_222'

Appendix J1: Evaluation of indoor environment, case I, 13.05, 0.0167 kg/s

Appendix J2: Evaluation of indoor environment, case II, 14.05, 0.0333 kg/s

Appendix J3: Evaluation of indoor environment, case III, 15.05, 0.0500 kg/s

Appendix J4: Evaluation of indoor environment, case IV, 20.05, 0.0667 kg/s

Appendix J5: Evaluation of indoor environment, case V, 21.05, 0.0667 kg/s, heater fan on

Appendix J6: Evaluation of indoor environment, case VI, 22.05, 0.0667 kg/s, heater I

Appendix J7: Evaluation of indoor environment, case VII, 23.05, 0.0667 kg/s, heater II

Appendix J8: Evaluation of indoor environment, case VIII, 25.05, 0.0667 kg/s, heater III

Appendix J9: Evaluation of indoor environment, case IX, 28.05, 0.0667 kg/s, heater II

Appendix J10: Evaluation of indoor environment, case X, 29.05, 0.0500 kg/s, heater II

Appendix K1: Accumulative quantities of temperature and air velocity allocated to different joint locations to the participant and the subject's evaluation, case I, 13.05, 0.0167 kg/s

Appendix K2: Accumulative quantities of temperature and air velocity allocated to different joint locations to the participant and the subject's evaluation, case II, 14.05, 0.0333 kg/s

Appendix K3: Accumulative quantities of temperature and air velocity allocated to different joint locations to the participant and the subject's evaluation, case III, 15.05, 0.0500 kg/s

Appendix K4: Accumulative quantities of temperature and air velocity allocated to different joint locations to the participant and the subject's evaluation, case IV, 20.05, 0.0667 kg/s

Appendix K5: Accumulative quantities of temperature and air velocity allocated to different joint locations to the participant and the subject's evaluation, case V, 21.05, 0.0667 kg/s, heater fan on

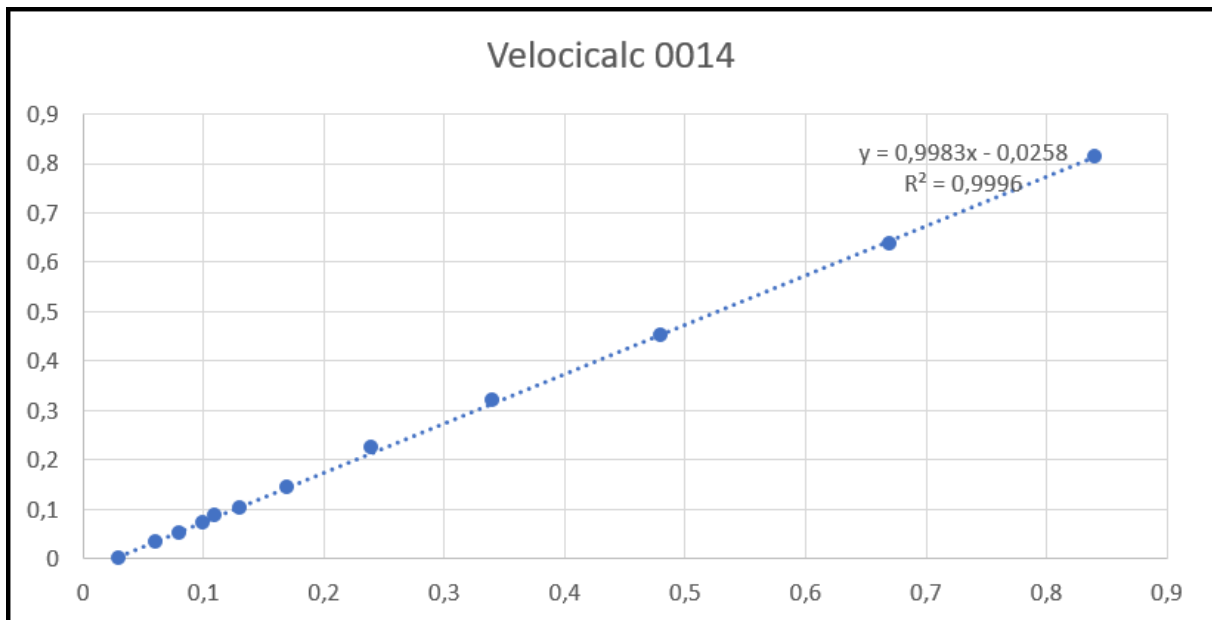
Appendix K6: Accumulative quantities of temperature and air velocity allocated to different joint locations to the participant and the subject's evaluation, case VI, 22.05, 0.0667 kg/s, heater I

Appendix K7: Accumulative quantities of temperature and air velocity allocated to different joint locations to the participant and the subject's evaluation, case VIII, 25.05, 0.0667 kg/s, heater II

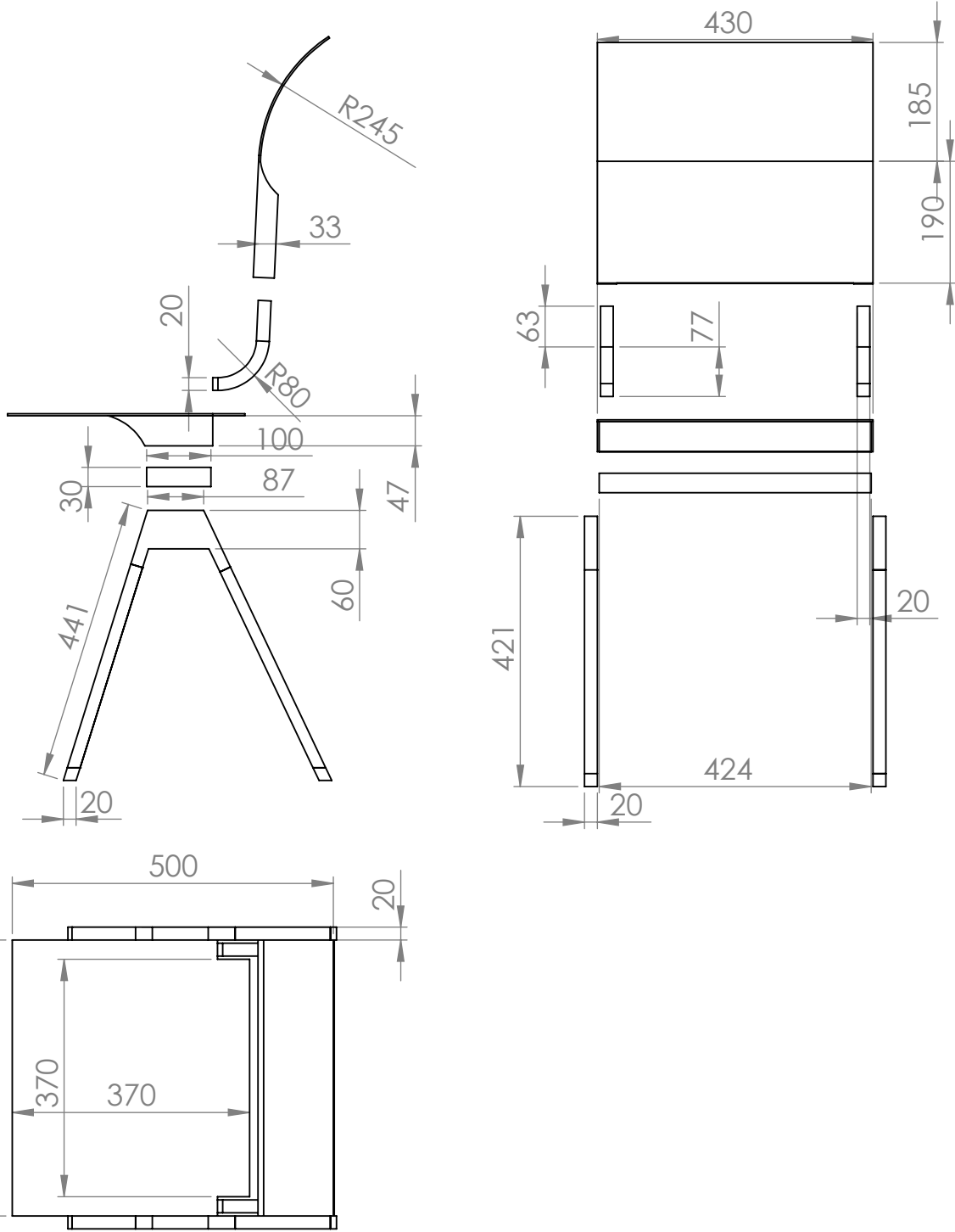
Appendix K8: Accumulative quantities of temperature and air velocity allocated to different joint locations to the participant and the subject's evaluation, case X, 29.05, 0.0667 kg/s, heater III

Appendix A : Calibration data for TSI VelociCalc 8388-M-GB

Can test humidity : 0014			
Pressure (Pa)	Measured velocity (m/s)	Real velocity (m/s)	Correlation
0	0.03	0	-0.0300
10	0.06	0.032	-0.0280
25	0.08	0.051	-0.0292
50	0.10	0.072	-0.0282
75	0.11	0.088	-0.0221
100	0.13	0.101	-0.0286
200	0.17	0.143	-0.0268
500	0.24	0.226	-0.0139
1000	0.34	0.319	-0.0206
2000	0.48	0.451	-0.0286
4000	0.67	0.638	-0.0320
6500	0.84	0.813	-0.0270



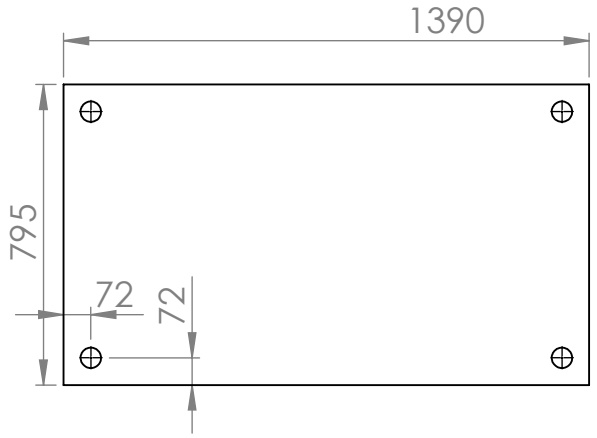
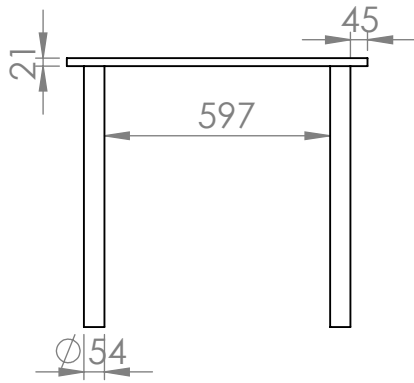
Appendix B1 : Drawing of chair



UNLESS OTHERWISE SPECIFIED: DIMENSIONS ARE IN MILLIMETERS SURFACE FINISH: TOLERANCES: LINEAR: ANGULAR:			FINISH:	DEBURR AND BREAK SHARP EDGES	DO NOT SCALE DRAWING	REVISION																								
<table border="1"> <thead> <tr> <th>NAME</th> <th>SIGNATURE</th> <th>DATE</th> <th></th> </tr> </thead> <tbody> <tr> <td>DRAWN</td> <td></td> <td></td> <td></td> </tr> <tr> <td>CHK'D</td> <td></td> <td></td> <td></td> </tr> <tr> <td>APPV'D</td> <td></td> <td></td> <td></td> </tr> <tr> <td>MFG</td> <td></td> <td></td> <td></td> </tr> <tr> <td>Q.A</td> <td></td> <td></td> <td></td> </tr> </tbody> </table>				NAME	SIGNATURE	DATE		DRAWN				CHK'D				APPV'D				MFG				Q.A				TITLE:		
NAME	SIGNATURE	DATE																												
DRAWN																														
CHK'D																														
APPV'D																														
MFG																														
Q.A																														
MATERIAL:				DWG NO.																										
WEIGHT:				SCALE:1:5		SHEET 1 OF 1																								

Assembly_Chair3 A4

Appendix B2 : Drawing of table



UNLESS OTHERWISE SPECIFIED:
 DIMENSIONS ARE IN MILLIMETERS
 SURFACE FINISH:
 TOLERANCES:
 LINEAR:
 ANGULAR:

FINISH:

DEBURR AND
 BREAK SHARP
 EDGES

DO NOT SCALE DRAWING

REVISION

	NAME	SIGNATURE	DATE		
DRAWN					
CHK'D					
APPV'D					
MFG					
Q.A					

TITLE:

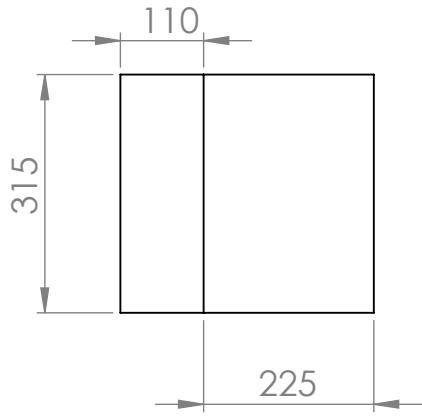
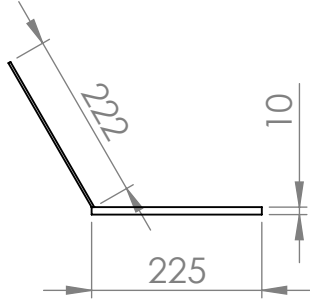
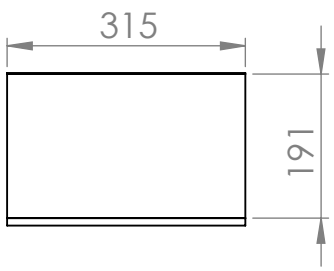
DWG NO. **Table**

SCALE: 1:20

SHEET 1 OF 1

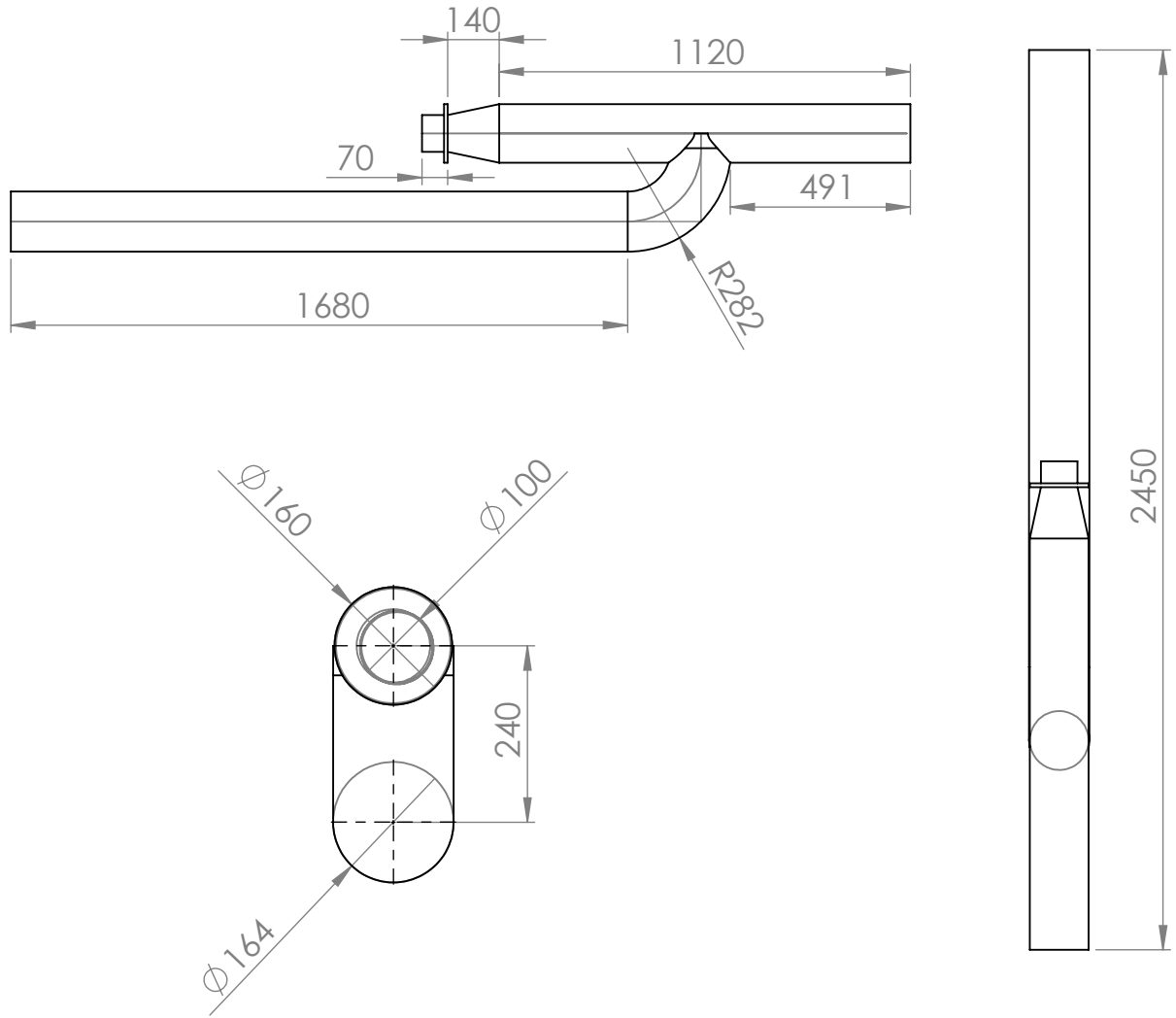
A4

Appendix B3 : Drawing of PC



UNLESS OTHERWISE SPECIFIED: DIMENSIONS ARE IN MILLIMETERS SURFACE FINISH: TOLERANCES: LINEAR: ANGULAR:		FINISH:		DEBURR AND BREAK SHARP EDGES		DO NOT SCALE DRAWING		REVISION	
DRAWN		SIGNATURE		DATE		TITLE:			
CHK'D						PC			
APPV'D									
MFG						DWG NO.		A4	
Q.A				MATERIAL:		SCALE:1:10		SHEET 1 OF 1	
				WEIGHT:					

Appendix B4 : Drawing of pipe

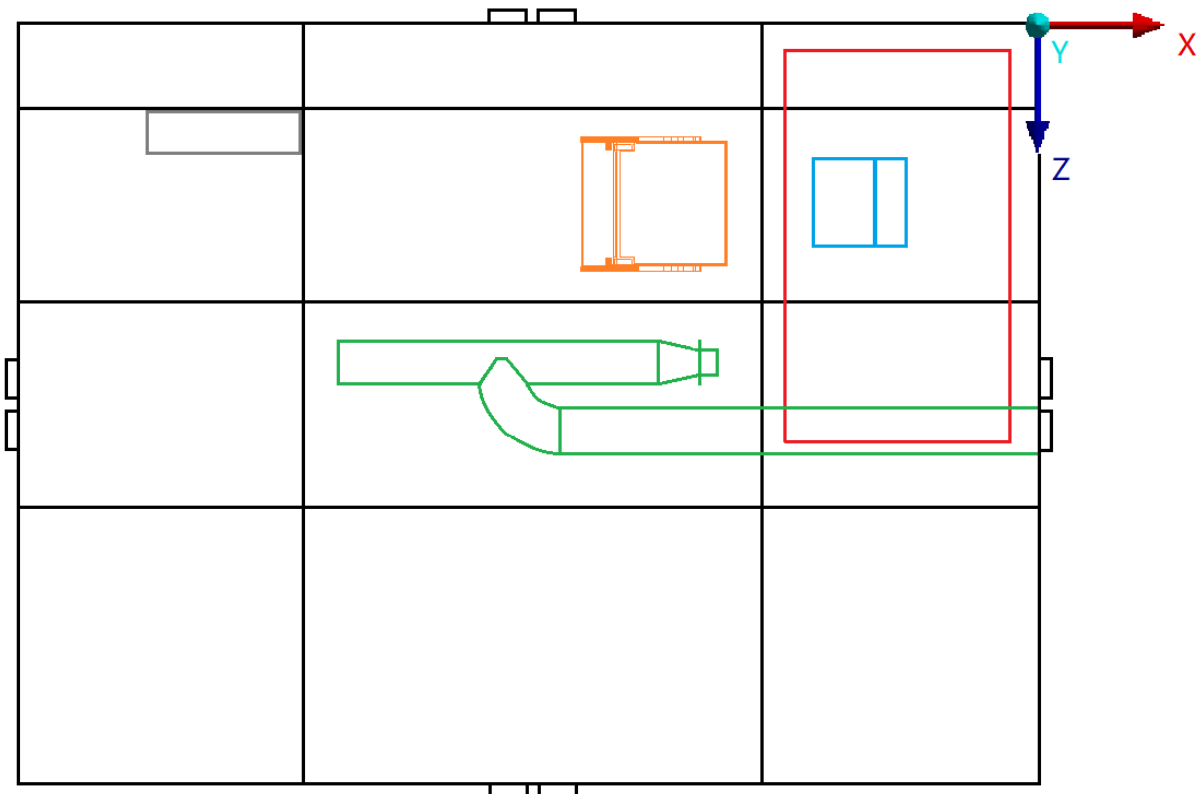


UNLESS OTHERWISE SPECIFIED: DIMENSIONS ARE IN MILLIMETERS SURFACE FINISH: TOLERANCES: LINEAR: ANGULAR:			FINISH:		DEBURR AND BREAK SHARP EDGES		DO NOT SCALE DRAWING		REVISION		
DRAWN			SIGNATURE		DATE		TITLE:				
CHK'D											
APPV'D											
MFG											
Q.A							MATERIAL:		DWG NO.		A4
									InletPipe2		
							WEIGHT:		SCALE:1:50		SHEET 1 OF 1

Appendix C : Cartesian coordinates

Name	X, Y, Z	Content
Table_111	-1, 1, 1	Air, table
Table_121	-1, 1, 2	Air
Table_131	-1, 1, 3	Air, table, outlets
Air_141	-1, 1, 4	Air
Air_112	-2, 1, 1	Air, outlets
Chair_122	-2, 1, 2	Air, chair
Air_132	-2, 1, 3	Air
Air_142	-2, 1, 4	Air, outlets
Air_113	-3, 1, 1	Air
Air_123	-3, 1, 2	Air, (radiator)
Air_133	-3, 1, 3	Air, outlets
Air_143	-3, 1, 4	Air
Table_211	-1, 2, 1	Air, table
Table_221	-1, 2, 2	Air, table, PC
Table_231	-1, 2, 3	Air, table
Air_241	-1, 2, 4	Air
Air_212	-2, 2, 1	Air
Chair_222	-2, 2, 2	Air, chair
Air_232	-2, 2, 3	Air
Air_242	-2, 2, 4	Air
Air_213	-3, 2, 1	Air
Air_223	-3, 2, 2	Air, (radiator)

Air_311	-1, 3, 1	Air
Air_321	-1, 3, 2	Air
Air_331	-1, 3, 3	Air
Air_341	-1, 3, 4	Air
Air_312	-2, 3, 1	Air
Air_322	-2, 3, 2	Air
Air_332	-2, 3, 3	Air
Air_342	-2, 3, 4	Air
Air_313	-3, 3, 1	Air
Air_323	-3, 3, 2	Air
Air_333	-3, 3, 3	Air
Air_343	-3, 3, 4	Air
Air_411	-1, 4, 1	Air
Air_421	-1, 4, 2	Air
Pipe_431	-1, 4, 3	Air, pipe
Air_441	-1, 4, 4	Air
Air_412	-2, 4, 1	Air
Air_422	-2, 4, 2	Air
Pipe_432	-2, 4, 3	Air, pipe
Air_442	-2, 4, 4	Air
Air_413	-3, 4, 1	Air
Air_423	-3, 4, 2	Air



Appendix D : Quality of elements in chamber mesh

Element quality for the chamber mesh:

	Tet10	Hex20	Wed15	Pyr13
0,95	3,15+e5	2,46+e6	2,45+e3	1,16+e4
0,85	3,54+e5	4,35+e4	2,54+e3	6,23+e3
0,751	1,53+e5	1,72+e4	1,77+e3	7,27+e3
0,651	5,15+e4	8,14+e3	1,64+e3	7,67+e3
0,551	1,84+e4	4,34+e3	1,41+e3	7,89+e3
0,452	7,61+e3	2,13+e3	1,63+e3	8,05+e3
0,352	4,85+e3	1,29+e3	1,11+e3	8,31+e3
0,252	5,35+e3	569	491	7,20+e3
0,153	3,32+e3	230	364	4,26+e3
0,053	589	14	14	1,13+e3

Aspect ratio of elements for the chamber mesh:

	Tet10	Hex20	Wed15	Pyr 13
465	9,12+e5	2,54+e6	1,34+e4	6,96+e4
1,39+e3	0	0	0	5
2,32+e3	0	0	0	2
8,82+e3	0	0	0	2

Skewness of elements for the chamber mesh:

	Tet10	Hex20	Wed15	Pyr13
0,05	1,87+e5	2,31+e6	188	4,64+e3
0,15	2,85+e5	9,93+e4	1,00+e3	6,05+e3
0,25	2,36+e5	5,61+e4	1,73+e3	2,39+e3
0,35	1,23+e5	3,57+e4	1,77+e3	4,81+e3
0,45	4,53+e4	1,80+e4	1,97+e3	7,82+e3
0,55	1,28+e4	9,55+e3	2,09+e3	1,10+e4
0,65	4,56+e3	4,93+e3	2,13+e3	1,36+e4
0,75	3,76+e3	1,70+e3	1,88+e3	1,22+e4
0,85	4,75+e3	566	636	5,94+e3
0,95	8,87+e3	308	31	1,09+e3

Appendix E : Air velocities [m/s] in chamber and in simulations

Mass flow: 0.0167 kg/s

	1	2	3	4	5
Standard	1.894	1.734	0.079	0.035	0.112
Realizable	1.894	20.856	14.752	19.055	6.622
RNG	1.894	1.836	0.0477	0.032	0.120
SST	1.894	8.621	5.071	6.328	7.650
Measured values	1.95-1.98	0.88-1.13	0-0.053	0-0.042	0-0.114

Mass flow: 0.0333 kg/s

	1	2	3	4	5
Standard	3.777	3.506	0.165	0.063	0.236
Realizable	3.777	3.844	6.540	3.456	19.999
RNG	3.777	3.693	0.095	0.111	0.230
SST	3.777	9.843	3.738	5.870	9.523
Measured values	3.95-4.00	1.71-1.87	0-0.054	0.048-0.112	0.112-0.143

Mass flow: 0.0500 kg/s

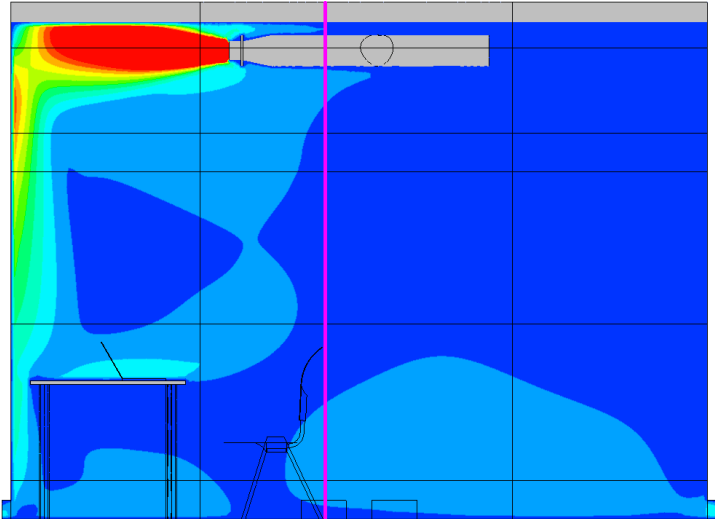
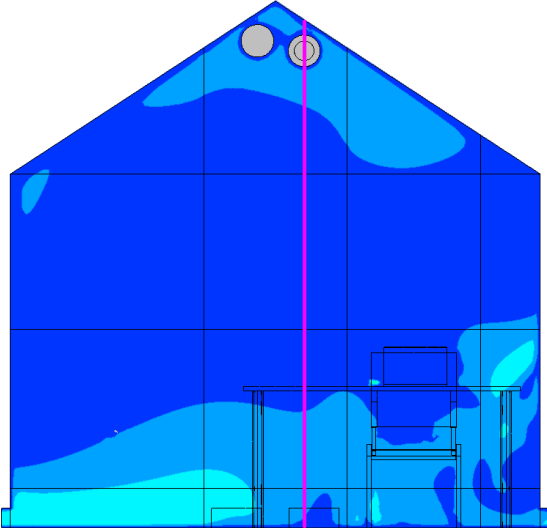
	1	2	3	4	5
Standard	5.672	5.3	0.258	0.109	0.347
Realizable	5.672	2.283	2.447	3.126	9.372
RNG	5.672	5.561	0.164	0.160	0.354
SST	5.672	4.175	8.330	8.011	29.236
Measured values	5.80-5.85	2.82-3.00	0.024-0.078	0.096-0.127	0.159-0.180

Mass flow: 0.0667 kg/s

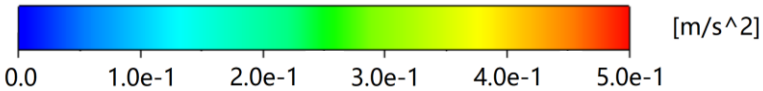
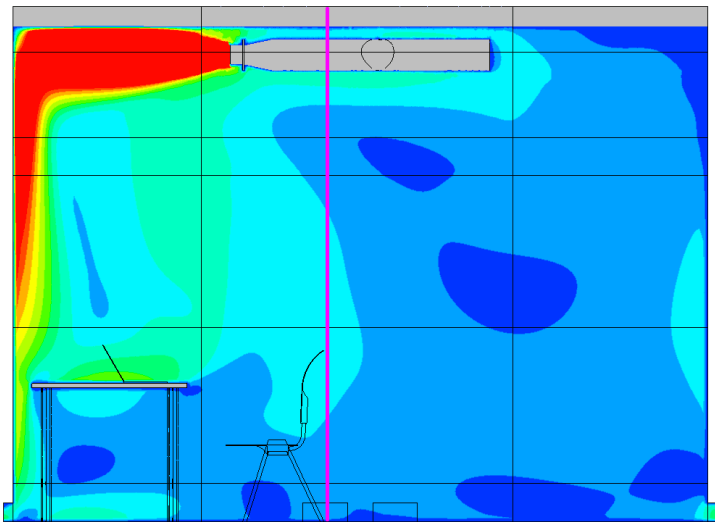
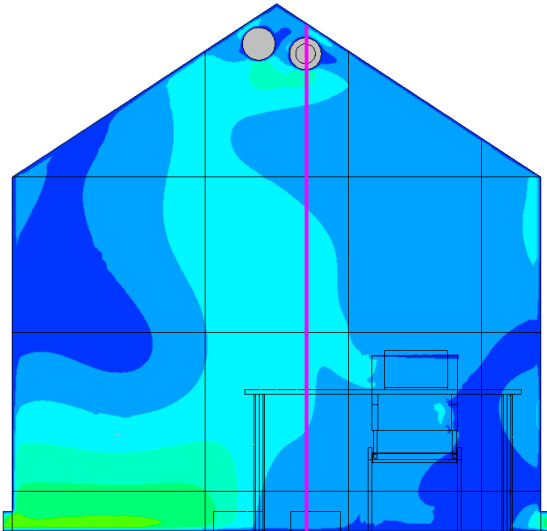
	1	2	3	4	5
Standard	7.566	7.083	0.317	0.129	0.467
Realizable	7.566	2.547	1.228	3.489	11.966
RNG	7.566	7.430	0.236	0.18	0.435
SST	7.566	6.433	5.604	8.687	20.867
Measured values	7.55-7.70	3.32-3.68	0.077-0.145	0.073-0.143	0.230-0.277

Appendix F1 : Cross-sectional view of chamber displaying air velocities for induced air flow of 0.0167 and 0.0333 kg/s

0.0167 kg/s:

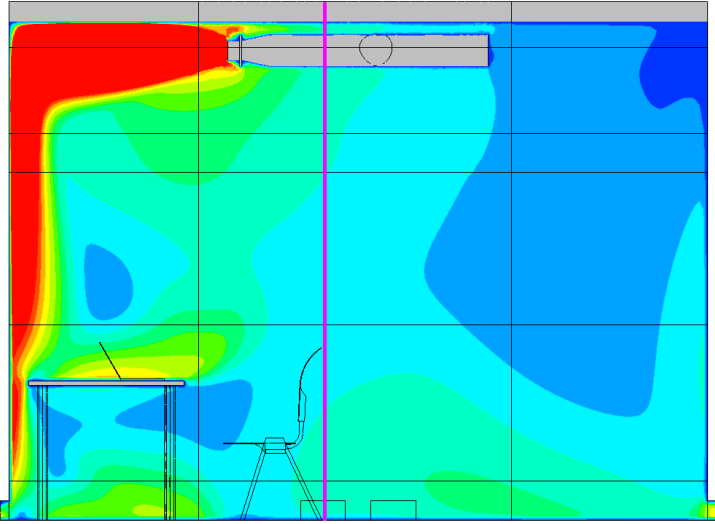
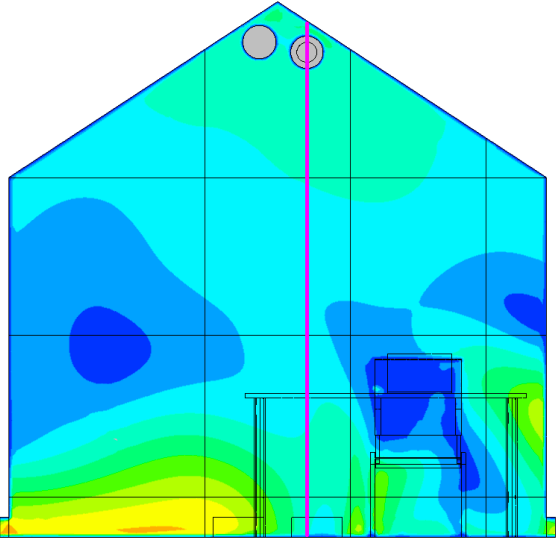


0.0333 kg/s:

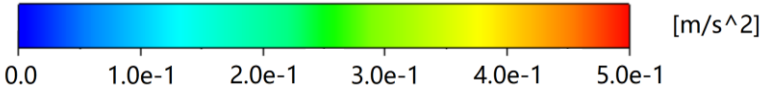
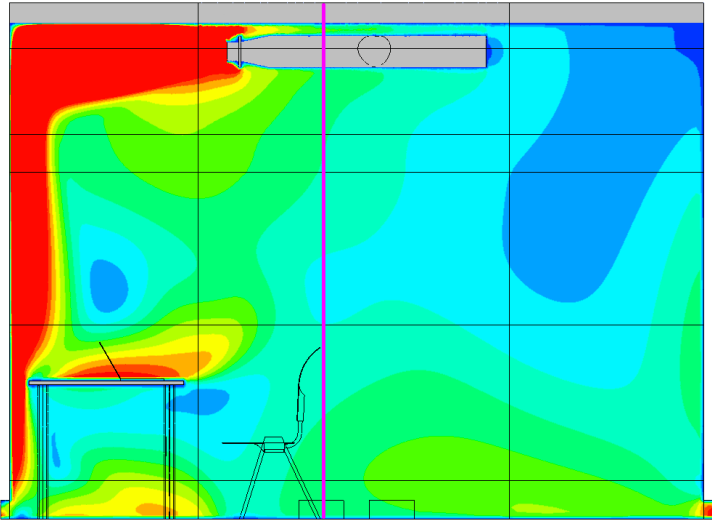
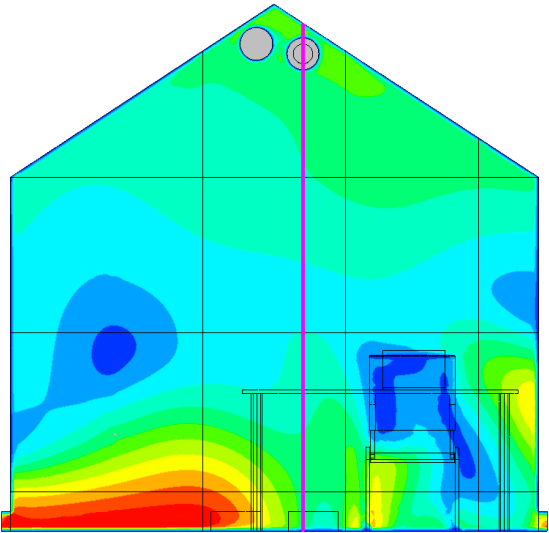


Appendix F2 : Cross-sectional view air velocities for induced air flow of 0.0500 and 0.0667 kg/s

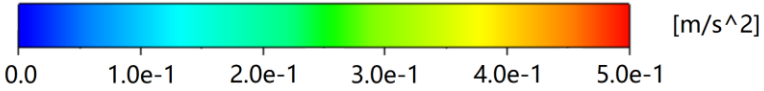
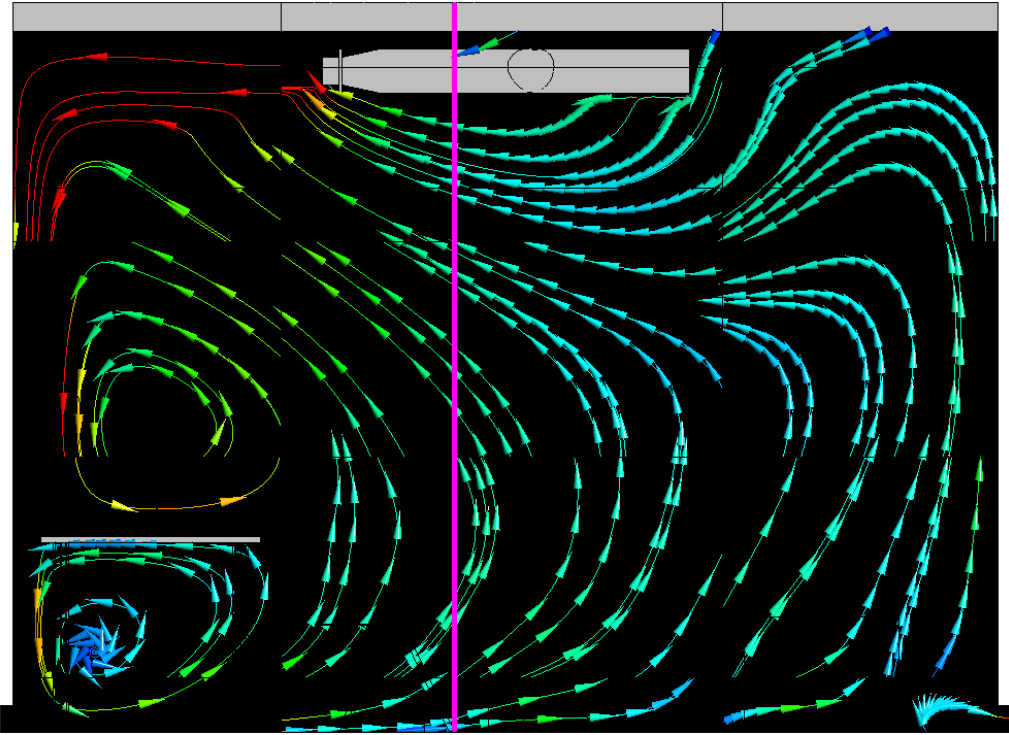
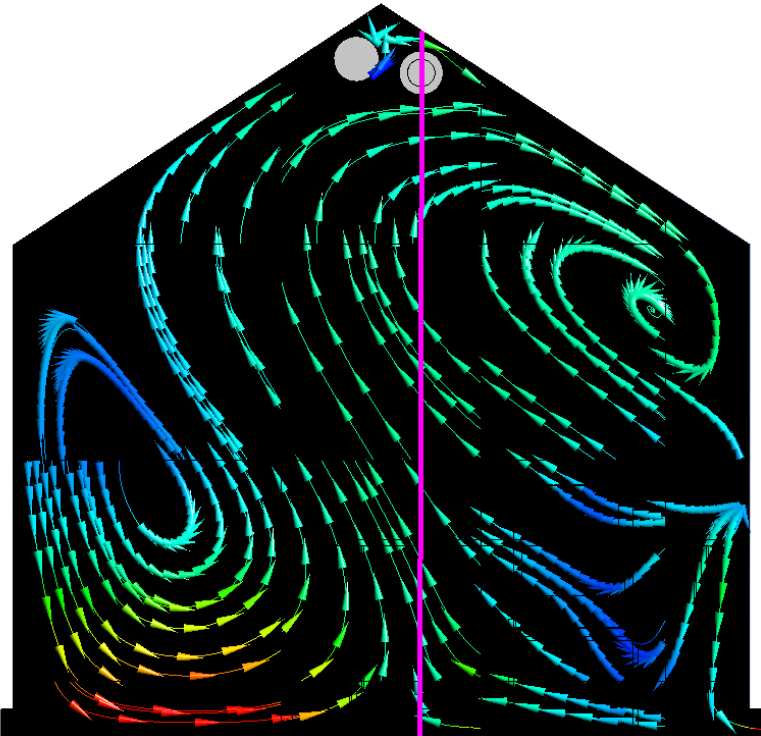
0.0500 kg/s:



0.0667 kg/s:

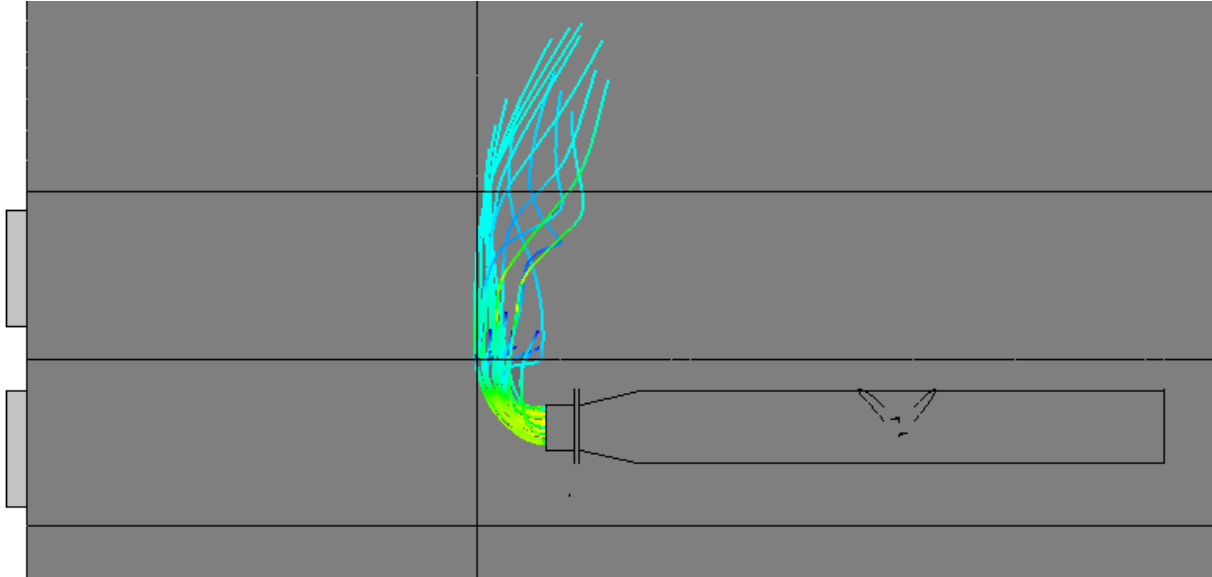


Appendix G : Cross-sectional view of streamlines for the RNG model with air flow of 0.0667 kg/s and display of velocity magnitude and direction

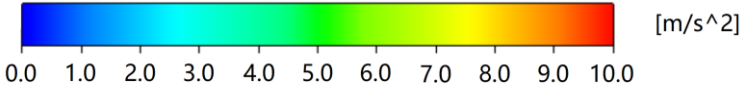
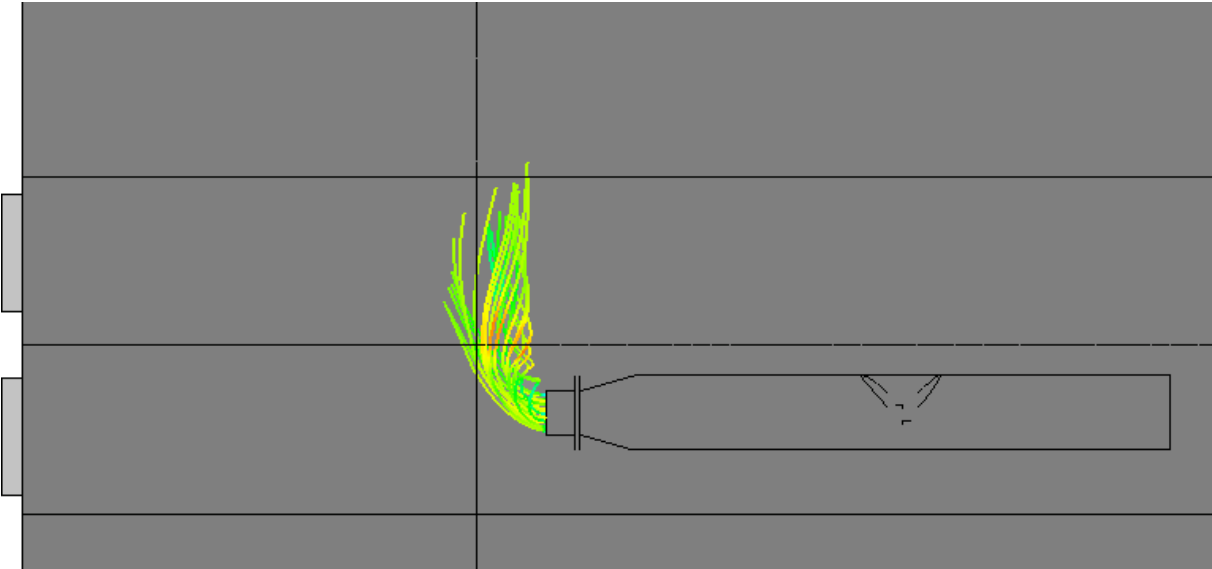


Appendix H : Streamlines of the Realizable and SST models with air flow of 0.0667 kg/s and displaying velocity magnitude

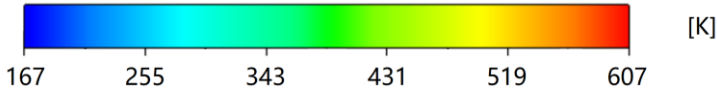
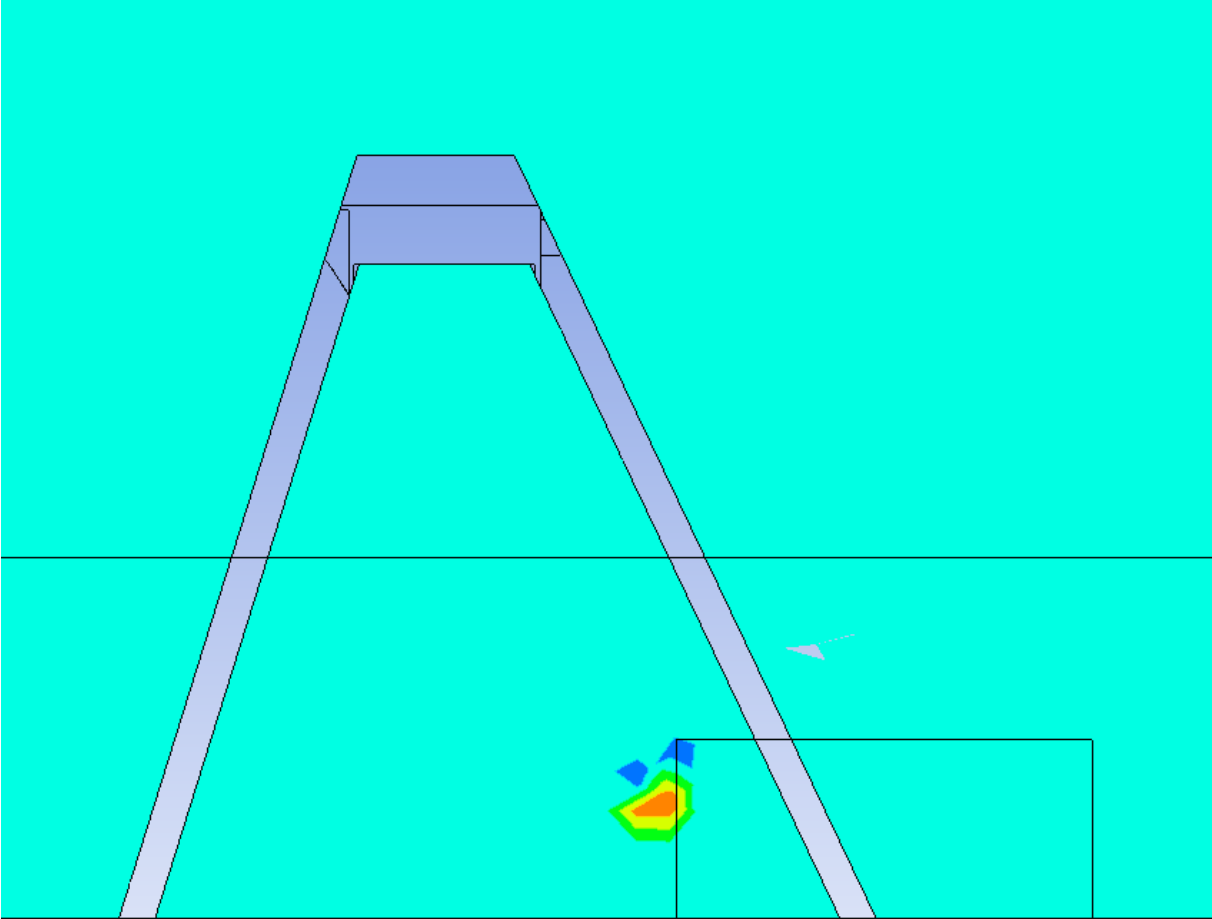
Realizable model:



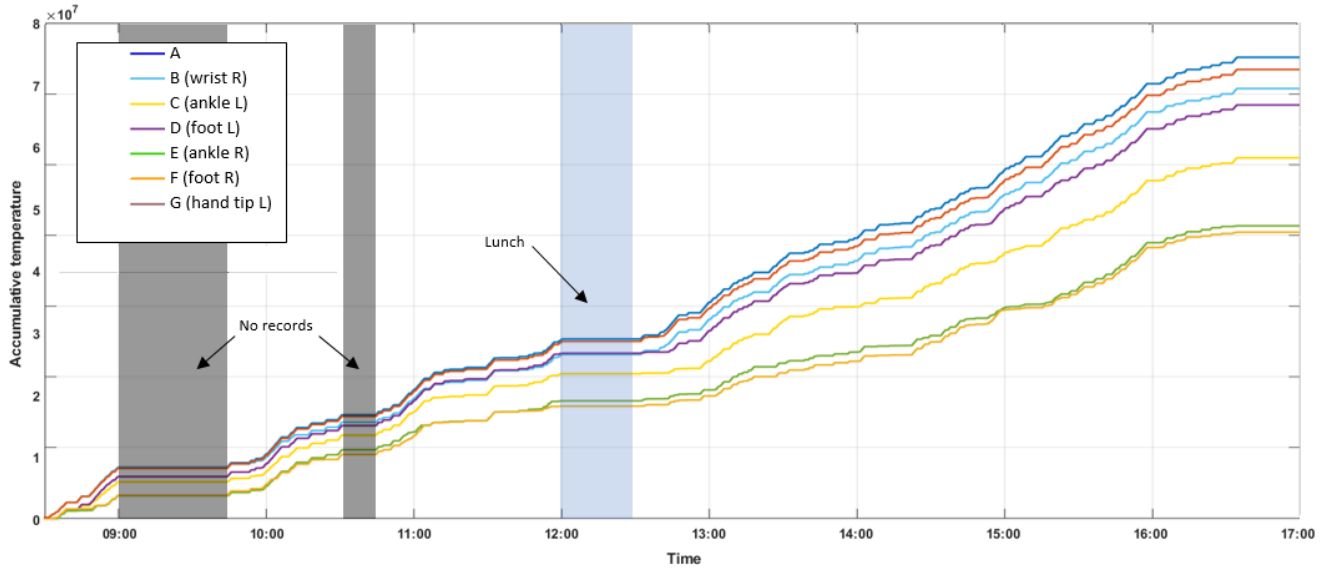
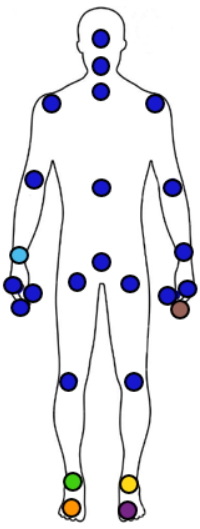
SST model:



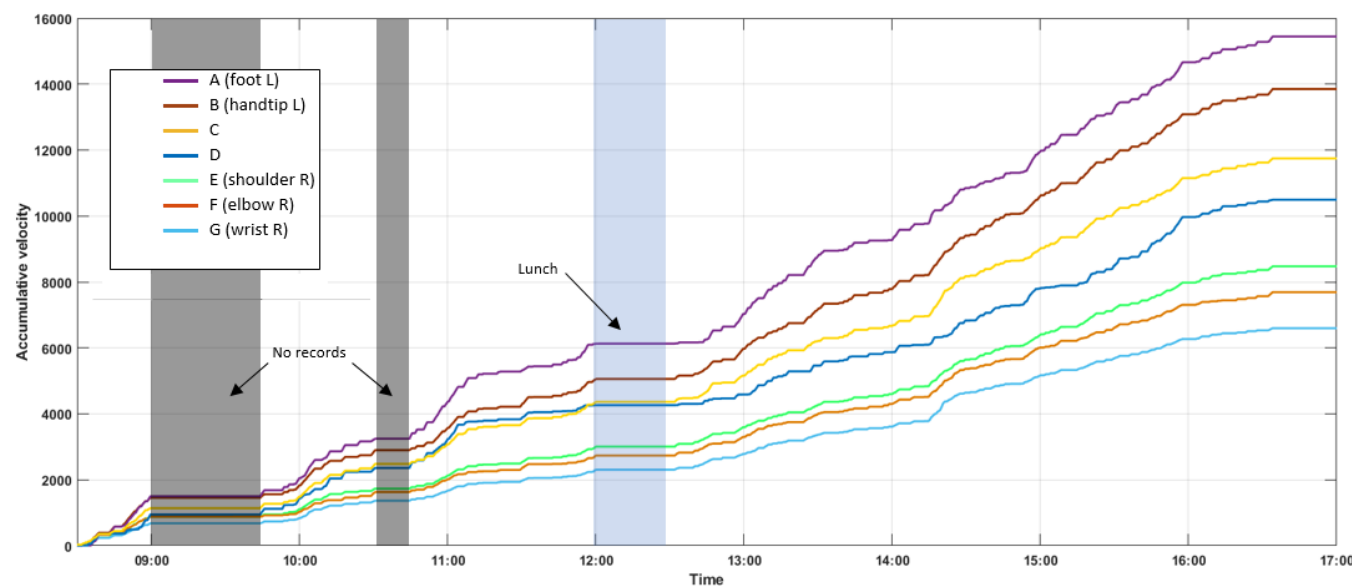
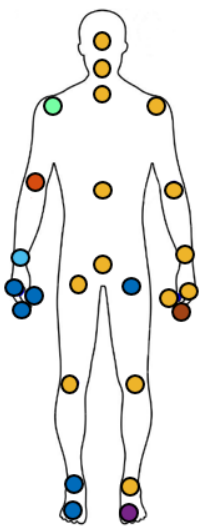
Appendix I : Accumulation of heat in zone 'Chair_222'



Appendix K1 : Accumulative quantities of temperature and air velocity allocated to different joint locations to the participant and the subject's evaluation, case I



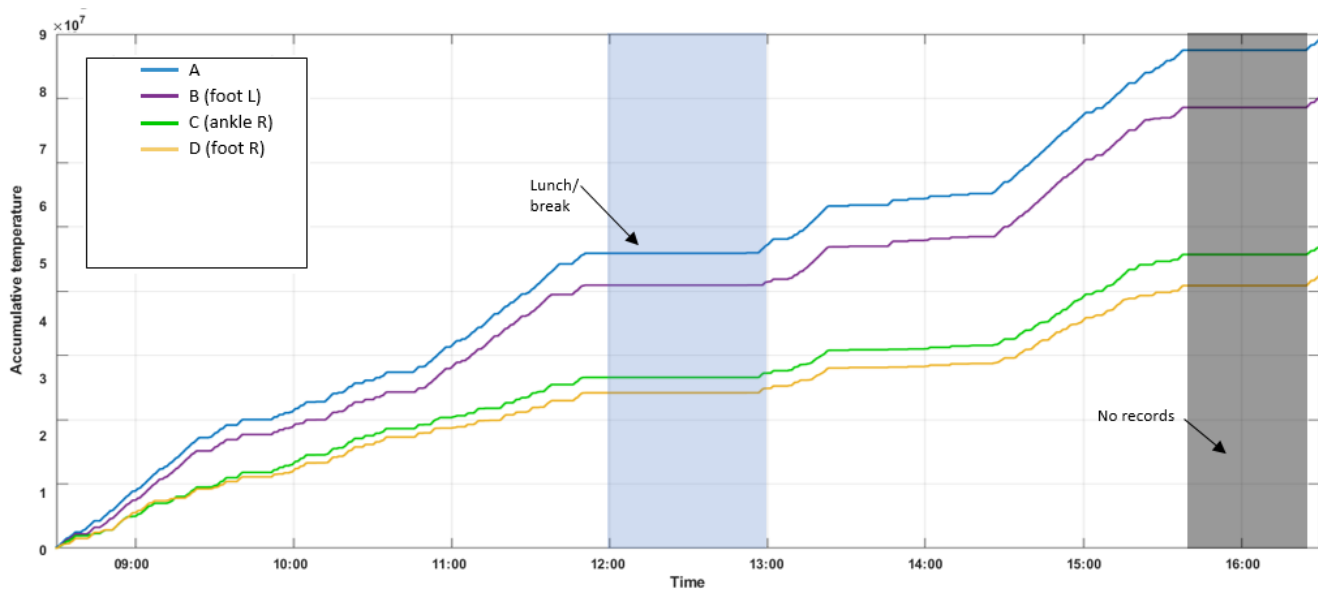
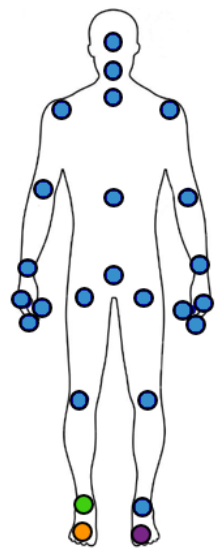
A: Spine mid (represent 19 other joint locations); B: wrist R; C: ankle L; D: foot L; E: ankle R; F: foot R; G: hand tip L



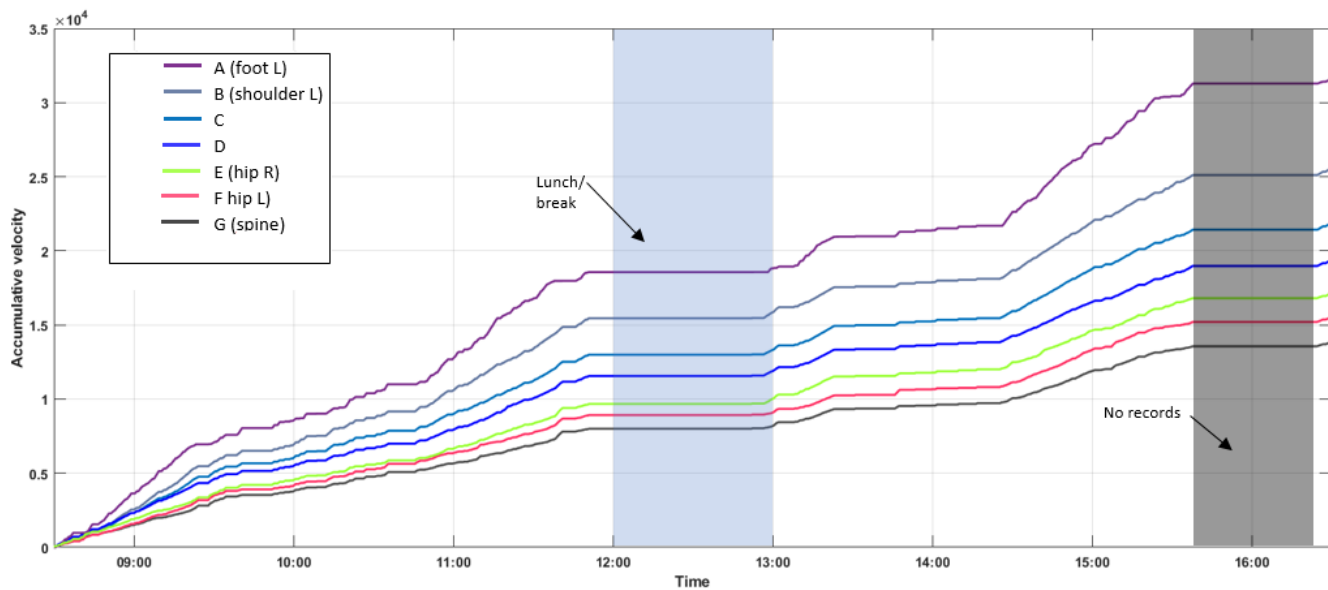
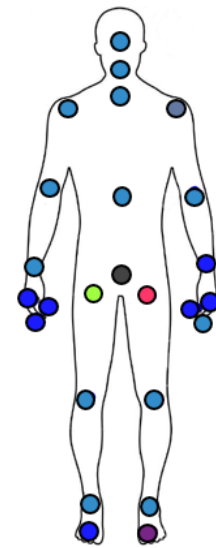
A: foot L; B: handtip L; C: spine mid (represent 13 other joint locations); D: foot R (represent 5 other joint locations); E: shoulder R; F: Elbow R; G: wrist R

Core thermal comfort (1-7)	4	4	4	4	3	3	4	4	4	4	4	4	4	4	4	4
Hand thermal comfort (1-7)	4	4	4	4	3	3	4	3	4	4	4	4	4	4	4	4
Feet thermal comfort (1-7)	3	4	4	3	4	4	3	3	2	2	3	3	3	2	2	3
Body movement (1-5)	2	1	1	2	1	3	1	1	1	1	2	1	1	2	1	1
Sweat rate (1-5)	1	1	1	1	1	1	1	1	1	1	1	1	1	1	1	1
Pulse (-)	66	67	62	63	57	60	57	58	56	58	58	37	47	51	54	52

Appendix K2 : Accumulative quantities of temperature and air velocity allocated to different joint locations to the participant and the subject's evaluation, case II



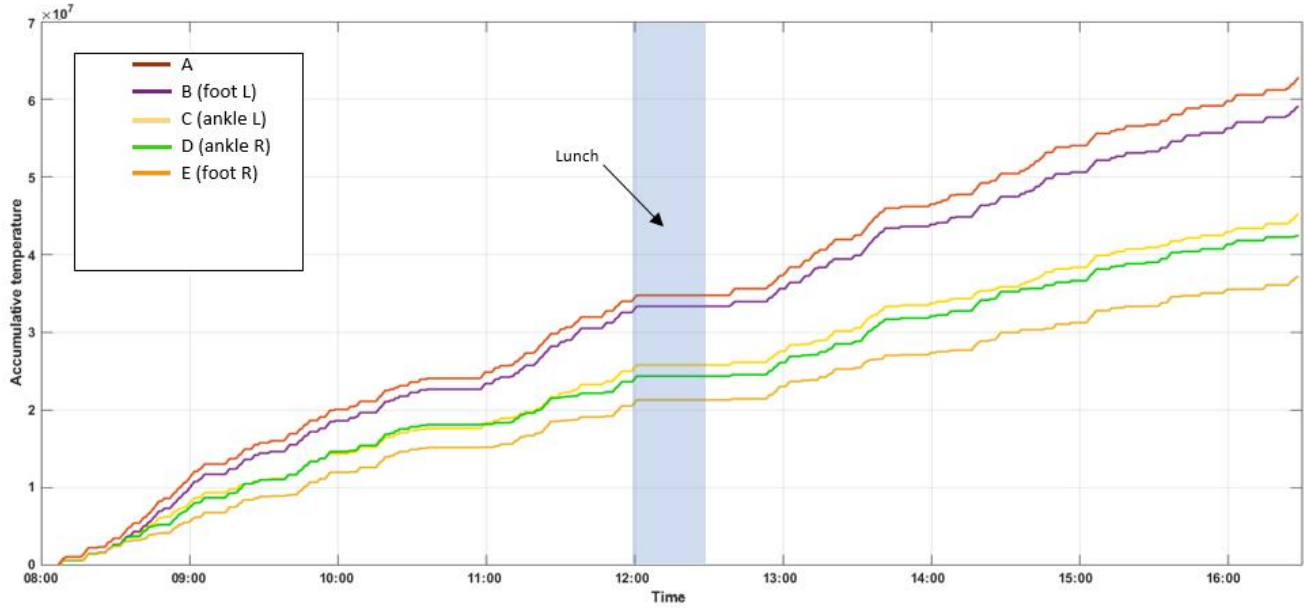
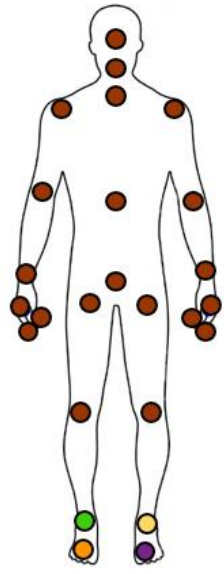
A: Spine mid (represent 22 other joint locations); B: foot L; C: ankle R; D: foot R



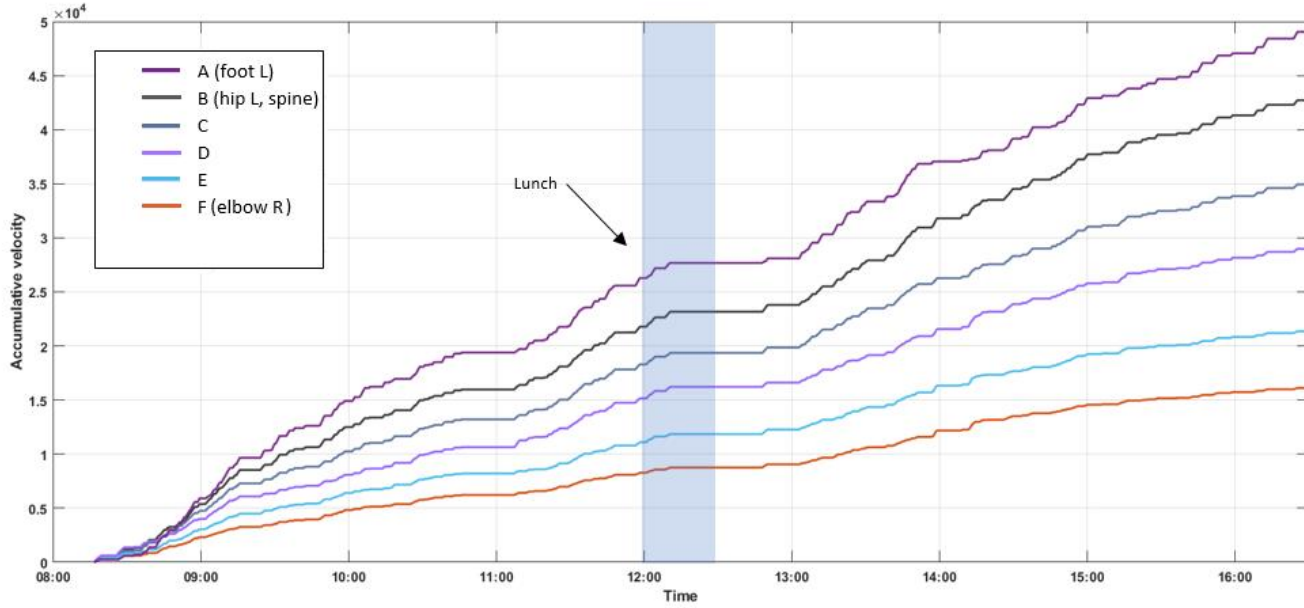
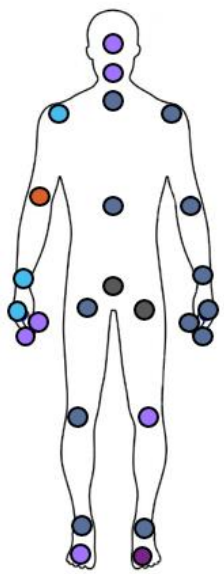
A: foot L; B: shoulder L; C: spine mid (represent 12 other joint locations); D: wrist L (represent 6 other joint locations); E: hip R; F: hip L; G: spine

Core thermal comfort (1-7)	5	4	4	4	4	3	4			4	4	4	4	4	4	4
Hand thermal comfort (1-7)	4	5	4	4	4	4	3			4	4	4	4	4	4	4
Feet thermal comfort (1-7)	4	5	5	4	5	3	3			5	4	5	5	5	5	5
Body movement (1-5)	3	2	2	2	2	1	3			3	1	2	1	1	1	2
Sweat rate (1-5)	2	1	1	1	1	1	1			1	1	1	1	1	1	1
Pulse (-)	70	64	62	61	60	59	54			50	61	60	60	60	60	66

Appendix K3 : Accumulative quantities of temperature and air velocity allocated to different joint locations to the participant and the subject's evaluation, case III



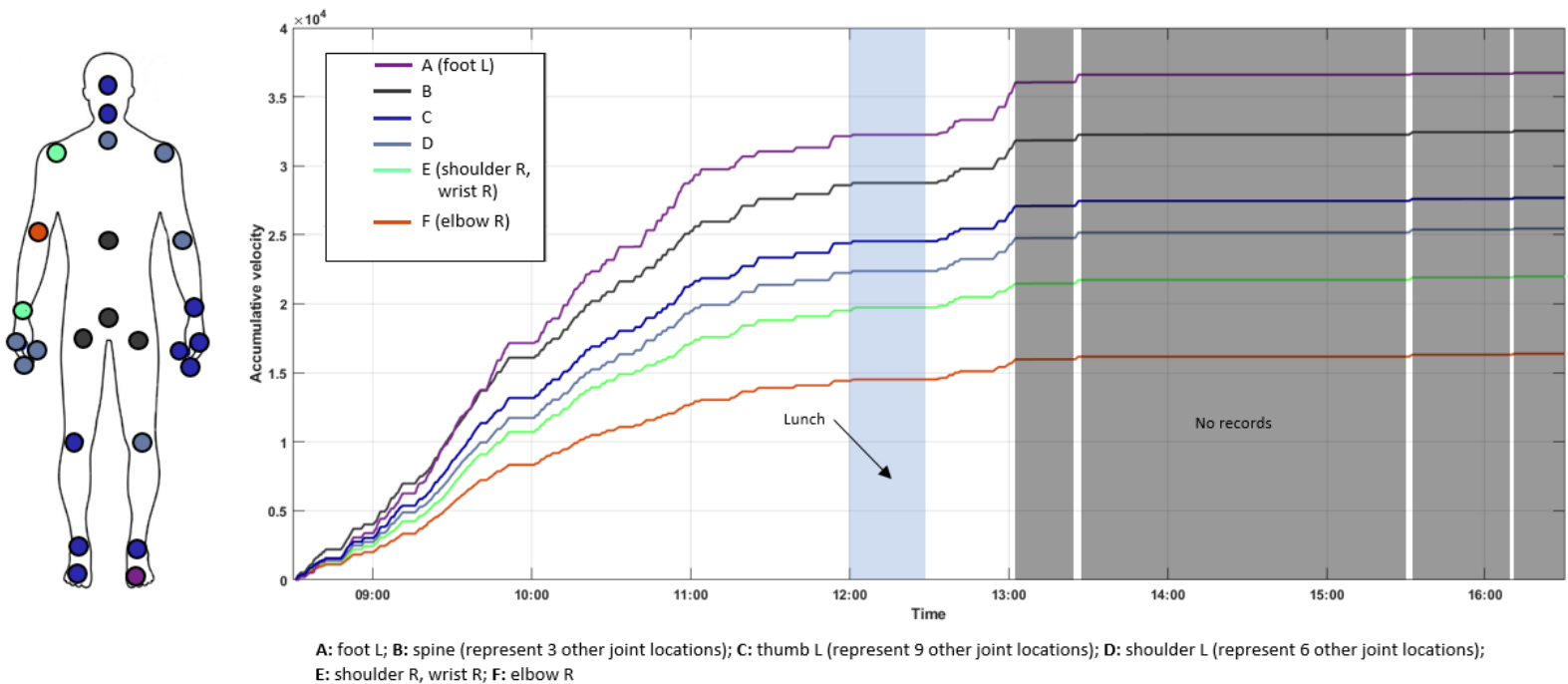
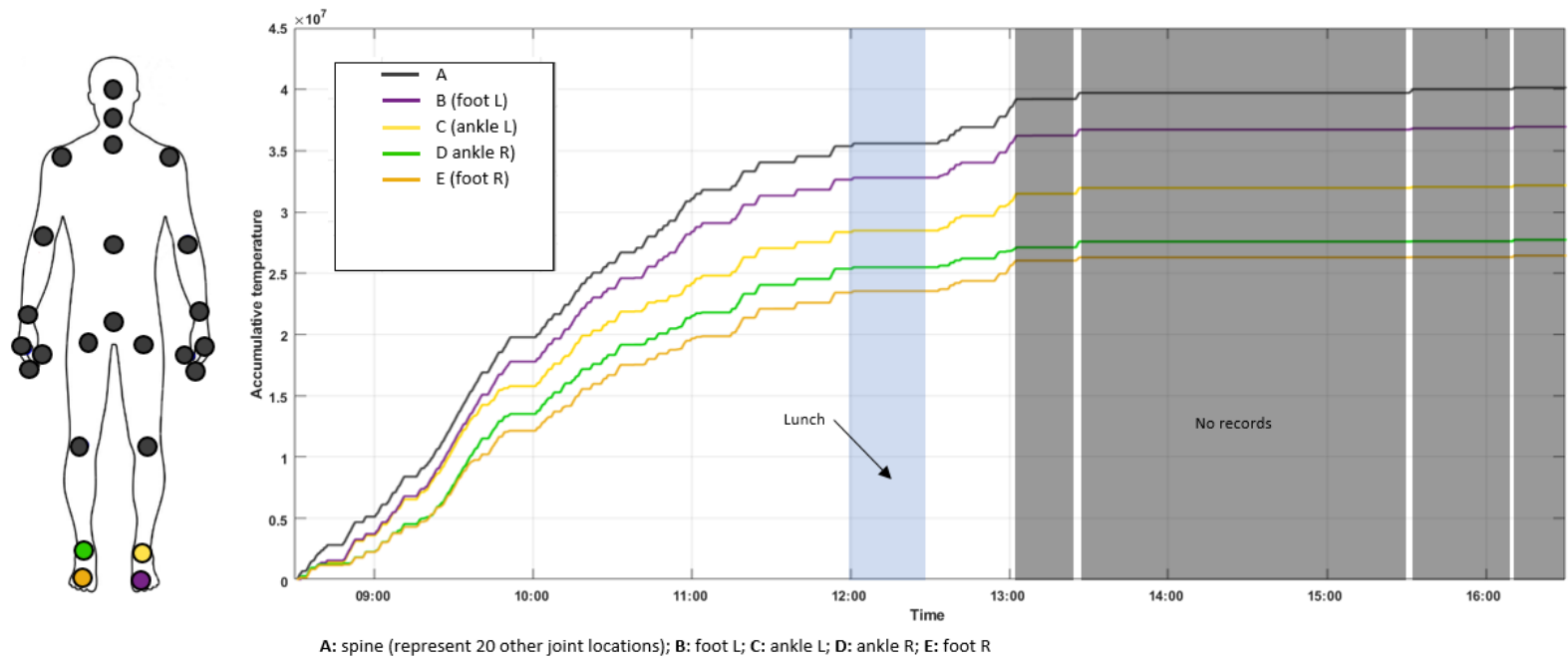
A: Handtip L (represent 20 other joint locations); B: ankle L; C: foot L; D: ankle R; E: foot R



A: Foot L; B: hip L, spine; C: Shoulder L (represent 11 other joint locations); D: knee L (represent 5 other joint locations); E: wrist R (represent 2 other joint locations); F: elbow R

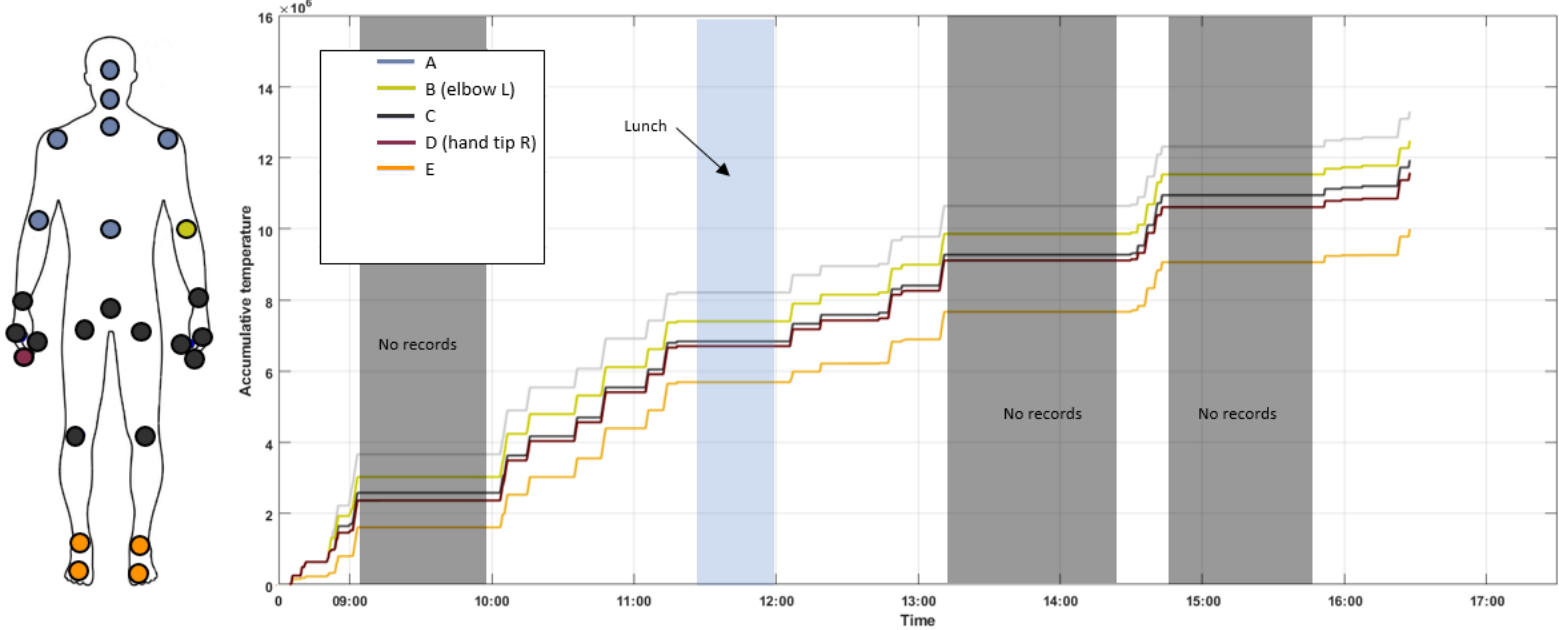
Core thermal comfort (1-7)	6	5	4	4	4	3	4	4	4	4	4	4	4	4	4	4	4
Hand thermal comfort (1-7)	4	4	5	5	4	4	4	4	4	4	4	4	4	4	4	4	4
Feet thermal comfort (1-7)	4	4	4	4	4	4	4	4	5	3	4	4	4	4	4	4	4
Body movement (1-5)	3	2	1	2	2	3	1	1	1	1	1	3	2	1	1	1	1
Sweat rate (1-5)	3	2	2	1	1	1	1	1	1	1	1	1	1	1	1	1	1
Pulse (-)	73	65	65	64	59	58	36	50	56	57	46	53	59	56	58	56	56

Appendix K4 : Accumulative quantities of temperature and air velocity allocated to different joint locations to the participant and the subject's evaluation, case IV

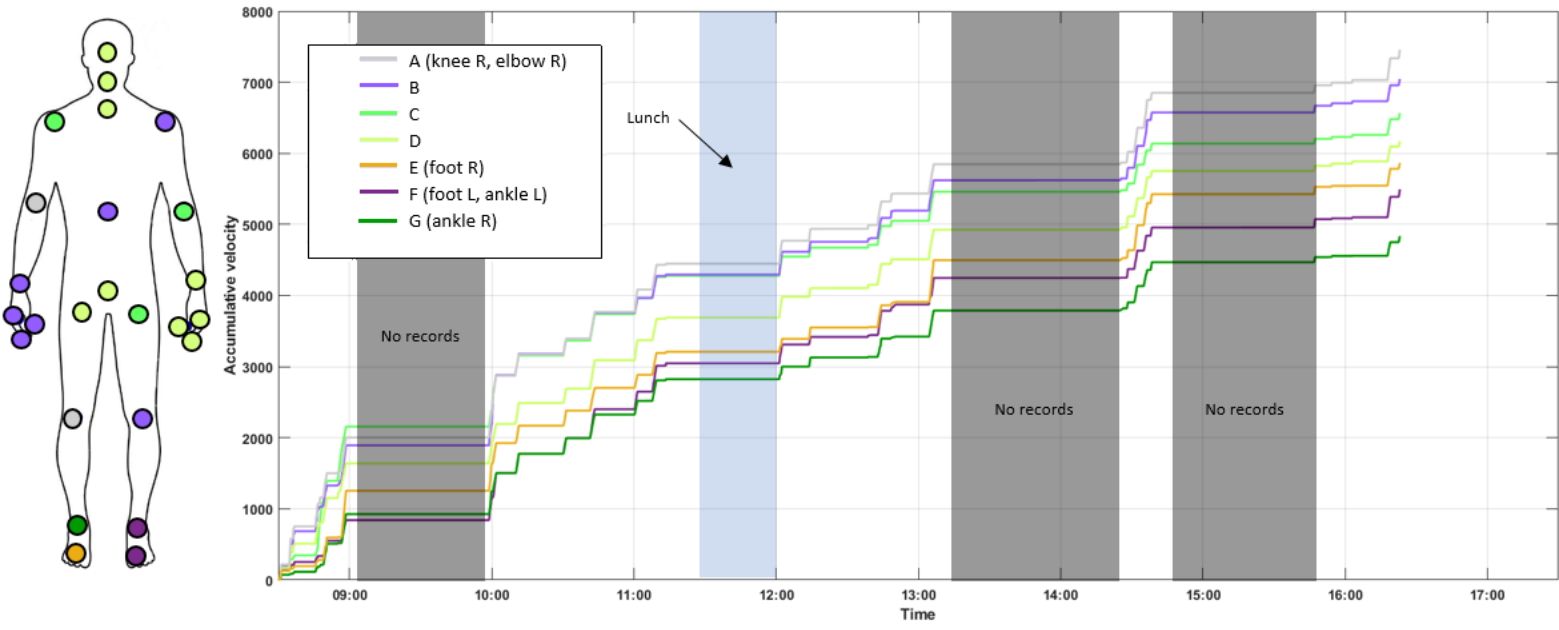


Core thermal comfort (1-7)	5	5	4	4	4	4	4	5	4	4	4	4	4	5	4
Hand thermal comfort (1-7)	4	4	4	4	4	4	4	4	4	4	4	4	4	4	4
Feet thermal comfort (1-7)	5	5	5	5	5	5	4	5	5	5	5	5	5	5	4
Body movement (1-5)	3	3	1	1	2	1	1	1	2	1	1	1	3	1	1
Sweat rate (1-5)	2	1	1	1	1	1	1	1	1	2	1	1	1	1	1
Pulse (-)	71	64	62	63	62	66	59	61	61	58	58	59	45	49	59

Appendix K5 : Accumulative quantities of temperature and air velocity allocated to different joint locations to the participant and the subject's evaluation, case V



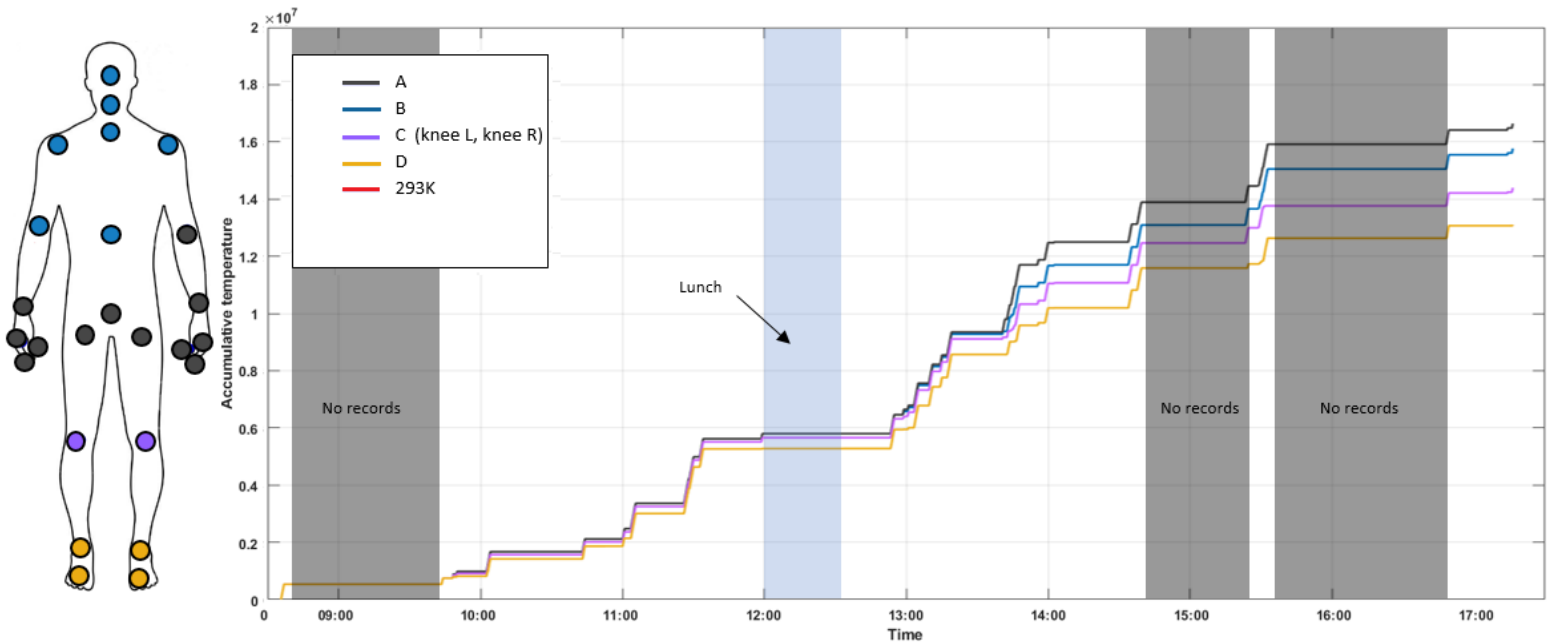
A: Shoulder L (represent 6 other joint locations); B: elbow L; C: spine (represent 11 other joint locations); D: hand tip R; E: foot R (represent 3 other joint locations)



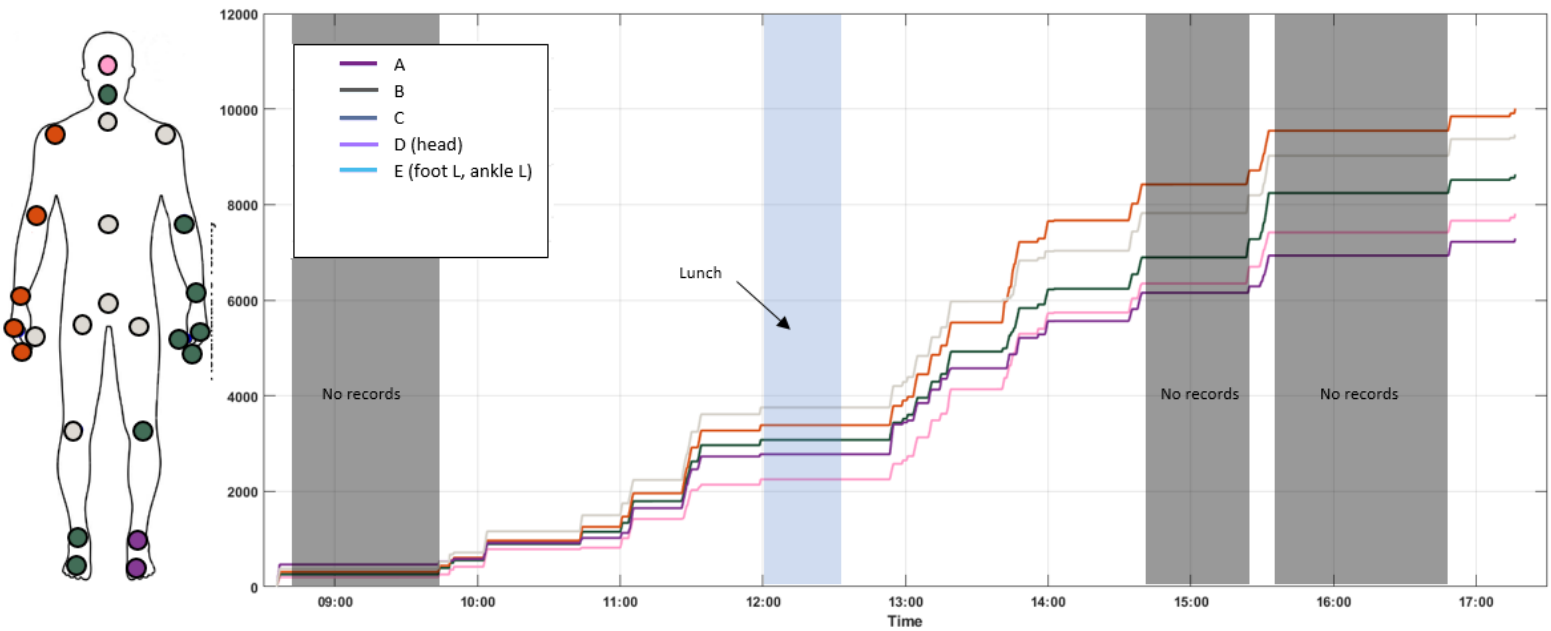
A: Knee R, elbow R; B: knee L (represent 6 other joint locations); C: shoulder R (represent 2 other joint locations); D: hip R (represent 8 other joint locations); E: foot R; F: foot L, ankle L; G: ankle R

Core thermal comfort (1-7)	5	5	4	4	4	4	4	4	4	4	4	4	4	4	4	4	4	5	4
Hand thermal comfort (1-7)	4	4	4	4	4	4	4	4	4	4	4	4	4	4	4	4	4	4	4
Feet thermal comfort (1-7)	5	4	5	5	4	4	4	5	5	5	5	4	5	5	5	5	5	5	5
Body movement (1-5)	3	1	1	2	1	1	1	1	3	1	1	1	1	2	1	1	1	1	1
Sweat rate (1-5)	2	2	1	1	1	1	1	1	1	1	1	1	1	1	1	1	1	1	1
Pulse (-)	79	63	62	66	59	56	45	52	55	57	56	64	60	57	55	55	59		

Appendix K6 : Accumulative quantities of temperature and air velocity allocated to different joint locations to the participant and the subject's evaluation, case VI



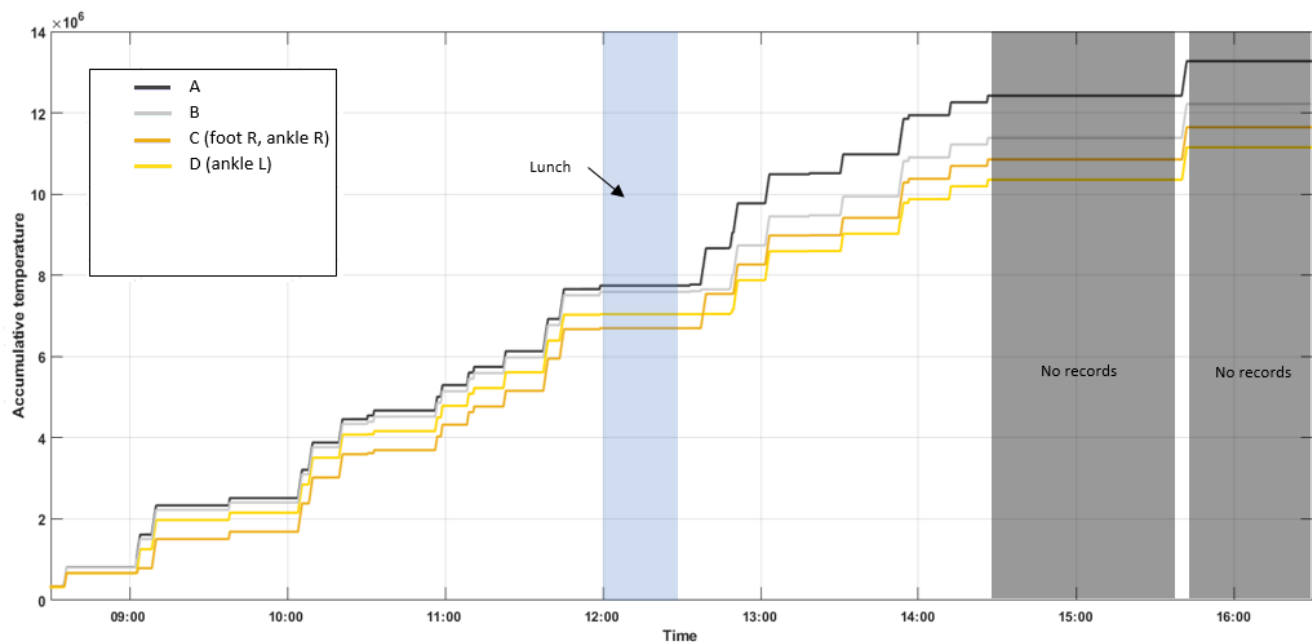
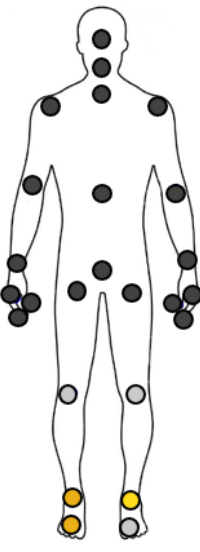
A: Spine (represent 11 other joint locations); B: spine mid (represent 6 other joint locations); C: (knee L, knee R) D: foot R (represent 3 other joint locations)



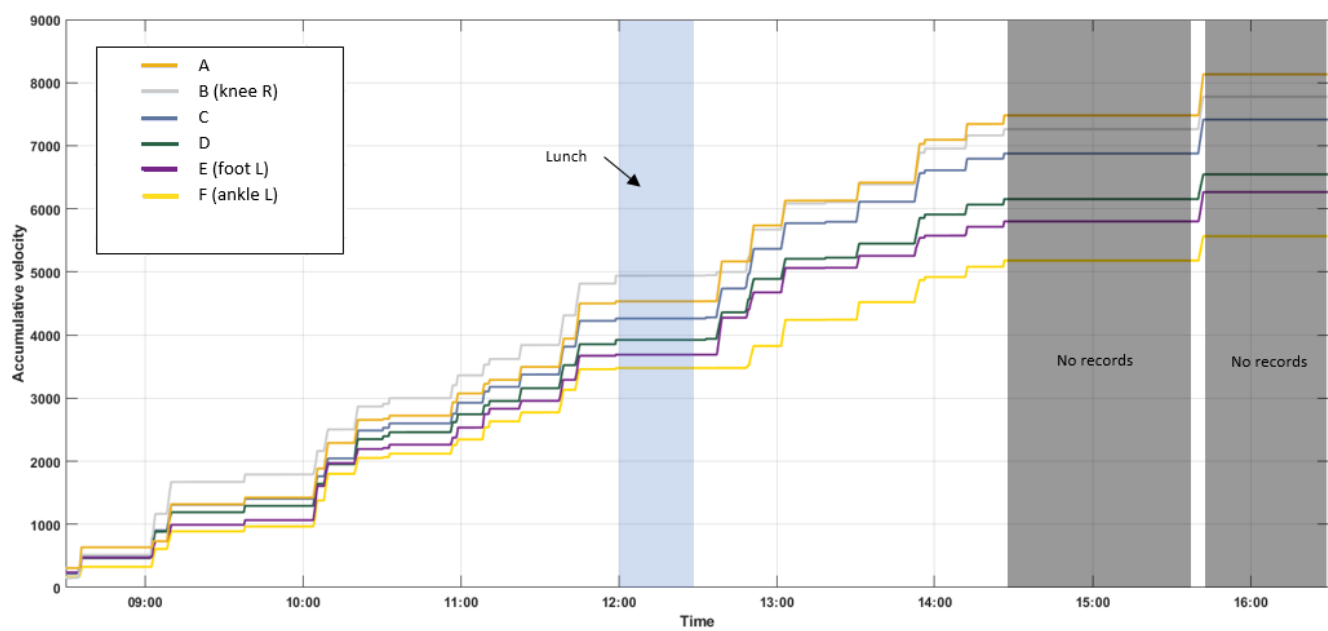
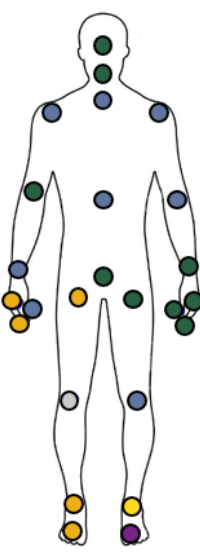
A: Elbow R (represent 4 other joint locations); B: knee R (represent 7 other joint locations); C: wrist L (represent 8 other joint locations); D: head; E: foot L, ankle L

Core thermal comfort (1-7)	5	6	5	5	5	5	5	6	6	6	5	5	5	5	5	5	6
Hand thermal comfort (1-7)	4	4	4	4	4	4	4	4	4	4	4	4	4	4	4	4	4
Feet thermal comfort (1-7)	4	4	4	4	4	5	5	5	4	5	4	5	4	4	4	4	4
Body movement (1-5)	2	1	2	1	1	1	1	2	1	2	2	1	1	1	1	1	2
Sweat rate (1-5)	2	3	2	1	2	1	2	3	4	4	3	3	2	3	3	3	3
Pulse (-)	67	65	63	62	58	65	49	63	63	65	62	60	60	61	59	62	60

Appendix K7 : Accumulative quantities of temperature and air velocity allocated to different joint locations to the participant and the subject's evaluation, case VII



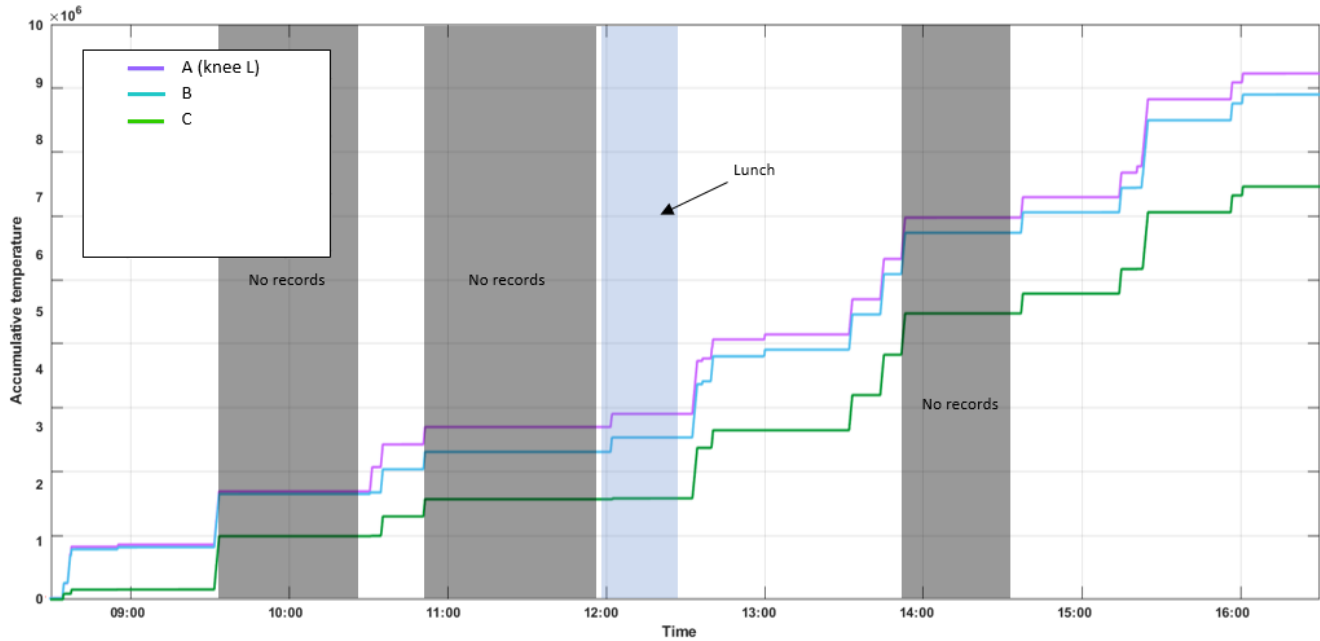
A: Spine (represent 18 other joint locations); B: knee R (represent 2 other joint locations); C: foot R, ankle R; D: ankle L



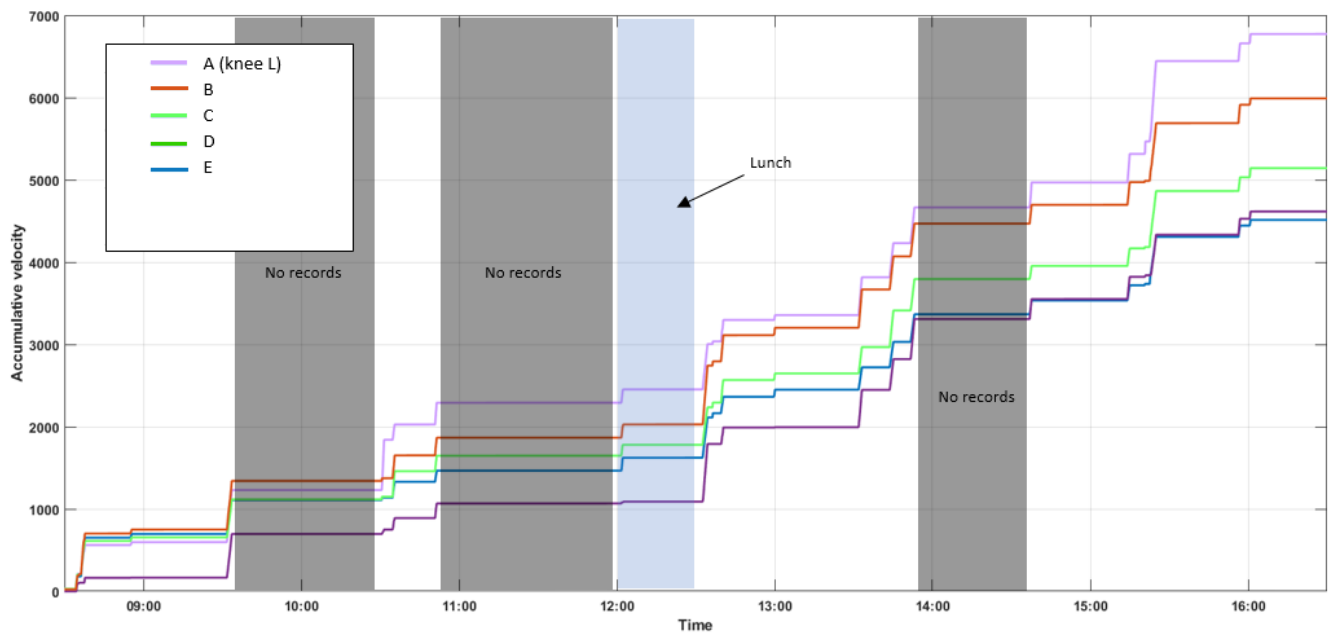
A: Foot R (represent 4 other joint locations); B: knee R; C: shoulder L (represent 7 other joint locations); D: wrist L (represent 8 other joint locations); E: foot L; F: ankle L

Core thermal comfort (1-7)	5	5	5	5	5	5	5	5	5	5	5	5	5	5	5
Hand thermal comfort (1-7)	4	4	4	4	4	4	4	4	4	4	4	4	4	4	4
Feet thermal comfort (1-7)	5	5	4	5	5	4	4	4	4	4	4	4	4	4	4
Body movement (1-5)	2	1	1	1	2	1	1	2	2	1	1	1	1	1	1
Sweat rate (1-5)	1	2	2	2	2	2	2	2	2	3	3	2	3	3	2
Pulse (-)	54	63	62	64	54	64	55	57	58	57	58	57	63	62	64

Appendix k8 : Accumulative quantities of temperature and air velocity allocated to different joint locations to the participant and the subject's evaluation, case VII



A: Knee L; B: wrist R (represent 19 other joint locations); C: ankle R (represent 3 other joint locations);



A: Knee L; B: hand tip L (represent 7 other joint locations); C: hip R (represent 8 other joint locations); D: spine mid (represent 2 other joint locations); E: foot L (represent 3 other joint locations)

Core thermal comfort (1-7)	4	5	5	5	5	5	5	5	5	5	5	5	4	5	5
Hand thermal comfort (1-7)	4	4	4	4	4	4	4	4	4	4	4	4	4	4	4
Feet thermal comfort (1-7)	4	5	4	4	4	4	5	5	4	4	4	4	4	4	4
Body movement (1-5)	2	1	1	1	2	1	1	1	1	1	1	1	2	1	1
Sweat rate (1-5)	2	2	2	2	2	1	1	2	2	1	2	2	2	1	2
Pulse (-)	61	61	61	66	61	59	51	59	55	51	60	54	57	57	52

